MACHINE LEARNING–BASED ASSESSMENT OF DEFORESTATION, SUCCESSIONAL STAGES, AND CARBON STOCKS IN A TROPICAL MONTANE FOREST USING RADAR AND OPTICAL SATELLITE IMAGERY

A Thesis submitted by

Richard Dein D. Altarez
B.Sc. Environmental Science (*magna cum laude*)
M.Sc. Environmental Science

For the award of

DOCTOR OF PHILOSOPHY

2024

ABSTRACT

Tropical montane forests (TMFs) play a crucial role in providing essential ecosystem services. However, these environments are increasingly threatened by deforestation and degradation. In the Philippines' TMFs, the extent of deforestation, successional stages, and carbon stocks remain poorly explored. Hence, this study focuses on the Province of Benguet, Philippines, with three specific objectives: 1) to demarcate deforestation using the fusion of Sentinel-1,-2, and biophysical data through a traditional classifier, machine (ML) and deep learning (DL) algorithms; 2) to map the successional stages in different vegetation types through Interferometric Synthetic Aperture Radar (InSAR), Global Ecosystem Dynamics Investigation (GEDI), Sentinel products and biophysical data with ML; and, 3) to estimate the above-ground biomass (AGB) and above-ground carbon (AGC) through optical, radar, biophysical data and ML. In addition to the field assessments conducted from December 2023 to January 2024, a systematic review of spaceborne remote sensing applications in global TMFs reinforced the significance of this study. The following results are the highlights of this study: 1) generally, RS investigations on TMFs are concentrated in the Americas (62%), with optical sensors (85.76%) being used more frequently than SAR (12.70%); 2) the fusion of Sentinel-1-2 and biophysical data with U-Net DL algorithm effectively demarcated the deforestation (Overall Accuracy (OA) = 86.77%, Kappa Index (KI) = 78.89); 3) elevation emerged as a significant predictor of vegetation type distribution, with Random Forest's (RF) top 10 features yielding the best predictive performance (OA = 84.22%, KI = 81.19%); and, 4) among the various algorithms utilized for AGB assessment, RF demonstrated the highest accuracy (r = 0.982; RMSE = 53.980 Mgha $^{-1}$). Above-ground carbon density varied from 0 to 434.94 Mgha^{-1}. This study underscores the urgency of formulating conservation and sustainable management policies. It also emphasizes the significance of Benguet's TMF in the context of carbon sequestration initiatives like REDD+.

CERTIFICATION OF THESIS

I, Richard Dein D. Altarez, declare that the PhD Thesis entitled *Machine learning-based assessment of deforestation, successional stages, and carbon stocks in a tropical montane forest using radar and optical satellite imagery* is not more than 100,000 words in length, including quotes and exclusive of tables, figures, appendices, bibliography, references, and footnotes.

This Thesis is the work of Richard Dein D. Altarez except where otherwise acknowledged, with the majority of the contribution to the papers presented as a Thesis by Publication undertaken by the student. The work is original and has not previously been submitted for any other award except where acknowledged.

Date: 09 January 2024

Endorsed by:

Prof. Armando A. Apan
Principal Supervisor

Prof. Tek N. Maraseni
Associate Supervisor

Student and supervisors' signatures of endorsement are held at the University.

STATEMENT OF CONTRIBUTION

The following information outlines the mutually agreed upon distribution of contributions for the candidate and co-authors in the publications provided within this thesis:

Paper 1:

Altarez, R.D.D., Apan, A. & Maraseni, T. (2022). Spaceborne satellite remote sensing of tropical montane forests: a review of applications and future trends, *Geocarto International, 37:26,* 11900-11928, DOI: 10.1080/10106049.2022.2060330

Altarez, R.D.D. contributed 70% to this paper. Collectively, Apan, A. & Maraseni, T. contributed the remainder.

Paper 2:

Altarez, R.D.D., Apan, A. & Maraseni, T. (2023). Deep learning U-Net classification of Sentinel-1 and 2 fusions effectively demarcates tropical montane forest's deforestation. *Remote Sensing Applications: Society and Environment, 29,* 100887, DOI: 10.1016/j.rsase.2022.100887

Altarez, R.D.D. contributed 70% to this paper. Collectively, Apan, A. & Maraseni, T. contributed the remainder.

This publication was presented at the Locate23 Symposium, organized by the Geospatial Council of Australia and awarded the best paper presentation. The symposium's theme was "Geospatial Evolutions: From Lands to Seas to the Stars." The event was held at the Adelaide Convention Centre in South Australia from 10 to 12 May 2023.

Paper 3:

Altarez, R.D.D., Apan, A. & Maraseni, T. (2023). Integrated multi-satellite data and machine learning approach in mapping the successional stages of forest types in a tropical montane forest. *Remote Sensing Applications: Society and Environment*. (Undergoing review)

Altarez, R.D.D. contributed 70% to this paper. Collectively, Apan, A. & Maraseni, T. contributed the remainder.

This publication was awarded for best research poster presentation at the UniSQ Centre for Sustainable Agricultural Systems, University of Southern Queensland, on November 8, 2023.

Paper 4:

Altarez, R.D.D., Apan, A. & Maraseni, T. (2023). Uncovering the hidden carbon treasures of the Philippines' towering mountains: A synergistic exploration using satellite imagery and machine learning. *PFG – Journal of Photogrammetry, Remote Sensing and Geoinformation Science*, 22 November 2023. https://doi.org/ 10.1007/s41064-023-00264-w

Altarez, R.D.D. contributed 70% to this paper. Collectively, Apan, A. & Maraseni, T. contributed the remainder.

This publication received the award for best research poster at the UniSQ GRS Virtual Poster Showcase and Competition, which ran from September 7 to September 14, 2023.

The overall contribution of Altarez, R.D.D. accounts for 70% in terms of developing the theoretical framework, conducting analysis, and refining the content of this thesis. Professor Apan, A. and Professor Maraseni, T. contribute significantly to the remaining percentage of the study's theoretical formulation, structural organization, data analysis, editorial work, and provision of substantial feedback.

ACKNOWLEDGEMENTS

I return all honor and glory to You, **Almighty God,** through this piece of work!

I also extend my sincere appreciation to my PhD Supervisory team. To Professor Armando Apan, who helped me become a professional remote sensing specialist. He has shaped me into a skilled researcher, an academic practitioner, and a humble person. I am very grateful to him for sharing his knowledge and helping his students to be a better version of themselves. To Professor Tek Maraseni, whose support has been indispensable in fostering my technical and critical skills in the realms of publication and scientific dissemination of my research findings. I am extremely proud to have been mentored by two prominent individuals in their respective fields.

This research was supported by the Philippines Department of Science and Technology – Science Education Institute (DOST-SEI) under the Foreign Graduate Scholarships in Specialized Priority Fields in Science and Technology. The Philippine Military Academy (PMA) and the Armed Forces of the Philippines (AFP) permitted the author to study PhD under the National Defense Act (NDA) Section 22 (k) (government time only).

Special gratitude is also extended to the following individuals and organizations for their significant contributions to the author's PhD journey:

To my mentors who turned a family, LTC RONNEL R ALMAZAN PROF (GSC), who has played a paternal role in my military career and consistently takes pride in my personal and professional growth. He untiringly helped me to go through all the problems I encountered throughout my 22 (k) application; he has been there for me when I almost lost my hope to do PhD. A sincere appreciation also goes to LTC WILFREDO L CLAVERIA JR PROF (GSC), who urged me to persevere in the face of discouragement and keep working toward my goal of getting the 22 (k) scholarship. Thanks to him and his wife, LTC LOURDES IMPERIAL-CLAVERIA PA (GSC). I will never forget how much you treated me like one of your family.

To COMMODORE CHESTON D VALENCERINA AFP (Ret), former Head of the Headquarters Academic Group (HAG), for allowing and supporting me to pursue this PhD

study in Australia. In addition, I would like to thank the late COL CLARO G UNSON JR PROF (GSC) (Ret) and COL EDWIN C POPA PROF (GSC) for their support and assistance during my application for 22 (k).

To Ma'am Fran and Ma'am Dina from the Department of Management, my extended family and friends at the Headquarters Academic Group, who have always supported and immensely encouraged me in all my career and educational undertakings. To the late Ma'am Tio, Ma'am Olive, and Ma'am Carol, pillars of the HAG, who gave me tremendous amounts of encouragement and advice throughout my life. Their support has been invaluable as I work toward pursuing my PhD.

To Glov and Gelo, fellow PhD scholars, for always being there to help me in various aspects of my PhD study. Thank you to Ma'am Bernz for the support and unending laughter. To Carmina Bacungan, thank you for connecting me with other international students who were also seeking a border restriction exemption in Australia around the time of the COVID-19 pandemic. Ms Leny Jane Pame, a PhD scholar at the University of Queensland, for generously providing her insight into the border exemption application process.

To the Department of Natural Resources Office - Cordillera Administrative Region (DENR-CAR) Regional Office, Mount Pulag Protected Landscape (MPPL) Protected Area Management Board (PAMB) and Protected Area Management Office (PMO), particularly the Superintendent Ms Mering Albas for allowing the author to conduct his PhD study in Kabayan Benguet.

To Center Head, Ms Helen A. Maddumba of the Watershed and Water Resources Research Development and Extension Center – Ecosystems Research and Development Bureau (WWRRDEC – ERDB), for assisting with the additional study plots in Baguio City.

To the staff of City Government of Baguio, particularly Forester Floro Bastian of CEPMO and some of his colleagues, the monitoring staff and park rangers of MPPL PMO for their support and assistance during the field data gathering.

To *kuya* Donald and Armina, thank you for helping me during my field work in Baguio City, Itogon, and Kabayan Benguet.

To my classmates and fellow students under the supervision of Prof. Apan, Sarasie and her husband, Prabath. They have been crucial in helping me adapt to this foreign land.

To Sir Rudolf, a former student of Prof Apan, for his support and kindness to me.

To Chea, for hosting wonderful get-togethers, complete with potlucks and barbecues with Jane, Wei, Steven, Cheryl, Johnny, Wil and the rest of the gang. To Dr. Peter, you have been a wonderful friend, and I look forward to playing badminton with you again.

To my UniSQ Badminton Club family, Kelvin, thank you for helping me bring the club to greater heights. You have been a wonderful friend as well as a valuable member of the committee. Thank you, Dr. Rob Wittenmyer, for being such a gracious host and everyone's best friend. Dr. Bidhan Nath, for the kindness and life lessons you have taught me.

To my friends from the Toowoomba Badminton Club, where camaraderie, friendship, and sportsmanship are highly valued. Isaac, who turned a good friend and helped me play well in badminton. Jay, who is funny and outspoken yet values friendship and company deeply. To Miao, Chen, and Melvis, the club's kindest and humblest players. I have been reminded of the importance of maintaining a positive attitude and a sense of humility and respect on the court at all times. Loom ge for showing an authentic kindness. Thanks everyone for the badminton coaching, I will remember all of it!

To MAJ KIMBERLY B CRUZ PROF, the constant laughter we shared on social media makes me feel at home all the time. The same goes for my friend from Toowoomba who relocated to Brisbane, Keerthi; I am grateful for our friendship and for not missing an opportunity to get in touch with me. Thank you as well to Dr. Yi Huang, my seatmate, who also became a good friend, and who also never misses getting in touch.

To all my housemates turned friends, thank you for all the good moments: Tian (Daniel), Meimei (Quy), and Elaine. I thoroughly appreciate the company. The Friday and Saturday night games and drinks that we shared were awesome. These are irreplaceable memories that I will always value.

To my *kababayan,* Karla, who has become a very good friend of mine. She has rescued me from the lowest point of my life as an international student in Australia. She consistently provides me with life-changing stories. I appreciate our friendship very much.

Ate Lolita Aranas, a fellow PhD student at UniSQ, and a mother figure to all the other students. All of the advice that she has given me has been invaluable. She is always there for me, ready to listen and offer support whenever needed. *Salamat ate!*

Dr. Hizam Rusmi, thank you for all the help and life lessons. He has become instrumental to me here in the Land Down Under. The strength I gained from his encouragement and support allowed me to recuperate and improve to be a good person. You truly are inspiring!

To Ma'am Hope, wife of my professor. You inspire me with your resilience and tenacity. Thank you so much, ma'am, for treating me like your son. I will always appreciate your kindness, compassion, and empathy.

To my parents, thank you for loving me unconditionally and inspiring me always to give my best. I am also grateful to both of you for motivating me to never stop dreaming and for teaching me that everything is possible if you have faith in God. You are one of the most important reasons why I am always dedicated to whatever I do. I am very proud of you regardless of our status in life. I hope I make you proud! I love you both!

To everyone I have missed, please know that you will forever be in my heart, and I am very thankful for your support!

I will forever be grateful to all of you! *Maraming salamat po sa inyong lahat!*

Richard Dein Altarez
Toowoomba, Queensland, Australia
January 2024

DEDICATION

To you,

I acknowledge the tremendous effort you have invested in this journey. You have encountered challenges and endured moments of being ignored, degraded, and humiliated, especially at the beginning of this voyage. There were times when giving up seemed like the only option, but you continued to pursue your ambitions with determination.

You have encountered heartbreaks and triumphs, moments of joy and painful downfalls. The harsh realities of life revealed the true nature and character of people. Some friends turned away, while others stood by your side. You discovered who fought for you and who remained loyal. These experiences polished you to become tougher than ever.

I can see your dedication to this, and now it's bearing fruit. Anticipate more challenges but remain optimistic. Maintain your feet on the ground and engage in every challenge head-on. Stay firm, tenacious, and resilient!

I am proud of you!

TABLE OF CONTENTS

LIST OF TABLES

LIST OF FIGURES

ABBREVIATIONS

AGB	Above-ground Biomass
AGC	Above-ground Carbon
AI	Artificial Intelligence
ANN	Artificial Neural Network
ASF	Alaska Satellite Facility
BGB	Below-ground Biomass
BOA	Bottom-of-Atmosphere
CAR	Cordillera Administrative Region
CEPMO	City Environment and Parks Management Office
CNN	Convolutional Neural Network
dB	Decibel
DBH	Diameter Breast Height
DEM	Digital Elevation Model
DENR	Department of Environment and Natural Resources
DL	Deep Learning
EOSDIS	Earth Observing System Data and Information System
ERDB	Ecosystems Research and Development Bureau
ESA	European Space Agency
EVI	Enhanced Vegetation Index
FAO	Forest Agriculture Organization
fAPAR	Fraction of Absorbed Photosynthetically Active Radiation
fCover	Fraction of Vegetation Cover
FMB	Forest Management Bureau
GEDI	Global Ecosystem Dynamics Investigation
GHG	Greenhouse Gas
GLCM	Grey Level Co-occurrence Matrix
GPS	Global Positioning System
GRD	Ground Range Detected
IoT	Internet of Things
IPCC	Intergovernmental Panel on Climate Change
KDTree	KD Tree Nearest Neighbor

KI	Kappa Index
KNN	K Nearest Neighbor
LAI	Leaf Area Index
LiDAR	Light Detection and Ranging
LULC	Land Use Land Cover
ML	Machine Learning
MLC	Maximum Likelihood Classifier
MODIS	Moderate Resolution Imaging Spectroradiometer
MPPL	Mount Pulag Protected Landscape
NASA	National Aeronautics and Space Administration
NDVI	Normalized Difference Vegetation Index
NFO	Non-Forest
NYDF	New York Declaration on Forests
OA	Overall Accuracy
OGF	Old Growth Forest
PAMB	Protected Area Management Board
PSA	Philippine Statistics Authority
Q1	Quartile 1
RADAR	Radio Detection and Ranging
REDD+	Reducing Emissions from Deforestation and Forest Degradation and other activities that increase C stocks
RF	Random Forest
RMSE	Root Mean Square Error
RS	Remote Sensing
SAR	Synthetic Aperture Radar
SNIP	Source Normalized Impact per Publication
SRTM	Shuttle Radar Topography Mission
SS	Successional Stage
SVM	Support Vector Machine
TMF	Tropical Montane Forest
TOA	Top-of-Atmosphere
UAV	Unmanned Aerial Vehicle
UN	United Nation
UNFCCC	United Nations Framework Convention on Climate Change

VH	Vertical transmit and Horizontal receive
VV	Vertical transmit and Vertical receive
WEKA	Waikato Environment for Knowledge Analysis
WWRRDEC	Watershed and Water Resources Research Development and Extension Center

CHAPTER 1: INTRODUCTION

1.1. Background

Tropical montane forests (TMF) are tropical rainforest ecosystems along the equator (Figure 1.1). Although experts have yet to agree on the elevation gradients of TMFs (Kappelle, 2004), which are influenced by a number of factors and environmental conditions, such as those found on volcanic islands, in archipelagic regions, and wind-sheltered mountain valleys (FMB - DENR, 2011; Kappelle, 2004; Bruijnzeel & Veneklaas, 1998; Soh et al., 2019), it is realistic to infer that they occurred between 500 and 4,000 meters in elevation (Richter, 2008). The Global Forest Resources Assessment (2001) of the FAO estimates that TMFs cover 4,524,967.60 km^2.

TMFs are often involved in manufacturing important ecosystem services such as water, oxygen, and biological diversity (Wallis et al., 2019). They also hold a significant amount of biomass, which is vital in regulating the global carbon cycle (Spracklen & Righelato, 2014). Pests and diseases, land conversion, and human reliance on water and food threaten TMFs (Körner, et al., 2005). In Asia, for instance, mountains are being encroached to make way for agriculture and human settlements. The mountain forest system in Africa is adversely impacted by fire and agricultural expansion (FAO, 2001). The world's tropical forests have lost more than 7 million hectares between 2000 and 2010, and agricultural land gained 6 million hectares (FAO, 2016). These deforestation and degradation have led to the loss of vital vegetation and biodiversity (Turner et al., 1996). The variations in the forest structure influence the forest growth and biogeochemical cycles, particularly carbon stock (Helmer et al., 2000). Forest succession, or the development of forest structure over time, is an essential ecological process in terrestrial ecosystems (Liu et al., 2008). Knowledge of forest successional stages can aid in predicting and comprehending the global carbon cycle (Helmer et al., 2000; Liu et al., 2008).

Figure 1.1 Mt Ulap, a tropical montane forest in Benguet Province, Philippines

In the Philippines, forest cover declined from 90% in 1900 to 23% (7 Mha) in 2015 (Pulhin et al., 2020). Several literature attribute forest decline to land conversion for agriculture and development, overexploitation, the prevalence of fire, and pest and disease outbreaks (Lasco & Pulhin, 2003; Miettinen et al., 2014; FAO, 2015; Hu et al., 2021; Kowaal, 1966; Philippine Statistics Authority, 2020). In the mountainous land-locked region of the Philippines, Cordillera Administrative Region (CAR), deforestation and forest degradation are also prevalent. It is anticipated that 300 hectares (0.022%) of the region's forest reserves will be lost annually (Walpole, 2010; ESSC, 2012). CAR has 44.6 percent (1.35 million hectares) of forested mountain terrain. The region's 1.81-million-hectare catchment serves Ilocos and Cagayan Valley regions, with a combined population of 10.8 million as of the 2020 Philippine census (Philippine Statistics Authority, 2021).

Forest management has been a significant topic of discussion across the globe up until this juncture (Grêt-Regamey & Weibel, 2020). Several global initiatives to manage the world's forests have been established, including the UN 2030 Agenda for Sustainable Development, the REDD+ program, and the New York Declaration on Forests (NYDF) (Albrich et al., 2020; Cadman et al., 2017; Kauffman & Donato, 2012). Despite these growing forest management

efforts, there are still concerns surrounding the sustainability of forest management (Soh et al., 2019). Restoring particular ecosystem functions and services necessitates a thorough evaluation (Camarretta et al., 2019). Also required is a greater understanding of the ecological significance of TMFs, particularly those in Southeast Asia, where little research has been conducted (Soh et al., 2019; Altarez et al., 2022).

Consequently, this study sought to assess, quantify, and map deforestation in the Philippines' TMFs, understand successional stages, and estimate carbon stocks using remote sensing (RS) particularly, the data derived from spaceborne optical sensors, Synthetic Aperture Radar (SAR), and Light Detection and Ranging (LiDAR), in conjunction with deep learning (DL) and machine learning (ML) algorithms.

1.2. Statement of the problem

The increasing human population entails a growing demand for space for housing and agricultural land, which leads to a continuous loss of forest cover (FAO, 2015). The Philippines, like many other developing Southeast Asian countries, has experienced extensive and rapid deforestation (Apan et al., 2017). The Philippines' forest cover has fluctuated profoundly over time, falling from 90% in 1521 to 22% in 1998 (ESSC, 1999), and then slightly improved to 23% in 2015 (Pulhin et al., 2020).

The CAR is composed of five provinces, namely Abra, Apayao, Benguet, Ifugao, and Mountain Province. The Province of Benguet, in particular, is an example of TMF that has three vegetation zones: tropical lower montane forest (pine forest), tropical upper montane forest (mossy/cloud forest), and grassland summit (DENR - FMB, 2011; Fernando & Cereno, 2010). Sadly, the province is a source of lumber for construction and other uses. It was also heavily altered for settlements, agriculture, and mining (Perez et al., 2020). Over half of the forests in Apayao, Kalinga, and Mountain Provinces have been logged over. Agro-forestry operations have encroached on protected forests in Benguet, Mountain Province, and Ifugao. Forest fires are causing significant forest disturbance and damage. From 2008 to 2018, fires destroyed 21,242.40 hectares of Cordillera forest (PSA, 2020). In Benguet, fires destroyed 899.53 hectares of natural forest in 2020 (Dionisio & Agoot, 2020).

Tropical rainforests are the most productive of all forest types (Wallis et al., 2019). They store 70-90 percent of the carbon (González-Jaramillo et al., 2018). TMFs, as one of the tropical forest types, store a lot of biomass in their steep slopes (Spracklen & Righelato, 2014). Estimating biomass helps researchers determine how much carbon is released into the atmosphere due to deforestation (Salvaña et al., 2019). Biomass assessment also determines the forest's ability to store carbon (DENR, 2009).

Unfortunately, the TMF's complex terrain makes estimating biomass difficult (González-Jaramillo et al., 2018). Likewise, the altitude also drives its ecological composition (Chapman et al., 2016) poses a challenge for an assessment. Wallis et al. (2019) highlighted that performing assessments in TMF is labor-intensive. Knowledge about carbon studies in TMFs is still lacking (Anderson-Teixeira et al., 2016)**.** Studies related to TMFs are scarce in Southeast Asia alone, and spatial comprehension of ecosystem dynamics is still in its infancy (Soh et al., 2019). Examples of research gaps include carbon stock and biomass in different vegetation zones or forest types across the TMF's elevation gradient (Salvaña et al., 2019).

With the advent of carbon payment schemes under REDD+ or the reporting of deforestation and forest degradation to global carbon emission under the UNFCCC, quantifying vegetation biomass became popular in tropical areas (Yuen et al., 2016**;** Gao et al., 2020). The reporting requires precise measurements of forest cover, land use, and biomass (González-Jaramillo et al., 2019)**.** Reich (2012) proposed quantifying and mapping TMF biomass to understand the carbon cycle better. RS gained popularity in forest studies due to its ability to map and monitor spatial conditions over time. However, processing is necessary for remotely sensed data to be useful. It frequently requires massive and complicated approaches to analyze the data manually (Ma et al., 2019). This gap can be bridged using machine and deep learning techniques, both of which fall under the scope of Artificial Intelligence (AI) (Maxwell et al., 2018). These techniques have become popular, as they have been successfully used for classification, regression, clustering, etc. (Camps-Valls, 2009). Thus, combining DL, ML and RS can improve forest and environmental assessments.

Considering the problems and opportunities stated above, this research sought to understand the forest dynamics in Benguet's TMF and explore its significance in carbon studies, which is underrepresented in the current literature.

1.3. Significance of the study

Unprecedented changes in land use have resulted in the loss of pristine forest cover around the world (Cronin et al., 2014). The FAO (2016) estimates that agricultural land increased by at least 6 million hectares per year for every 7 million hectares of forest loss from 2000 to 2010. The global climate change also affects the climate patterns of TMFs (Ray, 2013; Eller et al., 2020).

There is a need to understand the rate of deforestation and the importance of carbon stock in TMFs because global deforestation is still widespread and unwarranted (Ray, 2013). Likewise, there needs to be more defined research directions that could enable the long-term use of the world's TMFs (Soh et al., 2019). According to IPCC (2007), deforestation is projected to contribute between 17 and 20% of global greenhouse gas (GHG) emissions. These deforestations mainly occur in tropical forests, abundant in many developing countries, including the Philippines (Carandang et al., 2013). These phenomena threaten the country's remaining forests (Avtar et al., 2020).

The assessment of TMFs in space and time may lead to defining their dynamics and comprehension of carbon cycling (Paulick et al., 2017). However, unlike the tropical lowland forests, only a few studies investigate the TMFs (Anderson-Teixeira et al., 2016; Paulick et al., 2017), especially in South East Asia (Soh et al., 2019). In particular, Spracklen & Righelato (2014) emphasized the scarcity of carbon studies, including the measurement of above-ground biomass (AGB) and other carbon-related metrics along elevation gradients. Assessment of these parameters is critical for environmental studies and conservation initiatives, such as the program reducing emissions from deforestation and forest degradation and the role of conservation, sustainable forest management, and enhancement of forest carbon stocks in developing countries (REDD+) (González-Jaramillo et al., 2019), and the United Nations Framework Convention on Climate Change (UNFCCC) policies on issues relating to reducing emissions from deforestation and degradation in developing countries (Carandang et al., 2013).

This thesis has produced four (4) publications with the following specific significance:

1. The systematic review of spaceborne RS to TMFs shifted the current knowledge of its application to tropical areas with towering terrain, which has received

disproportionate attention compared to other forest types worldwide. In addition to advancing our understanding of RS's role in forest research, this study shed light on how far the technology has been used for monitoring and mapping TMFs (Publication 1);

2. Mapping the extent of deforestation enabled the opportunity to comprehend the effects of deforestation in Benguet, Philippines' TMF. The generated data provided essential knowledge and a basis for policy formulation, conservation strategies, and appropriate land resource management measures (Publication 2);

3. The evaluated successional stages of the TMF addressed the knowledge gap about the distribution and growth patterns of Benguet's three vegetation zones. The study also revealed which parts of the TMF can store more carbon and which areas need improvement. The findings also keep track of the disruptions that necessitate the keen intervention of relevant government agencies (Publication 3); and,

4. Quantifying the magnitude of carbon stock in the three vegetation zones of the province is helpful in various applications (i.e., conservation planning, comprehensive land-use plan, policymaking). Similarly, TMF's carbon stock and density calculation are particularly relevant in REDD+ greenhouse gas emission reporting (Publication 4).

Finally, the novel methods applied in this study (e.g., the use of multi-temporal SAR bands, optical imagery, and DL and ML) to understand the Philippines' TMFs dynamics can be applied to other TMFs globally. It is noted from the various published literature that more work needs to be done on the aspect of carbon stock estimation using radar applications in the Philippines' TMF. Hence, this study is novel in the country as it hoped to estimate biomass and carbon density using RS technologies and emerging DL and ML algorithms for a more accurate assessment. Subsequently, this research is valuable for monitoring local and national government reforestation and restoration efforts.

1.4. Aim and objectives

The broad aim of this study is to assess, quantify, and map deforestation and successional stages of tropical montane forest (TMF) of the Philippines, as well as their carbon stocks, using Remote Sensing (RS), Deep Learning (DL) and Machine Learning (ML). Specifically, this study has the following objectives:

1. to evaluate the utility of Sentinel-1 and Sentinel-2 data and their fusion to compare the image classification performance of the traditional classifier (Maximum Likelihood), ML algorithms (Random Forest, K Nearest Neighbor, KD Tree Nearest Neighbor), and DL (U-Net). The Objective 1 paper also intended to determine which satellite input and AI algorithm is best for assessing the extent of deforestation in the area under investigation.

2. to refine the classification and map successional stages of a TMF in the Philippines based on forest types as determined by topographic factors through GEDI, Sentinel-1 InSAR, Sentinel products, and biophysical data. The Objective 2 paper also aspired to contribute to the growing interest in using GEDI and InSAR in a TMF utilizing ML regression for continuous data.

3. to test the synergistic approach of ML, optical and radar-derived satellite images, and other biophysical parameters to investigate its potential to estimate both the above-ground biomass (AGB) and above-ground carbon (AGC) in the tropical montane forest in the northern Philippines. In particular, the Objective 3 paper aimed to (1) determine the AGB and AGC of the three vegetation zones in the Province of Benguet; (2) evaluate the predictive capacity of ML algorithms using the combination of Sentinel-1 and 2 imagery and biophysical data; and, (3) map the carbon stock in the study area using ML.

1.5. Scope and limitations of the study

The study is concentrated on the province of Benguet, where multiple cases of forest degradation have been documented. This thesis focused on mapping the deforestation in the province, modelling the successional stages of three vegetation types, namely pine forest, mossy forest, and grassland summit, including the quantification of above-ground biomass and carbon density. At present, no definite elevation gradient defines the stratification of the three vegetation zones. Hence, we defined pine forests as areas with an elevation from 700 – 1,400 meters, mossy forests as areas with an elevation between 1,400 – 2,600 meters, and grassland summit as areas over 2,600 meters. These assumptions were based on the available literature (Whitford, 1911; DENR - FMB, 2011; Fernando & Cereno, 2010), satellite data inspection, and observations during fieldwork.

The seasonal variability of data collection is not taken into account in this study. Data collection took place from December 2023 to January 2024 to facilitate more accessible field sampling and to avoid unintended mishaps because the steep slopes of the montane ecosystem in Benguet are harshly eminent, especially during the rainy season. Allometric equations determined the biomass and carbon density of vegetation in the TMF because sampling of soil and living and dead plants are strictly prohibited in Benguet's protected areas per Philippine Republic Act number 7586. Sentinel-1 C band SAR imagery, which has readily accessible data for the province, was utilized for Objectives 1-3. Relatively cloudless Sentinel-2 bands 2-8a and 11-12 were utilized. Finally, the DL and ML approaches included in programs like ArcGIS Pro, SNAP, WEKA, and Whitebox Runner aided in the development of classification and regression models. Further information about the software is discussed in Chapters 4-7, and specific technical limitations were also provided

1.6. Conceptual framework

The conceptual framework of the study is depicted in Figure 1.2. The systematic review of RS applications to TMFs strengthens the comprehension of the spaceborne RS application to TMFs globally and in the local context. The findings were used to justify the necessity of conducting the three forest assessments in Benguet’s TMF. The TMFs' dynamics can be better understood by integrating data from three studies that all have interconnected relationships:

deforestation, succession stages, and carbon stock analyses. Like many other forest ecosystems, deforestation and degradation potentially affect the pattern of vegetation growth and carbon stocks on TMFs. To determine the extent of deforestation and degradation in Benguet, a study that focuses on mapping deforestation and degradation using radar and optical imagery and deep learning was employed. The stages of succession per forest type were also modelled through various integration of spaceborne RS and ML. Further, the carbon stocks of the different vegetation types were estimated using the same approach. The successional stages and carbon stock assessment were all validated through field data observations.

Apart from the eminent knowledge of deforestation rate, successional growth patterns, and carbon stock information, the study's results offer a crucial basis for developing policy and conservation strategies and measures. The science-based plans may be used to generate sensible land resource management approaches, sustainable utility of forests, and biodiversity conservation and restoration methods.

1.7. Organization of the dissertation

This thesis is organized into eight (8) chapters. **Chapter 1** presents the Introduction. This section includes the background of the study, statement of the problem, significance of the study, aims and objectives, scope and limitations and the conceptual framework.

In **Chapter 2**, the literature review covers the latest knowledge on the TMF and the use of RS technologies, as well as the emerging trend of artificial intelligence in TMF research.

In **Chapter 3**, the research methodologies used to describe the study area, the general design of this thesis, and field data gathering and processing are discussed.

The published papers from this thesis are included in chapters 4-7. In **Chapter 4**, a comprehensive assessment is presented of the use of spaceborne RS and emerging ML techniques in the investigation of TMFs located all over the world. **Chapter 5**

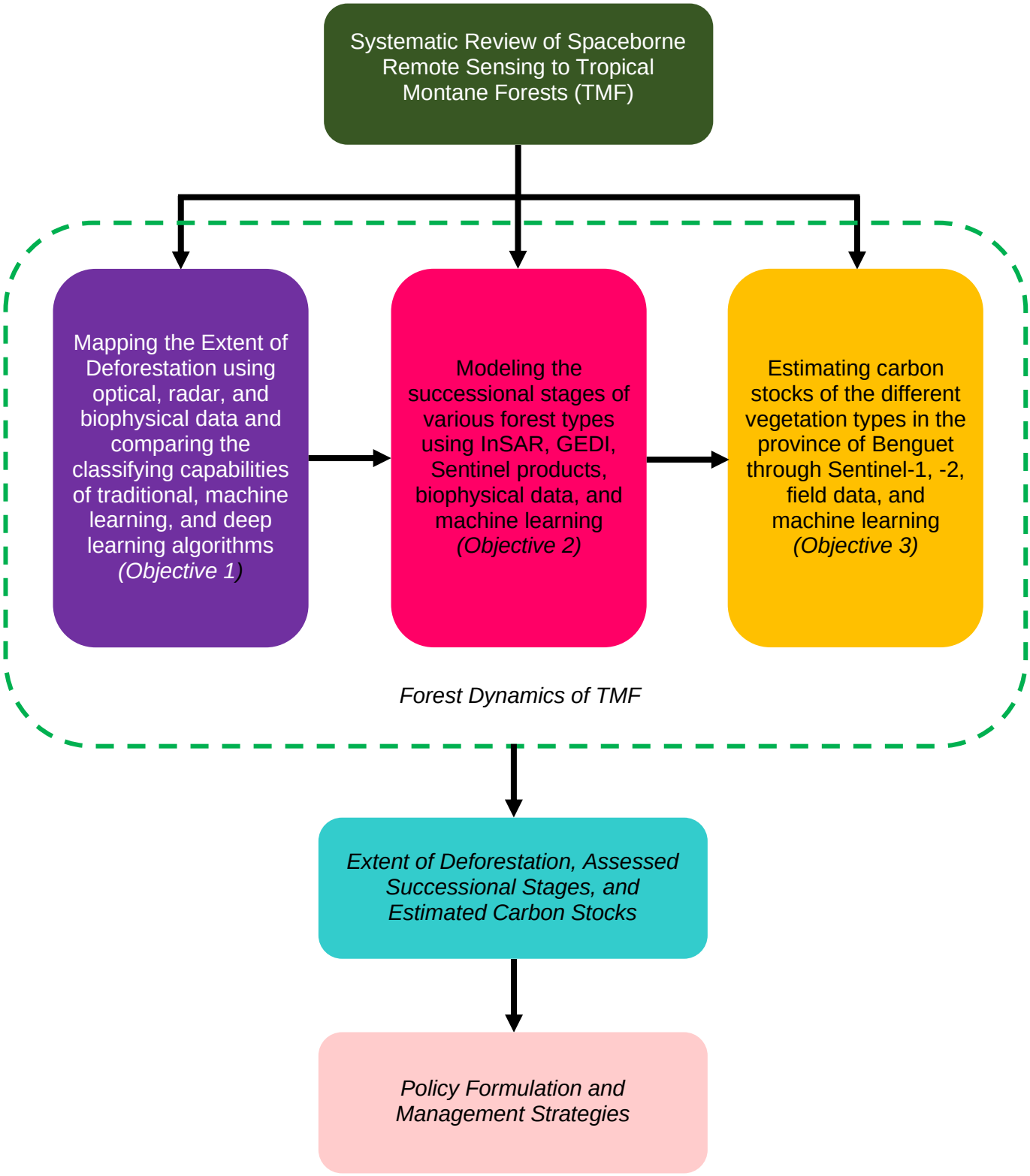

Figure 1.2 Conceptual framework of the study

talks about mapping deforestation in Benguet by integrating radar, optical, and biophysical raster data with deep learning algorithms, particularly the U-Net convolutional neural network. In this chapter, the method described which combinations and algorithms gave the most accurate representation of the forest loss.

The findings of the study that mapped the succession stages of the pine forest, mossy forest, and grassland summit found in the province of Benguet are presented and discussed in **Chapter 6**. The InSAR, GEDI, and Sentinel products were used with ML methods to predict the successional stages. The method employed in this study was novel in a way that InSAR and GEDI have been used to model forest attributes in a TMF, which was not done in the Philippines and South East Asia.

Chapter 7, on the other hand, presents the results of the above-ground biomass and above-ground carbon density estimations using RS and ML. These estimates were complemented by field observations and data obtained through RS. Several ML algorithms in the WEKA software were tested to determine which highly corresponds to estimating the biomass. In this chapter, we also covered the topic of the spatially explicit model that uses Random Forest in Whitebox Runner.

The overall findings, implications, research contributions, and recommendations for further study are presented in the eighth and final chapter, "**Chapter 8**".

CHAPTER 2: LITERATURE REVIEW

2.1. Introduction

The previous Chapter presented the overall background of the study, highlighting the need to investigate the TMF using spaceborne remote sensing (RS), deep and machine learning (DL and ML). This Chapter, reviews the current literature on TMF about mapping its deforestation, successional stages, and estimation of above-ground biomass and density. A comprehensive discussion of the application of spaceborne RS to TMF across the globe and its future trends is elaborated in Chapter 4. Additional reviews specific to each technical chapter (i.e., pertaining to Objectives 1, 2, and 3) are presented in Chapters 6 to 7.

The remainder of this Chapter is organized into seven sections. Section 2.2 discusses the distribution and status of TMFs across the globe. Section 2.3 talks about the importance and threats to TMFs. Section 2.4 is about using RS and ML to TMF for improved assessment of deforestation and land conversion. Section 2.5 outlines the implication of ML for forest assessment. Section 2.6 deals with mapping and monitoring TMF's successional stages and regeneration. Section 2.7 presents the estimation of biomass and carbon density using SAR and ML. This Chapter ends in Section 2.8, which summarizes the literature review.

2.2. Tropical montane forests: Distribution and status

TMFs are one of the types of tropical rainforest ecosystems found at middle to high elevations (Richter, 2008). According to the FAO's Global Forest Resources Assessment (2001), they cover 4,524,967.60 km^2 of the earth's surface area and are found in North and South America, Eastern Africa, and Asia (Figure 2.1).

TMFs are classified into three mountain zones based on their ecotones: tropical lowland, tropical lower montane, and tropical upper montane (Ohsawa, 1991). Scholars have expressed concern about identifying TMFs based on elevation gradient (Kappelle, 2004) because vegetation types inherent to TMFs can occur at lower elevations than the conventional guideline of 500-4,000 masl. For instance, it appears at 300 masl on volcanic islands and other

archipelagic regions (Kappelle, 2004; Bruijnzeel & Veneklaas, 1998; Soh et al., 2019), and vegetation also changes at wind-protected valleys (FMB - DENR, 2011).

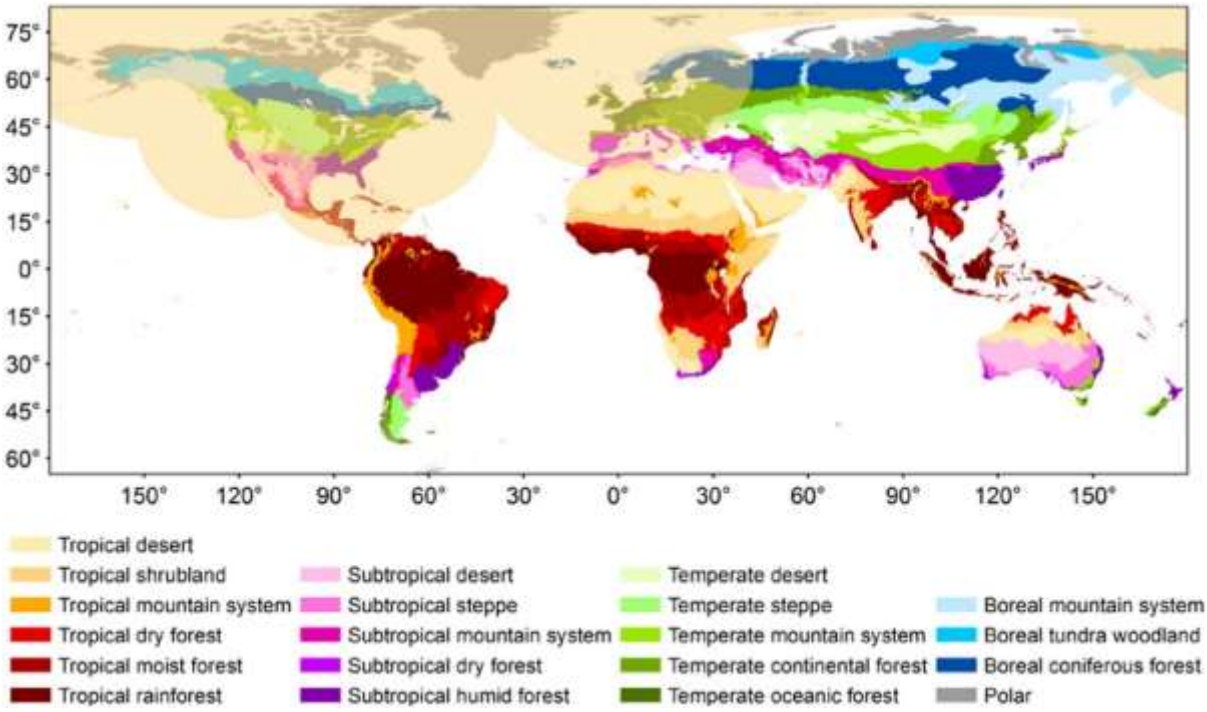

Figure 2.1 The global ecological regions of the world (FAO, 2012)

In the Philippines, TMFs are found in the mountains of Luzon, Zambales, Mindoro Island, and Mindanao (DENR - FMB, 2011; Wikramanayake, 2021). Figure 2.2 illustrates the Philippines' elevation map, emphasizing the mountain zones where TMFs can be found.

The vegetation zones in the Philippines' TMF can be classified as the following: lower montane forest, upper montane forest, subalpine forest (DENR - FMB, 2011), and grassland summit in some mountains (Fernando & Cereno, 2010). This vegetation stratification can be linked to elevation changes. Elevation influences important environmental parameters (Jin et al., 2008; Benner et al., 2011); for instance, the amount of sunshine that plants receive lessens, the amount of water that plants absorb varies (Mc Daniel, 2017), and the nutrient content in the soil decreases (Bruijnzeel & Veneklaas, 1998). As a result, particular vegetation grows best at higher elevations but not at lower elevations. However, based on extensive literature and research, no map delineates the aforementioned vegetation stratifications in the Philippines.

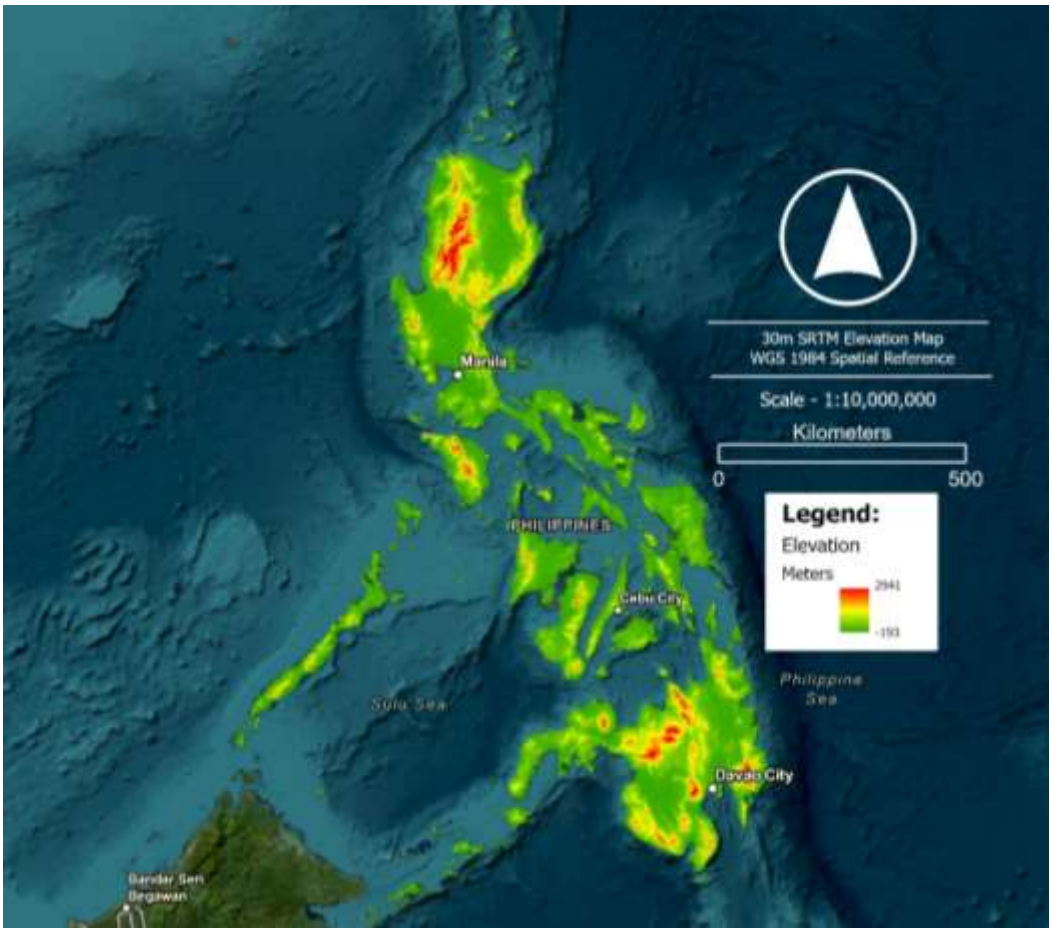

Figure 2.2 Relief map of the Philippines

The lower montane forest is most commonly referred to as the pine forest. Benguet pine (*Pinus kesiya)* (which was treated conspecific with *Pinus insularis*) and Mindoro pine (*Pinus merkusii)* are two types of pine trees that thrive in the Philippines. The Benguet pines flourish in the high mountains of the Cordillera Administrative Region, where altitudes range from 700 to 1,800 meters (Figure 2.3). *Pinus insularis* and *Pinus merkusii* are found at elevations ranging from 500 to 1,500 masl in Zambales, but Mindoro pine is found scattered in as low as 60 masl. In Mindoro, a pure stand of *Pinus merkusii* grows at elevations ranging from 500 to 1,500 masl (Whitford, 1911; DENR - FMB, 2011).

Figure 2.3 Pine forest ecosystem in Baguio City, Philippines

The tropical upper montane forest, also known as the mossy or cloud forest, occurs on mountains above 1,000 masl, with upper limits varying depending on the locality and height of the mountains. Mossy or cloud forest comprises rugged ridges, canyons, shallow soil, landslips, and exposed rocks (Whitford, 1911). In general, the climatic conditions are extremely wet, with high exposure to winds. As a result, the vegetation is usually stunted, and the trees are frequently twisted (Figure 2.4). The trunks and branches of trees are typically covered with mosses, giving rise to the name "mossy forest" (DENR - FMB, 2011). Dwarfed trees found in this forest are *Dacrydium and Poducarpus spp., Eugenia spp., Tristania decorticates, Leptospermum ambionense, Decaspermum spp., Quercus spp., Myrica spp., Englehardtia spicata, Acronuchia laurifolia, Symlocos sp.* (Whitford, 1911; DENR - FMB, 2011). *Lithocarpus jordanae, L. luzoniensis, L. woodii* are other common oaks (Fernando & Cereno, 2010).

Figure 2.4 Mossy forest of Mt Pulag, Kabayan, Benguet

The subalpine forest is only found in the peak of Mindoro Island's Mt Halcon-Mt Sialdang range, an elevation range of 2,470 – 2,587 masl. The soil is shallow, acidic, and nutrient deficient, resulting in open vegetation. Small and woody dicots dominate the vegetation in subalpine forests (DENR - FMB, 2011). Unlike Mt Halcon, the summits of Mt Pulag and Mt Akiki are dominated by grasses, which continue till the rolling terrain, gentle slopes, and plateaus (Fernando & Cereno, 2010). In Mt Pulag, dwarf bamboo *(Yushania niitakayamensis),* locally known as *útod,* is also present other than grasses and sedges (Figure 2.5). During the wet season, mini marshes occur on these grasslands; during the dry season, they become susceptible to fires (Fernando & Cereno, 2010).

Figure 2.5 Grassland summit in Mt Pulag, Kabayan, Benguet

2.3. The importance and threats to tropical montane forests

TMFs are crucial in providing various ecosystem services. These services include a source of clean water (Martínez et al., 2009), a host of biodiversity richer than lowland forest (Kappelle, 2004; Wallis et al., 2017), a large quantity of carbon stored on steep slopes (Spracklen & Righelato, 2014) and soil erosion prevention (Brenning et al., 2015). Unfortunately, TMFs are also prone to several threats (Paulick et al., 2017).

Humans have become more pervasive and abusive in resource consumption, and the rapid changes in land use have resulted in the loss of forest cover (Cronin et al., 2014). As mentioned in Chapter 1, between 2000 and 2010, agricultural land increased by at least 6 million hectares per year in exchange for more than 7 million hectares of forest (FAO, 2016). Global climate change also affects the climate patterns in TMF, subsequently affecting its forest composition (Ray, 2013; Eller et al., 2020). The loss of natural landscape structure in a TMF may cause fires that may destroy other areas of the environment (Ray, 2013). In the Philippines, deforestation and forest degradation strain the country's remaining forest cover

(Avtar et al., 2020). In 2015, the forest cover of the Philippines was only 23% or 7 Mha (Pulhin et al., 2020). Literature points out land conversion for agriculture and habitation, undervalued environmental services, overexploitation, and natural occurrences such as fire and the presence of pests and diseases as causes of deforestation and degradation (Lasco & Pulhin, 2003; Miettinen et al., 2014; FAO, 2015; Hu et al., 2021; Kowaal, 1966; Philippine Statistics Authority, 2020). The Cordillera Administrative Region (CAR), which serves as a watershed zone for surrounding low-lying regions in North Luzon, faces the same fate, with 300 hectares of forest reserve estimated to be lost each year (Walpole, 2010).

2.4. Application of RS and ML to improved assessment of TMFs' deforestation and land conversion

The ecological significance of forests has always been of interest to many as the rate of deforestation and its causes are still alarming (Liu et al., 1993). Forest evaluation necessitates accurate forest information, which is frequently unavailable in TMFs. Remote sensing (RS) is a very effective method for addressing this issue (Ochego, 2003).

RS provides an opportunity to analyze and monitor deforestation, degradation, and fragmentation. It enables us to work at varying scales (i.e., kilometer to centimeter spatial resolutions). Remotely sensed data could be obtained regularly, allowing us to monitor forest resources in real time, which is extremely useful for monitoring natural calamities such as forest fires. Because RS data provides synoptic coverage, information can be acquired even in difficult-to-reach areas. As a result, RS is one of the most effective means of assessing and monitoring forest resources in TMFs. However, it is crucial to know that RS does not replace field surveys but instead supports them (FAO, 2007). dos Santos et al. (2014) summarize the benefits and limitations of remote sensing for forest studies (Table 2.1). RS, particularly time series analysis, has seen a significant advantage in detecting deforestation and land conversion globally (Stone et al., 1991; Biggs et al., 2008; Reiche et al., 2018). Ochego (2003) used Landsat TM to detect forest loss in Kenya with an unsupervised classification method. Buchanan et al. (2008) and Masum et al. (2017) used a similar method to identify conservation priority but with classification. Elhag et al. (2021) used Landsat-derived vegetation indices, including the Normalized Difference Vegetation Index (NDVI) and Enhanced Vegetation Index (EVI) along with MODIS to monitor and record changes in vegetation cover across

Greece from 1995 to 2015. Richards & Friess (2016) identified deforestation in Southeast Asian mangrove regions from 2000 to 2012 by categorizing patches connected to direct deforestation causes (aquaculture, rice-dominated arable, oil palm plantation, urban and other terrestrial forests). Apan et al. (2017) analyzed the rate and extent of forest loss in the Philippines' terrestrial protected areas from 2000 to 2012 using Hansen et al. (2013) high-resolution global maps of forest cover data. As a result, the study could distinguish forest changes in the period by classifying the map as loss (1) or no loss (0). Perez et al.'s (2020) use of time series analysis of Landsat and MODIS satellite imagery from 2001 to 2018 fully justified the forest cover change in Northern Luzon.

Table 2.1 Benefits and limitations of remote sensing data to forest studies.

Products	Description	Benefits	Limitations	Uncertainty
Optical remote sensors	• Use visible and infrared wavelengths to measure spectral indices and correlate to ground-based forest biomass measurements (Examples: Landsat, AVNIR/ALOS, HRV/SPOT, MODIS)	• Satellite data routinely collected and available on regional and/or global scale • Regionally and/or globally consistent	• Limited ability to develop good models for tropical forests • Spectral indices saturate at relatively low C stocks • Can be technically demanding	High
Very high resolution optical remote sensors	• Use very high-resolution images to measure tree height and crown area and allometry to estimate biomass stocks (Examples: 3D digital aerial imagery, IKONOS, QuickBird)	• Reduce time and cost of collecting forest inventory data • Reasonable accuracy • Excellent ground verification for deforestation baseline	• Only cover small areas (10 000s ha) • Can be expensive and technically- demanding • No allometric relations based on crown area are available	Low to medium
Radar remote sensors	• Use microwave signal to measure forest vertical structure (Examples: ALOS/PALSAR-2, RADARSAT-2, COSMOSkyMed, TanDEM/TerraSAR-X)	• Some satellite data are generally free • Can be accurate for open or sparse primary forest and secondary succession	• Less accurate in complex canopies of mature tropical forests because signal saturates • Mountainous terrain also increases the number of errors • Can be expensive and technically- demanding	Medium
Laser remote sensors	• LiDAR uses laser light to estimate forest height/vertical structure (Examples: Structure and biomass 3-D satellite system combines Vegetation canopy LiDAR (VCL) with horizontal imager)	• Accurately estimates full spatial variability of forest carbon stocks • Potential for satellite-based system to estimate global forest carbon stocks	• Airborne-mounted sensors only option • Requires extensive field data for calibration • Can be expensive and technically- demanding	Low to medium

While countries increasingly monitor forest cover change using RS, it is vital to have field observations to accurately identify the land changes (Romijn et al., 2015). Misrepresentation of forest cover change in forest change mapping is likely, leading to inefficient policy action and, in some cases, increased illegal logging (Ahrends et al., 2021). Despite this interest, there has yet to be a consistent method of mapping the deforestation rate based on the reviewed literature. Interestingly, various developments in forest mapping have significantly increased to accurately assess the deforestation rate. The improvements made in forest assessment are as follows:

- inclusive mapping with the community (Galido-Isorena, 2011);
- collaboration with the government sector of the country of interest (FAO, 2010);
- the use of constantly improving satellite and airborne sensors to include analysis and methods (De Sy et al., 2012); and,
- the integration of artificial intelligence, primarily ML, for improved forest classification (Xu et al., 2016).

2.5. The implication of ML for forest assessment

Machine learning (ML) is a subset of Artificial Intelligence. ML is a robust empirical approach for regression or classification (supervised or unsupervised) of various systems. Such systems can be massively multivariate, with a few to thousands of variables (Lary et al., 2016). ML is concerned with methods and strategies that allow computers to "learn" by example, which is especially valuable for predictions (Lary et al., 2018).

RS necessitates processing techniques for correct analysis. With ML at their fingertips, the RS community could fine-tune components such as pre-processing, segmentation, and classification (Ma et al., 2019). Several studies have shown that various ML algorithms provide higher accuracy than traditional parametric classifiers, particularly for complex data with a high-dimensional spatial characteristic (Maxwell et al., 2018). Many ML algorithms have been developed for various applications, yet their results vary substantially. As a result, locating suitable ML algorithms for your research is challenging (Sarker, 2021).

The artificial neural network, the first algorithm to detect patterns and forms, was created in 1958. Since its inception, the development of ML has grown in popularity (Liu et al., 2018; Sarker, 2021). Figure 2.6 shows the trend of the classical, ML and deep learning (DL) emergence in ecological studies. ML algorithms can be classified as supervised or unsupervised, and some authors classify other algorithms as reinforcement as they learn data and discover patterns from their surroundings (Alloghani et al., 2020). This review will concentrate on supervised learning, commonly used in forest assessments (Lapini et al., 2020). Studies such as the paper of Olaode & Todd (2014) provided a rigorous analysis of unsupervised learning algorithms for special applications.

Support vector machine (SVM) and Random Forest (RF) are two of the most widely utilized ML algorithms in forest assessment nowadays (Ma et al., 2019). SVM uses higher-dimensional space to gain improved prediction power (Mantero et al., 2004) or offers good results with a small number of training data (Mountrakis et al., 2011). On the other hand, RF is an ensemble learning classification method that decides on the aggregated classification result from multiple weak classifiers (Lapini et al., 2020). It is noted in the study of Belgiu & Drăgu (2016) that RF has high accuracy in classifying land uses.

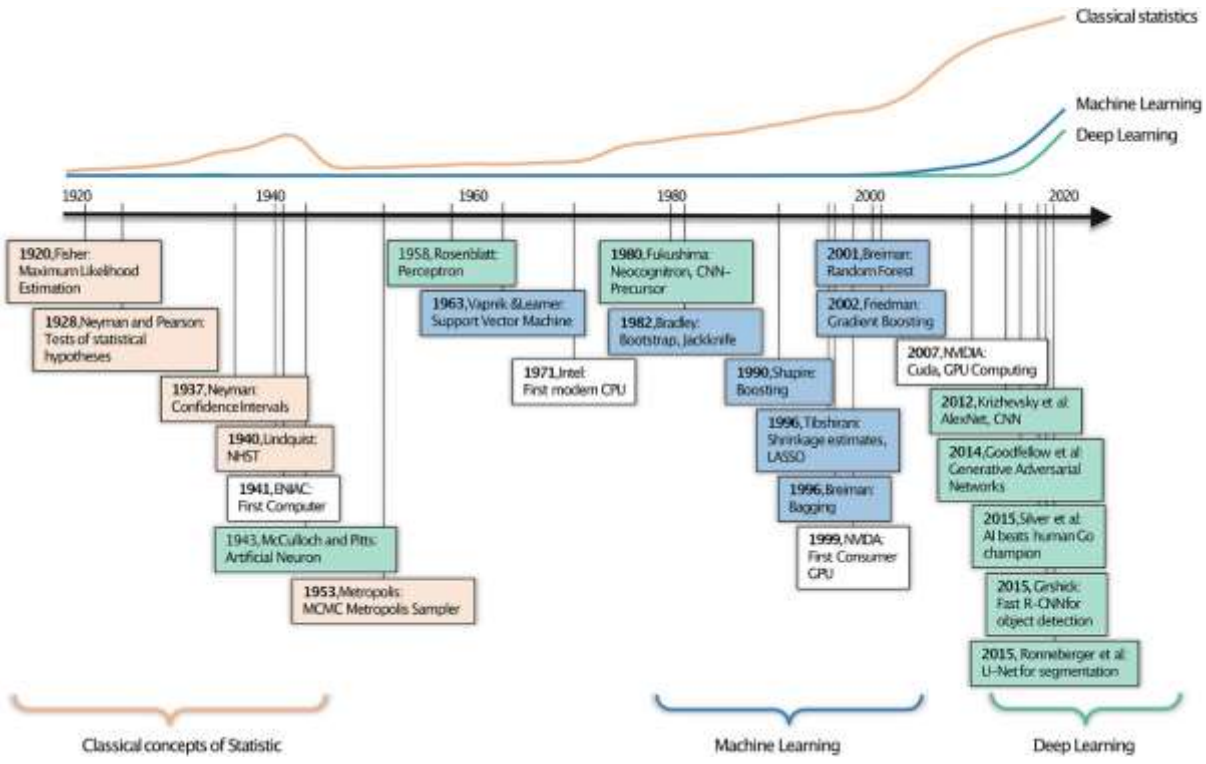

Figure 2.6 The three eras of statistical learning from 1920 to the present (Pichler & Hartig, 2023)

DL, such as the Artificial Neural Network (ANN), is also a standard algorithm for geoscience problems (Lary et al., 2015). ANN can estimate the non-linear relationship between the input data and the intended outputs. ANN has been shown in multiple studies to be more accurate than traditional classification methods (Yuan et al., 2009).

DL and ML were powerful in classification and regression investigations for forests and ecological settings however Hütt et al. (2016), Shivakumar & Rajashekararadhya (2018), and Norovsuren et al. (2019) found that the classic Maximum Likelihood Classification (MLC) was equally superior. MLC is a typical classifier that requires a normal or near-normal spectral distribution of reach features of interest and an equal prior probability among classes, which means that the MLC assumes a given pixel belongs to a specific category (Li et al., 2011).

The accuracy of the traditional, ML, and DL in classifying land use land cover change in TMFs have never been compared. A comparison analysis of the four ML algorithms is an interesting concept for this study. Likewise, the trend of artificial intelligence application and how these techniques were applied to remote sensing for studying TMF would be another valuable topic of future research.

2.6. Successional stages and regeneration of TMF: Mapping and monitoring

The successional stages in the forest have profound biophysical, biological, and biogeochemical implications in the terrestrial environment (Liu et al., 2008). In earlier studies by Foody & Curran (1994) and (Yanasse et al., 1997), there were up to six forest succession stages; however, three (3) stages of Secondary Succession (SS) with non-forest (NFO) and mature/old-growth forest (OGF) are now accepted: Initial (SS1), Intermediate (SS2), and Advance (SS3) (Lu, 2005; Li et al., 2011; Bispo et al., 2019). Identifying forest successional stages is immensely useful for reducing the uncertainty of carbon emission and sequestration measurements and determining their effect on soil fertility, degradation, and restoration (Lu, 2005). The old-growth forest is believed to be carbon neutral, but the secondary forest is partially accountable for the "missing sink" in the global carbon budget if it is incorrectly characterized (Brown & Lugo, 1990; Helmer et al., 2000).

Mapping land cover and forest successional stage using satellite data in the tropical regions was primarily done at mildly flat or lower elevations. Researches on TMFs are affected

by the challenges imposed by the complexity of the terrain and the variability of vegetations within them (Helmer et al., 2000; Mukul et al., 2016; Perez et al., 2020; Ferrer Velasco et al., 2022). A systematic search at Scopus search engine using "The Philippines," "Succession," "Forest" keywords coupled with "*" wild card revealed 149 hits from 1995-2021, with 0 studies that focus on forest succession in the Philippines. This result demonstrates that, unlike other tropical regions, forest succession studies in the Philippines have not been thoroughly investigated (Espírito-Santo et al., 2005; Li et al., 2011; Caughlin et al., 2021). According to the literature reviewed, no standard method for delineating successional stages exists. As a result, numerous efforts have been made to define forest succession through field measurements (Lu, 2005; Liu et al., 2008) and RS (Song et al., 2002; Vieira et al., 2003; Liu et al., 2008; Li et al., 2011; Schwartz et al., 2017; Caughlin et al., 2021).

Field-measured parameters such as vegetation age, basal area, diameter breast height (DBH), and canopy height were utilized to define forest succession (Moran et al., 1994; Vieira et al., 2003). Lu et al. (2003) used the ratio of tree biomass to total biomass. However, this measurement is limited by the typically labor-intensive process of calculating biomass (Moran et al., 1994). Others (Pettorelli et al., 2005; Requena-Mullor et al., 2018) utilized vegetation indices (VI), such as the Normalized Difference Vegetation Index (NDVI), to simplify the distinction of forest succession. Recent initiatives have utilized multidate satellite imagery to determine the age of a forest and relate it to its stage of succession (Helmer et al., 2000; Espírito-Santo et al., 2005; Liu et al., 2008; Caughlin et al., 2021). Although VIs can be determined from satellite reflectance, they lack a direct physical interpretation of forest succession, and their relevance to forest structure during regrowth requires further study (Frolking et al., 2009).

A novel approach by Bispo et al. (2019) used canopy height derived from TanDem-X SAR interferometry. He used the height to map out forest successional stages in the Brazilian Amazon. He discovered a strong association with extremely low uncertainty in the reference data. Further, he concluded that forest height could be utilized to detect distinct stages of forest succession using SAR interferometry. Ghosh et al. (2020) discovered that forest height could be approximated by combining Sentinel-1 Interferometry with the integration of optical imagery-derived vegetation indices and Random Forest and Symbolic Regression ML techniques. Mapping successional stages through forest height in tropical areas is very rare (Berveglieri et al., 2016). Most studies used it in mangrove forests, with only a fraction

attempting it in tropical forests (Aslan et al., 2018; Ghosh et al., 2020). Classifying RS images using ML algorithms has clearly delineated forest succession (Li et al., 2011).

Given the scarcity of researches on forest succession in the Philippines' TMFs, this study's innovative attempt is to delineate forest succession using available spaceborne remote sensing data and ML.

2.7. Synthetic aperture radar and ML application to TMF for biomass and carbon density estimation

Global concern regarding greenhouse gas accounting has prompted efforts to accurately measure forest carbon stock or the total amount of carbon stored in an environment (e.g., above-ground and below-ground biomass). It is widely acknowledged that tropical rainforests capture more carbon than other terrestrial forests worldwide (Figure 2.7) (González-Jaramillo et al., 2018; Wallis et al., 2019). In addition, Spracklen & Righelato (2014) outlined the significance of TMFs in REDD+. They discovered that steep slopes of TMFs contain a substantial volume of biomass. However, compared to lowland tropical rainforests, many critical processes related to carbon cycling remain unclear (Anderson-Teixeira et al., 2016). Similarly, there is a lack of knowledge about carbon stocks and density in the Philippines and other Southeast Asian countries' montane environments (Soh et al., 2019). Carbon density refers to the concentration or amount of carbon per unit area. Given the conditions whereby forest degradation pressure remains and will likely continue, sustained forest assessment in these areas is necessary (Miettinen et al., 2014).

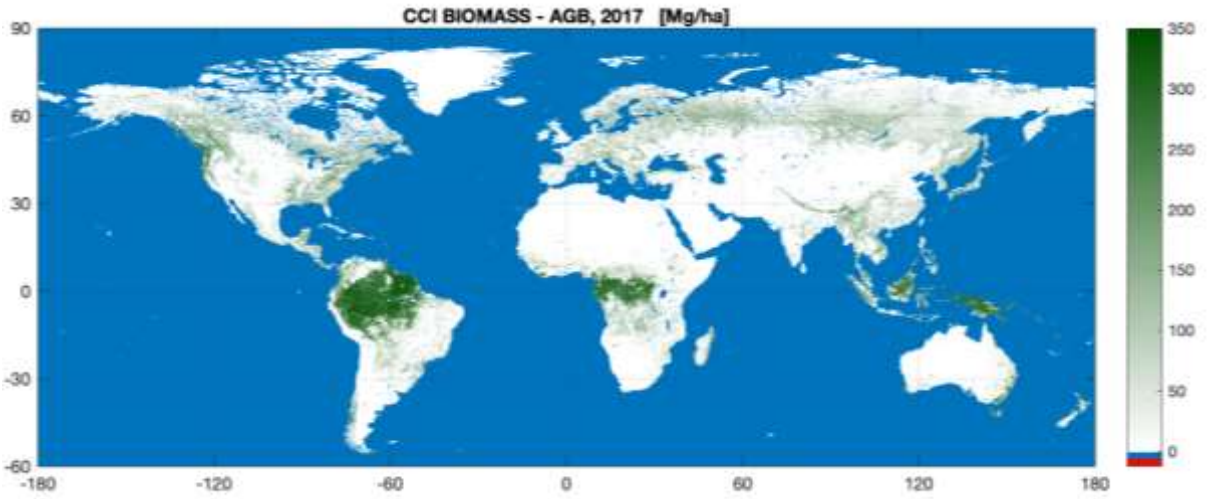

Figure 2.7 The world's above-ground biomass map in 2017 (European Space Agency, 2019)

TMFs have a difficult terrain that hinders field measurements for biomass assessment (González-Jaramillo et al., 2018). Thus, RS, which can monitor and map areas remotely, has been utilized for numerous mountain forest analyses (Timothy et al., 2016). Several studies highlighted its synergy with RS to categorize land use/cover (Moumni et al., 2021) and collect data on above-ground biomass (Santi et al., 2020).

Some studies approach the measurement of above-ground biomass using airborne light detection and ranging (LiDAR) data, which may be expensive and not all present in developing countries (González-Jaramillo et al., 2018; Loh et al., 2020). Optical sensor satellite data are robust in multidate analysis but possess frequent cloud coverage (Wallis et al., 2019). Unmanned aerial vehicle (UAV) was used to tackle cloud difficulties inherent in space-borne optical imagery (González-Jaramillo et al., 2019). However, the method's limitations in terms of cost and technical expertise in operating the equipment are an issue for forest evaluation. Utilizing Synthetic Aperture Radar (SAR), which can see through clouds, is an additional emerging method for assessing forest carbon stock (Timothy et al., 2016). The literature demonstrates that SAR backscatter correlates with forest structure and can be utilized to estimate the AGB of TMFs (Castel et al., 2000; Liao et al., 2019; Rodríguez-Veiga et al., 2017; Joshi et al., 2015). Longer wavelength (L- and P-band) and cross-polarized (HV and VH) sensor configurations should be considered when using SAR data to estimate AGB measurements (Rodríguez-Veiga et al., 2017). Longer SAR wavelengths are more vital to

penetrate the surface and canopy cover, and cross-polarized sensor configurations are sensitive to scattering factors within a tree canopy (Mitchard et al., 2011).

A growing number of studies in the Philippines use SAR data backscatter to estimate AGB in mangrove forests (Castillo et al., 2017; Singh et al., 2017; Argamosa et al., 2018; Makinano-Santillan et al., 2019). SAR data has also been used to study the AGB of other habitats, including the Northern Sierra Madre Natural Park and Mt. Apo Natural Park (Monzon et al., 2015; Washington-allen, 2015). Only Avtar et al. (2020) attempted to investigate the efficacy of SAR data in calculating AGB in Ifugao's upper montane environment. The forest stock evaluation of the various vegetation zones in the elevation gradients of TMF in CAR is still inadequate. Its function in the global carbon cycle has never been evaluated. Using SAR data to estimate AGB could be an innovative method for assessing this environment.

Gibbs et al. (2007) note that there is no standard approach for assessing forest carbon stocks. Rodríguez-Veiga et al. (2017) state that the AGB-derived information from SAR data is uncertainty. Validation of its data from field-measured AGB is essential to reduce the ambiguity in the outcome (Gibbs et al., 2007).

There are two methods for measuring forest biomass on the ground: destructive and non-destructive. The destructive method can precisely measure the carbon biomass, but it requires harvesting all tree parts, which is time-consuming, expensive, and sometimes illegal (Yuen et al., 2016). The alternative is to use regression equations (derived from a previously felled sample of trees) that estimate biomass through observable predictors such as tree diameter or height (Banaticla et al., 2007). Allometric equations are fundamental for the non-destructive estimation of vegetation (Kuyah et al., 2012). The most common allometric equations for tropical forest trees are the ones proposed by Brown (1997), and the improved Chave et al. (2014). In the Philippines, Banaticla et al. (2007) reviewed the applicability of current equations in the tropical tree plantation species common in the country. Mangrove allometry was also taken into account by Gevana & Im (2016). In the highlands, the work of Napaldet & Gomez (2015) showed an allometry equation specific for *Pinus kesiya*.

Species-specific allometry can provide accurate carbon stock analysis (Kuyah et al., 2012). The lack of specific equations for some tree species in the Philippines necessitates the utilization of generic equations for predicting the biomass of individual trees and other

vegetation (Banaticla et al., 2007). Brakas & Aune (2011) and Avtar et al. (2020) utilized generic allometry equations in their study. Researchers must use caution when employing generic equations because they could overestimate the actual biomass of a tree. Consequently, the requirement to evaluate its relevance to species and sites may reduce uncertainty (Banaticla et al., 2007).

2.8. Summary

The following research gaps were identified in order to comprehend deforestation, successional stages, biomass, and carbon density of the three vegetation types in Benguet's TMF:

- There is a lack of defined research directions that could enable the long-term or sustainable use of the world's TMFs (Soh et al., 2019). Deforestation is still prevalent in relation to the continuous need for space for human settlements and agriculture. Deforestation is projected to contribute between 17 and 20% of global greenhouse gas (GHG) emissions (IPCC, 2007). These deforestations mainly occur in tropical forests, abundant in many developing countries, including the Philippines (Carandang et al., 2013). Because global deforestation continues to grow, it is imperative that we understand the rate of deforestation and determine the significance of carbon stocks in TMFs (Ray, 2013).

- Investigation of TMFs is not intensively considered unlike the tropical lowland forests (Anderson-Teixeira et al., 2016; Paulick et al., 2017), especially in South East Asia (Soh et al., 2019). The spatial and temporal evaluation of TMFs may lead to the definition of their successional growth dynamics and a greater comprehension of the carbon cycle (Paulick et al., 2017).

- Carbon studies, including the measurement of above-ground biomass and other carbon-related metrics along the elevation gradients of TMFs, are scarce (Spracklen & Righelato, 2014). Numerous environmental research and conservation efforts to reduce global warming rely on the precise evaluation of such defining studies (González-Jaramillo et al., 2019).

- The REDD+, or the reducing emissions from deforestation and forest degradation and the role of conservation, sustainable forest management, and enhancement of forest carbon stocks in developing countries, and the UNFCCC policies on issues relating to reducing emissions from deforestation and degradation in developing countries are among the initiatives that require carbon measurements (Carandang et al., 2013).

- Remote sensing (RS) demonstrates strength in approaching temporal and spatial TMFs assessment (Timothy et al., 2016). The ability of RS to monitor and study forest degradation and estimate forest biomass without requiring fieldwork has long been its main advantage (González-Jaramillo et al., 2018). Utilizing DL and ML algorithms with a large quantity of RS data can expedite the detection of patterns and their association with forest parameters for enhanced assessment.

The next Chapter outlines the overarching technique and approaches employed to accomplish the objectives outlined in Chapter 1, namely Objectives 1 to 3.

CHAPTER 3: RESEARCH METHODS

3.1. Introduction

The preceding chapters established the foundation for understanding the importance of studying the tropical montane forest (TMF) in the Philippines and its unique environment. Deforestation, successional stages, carbon stocks, and density were all discussed in detail in Chapters 1 and 2. Further, Chapter 2 outlined the current research gaps in TMF studies in the Philippines, highlighting the need for more in-depth investigation into this topic. The study's goals and methods were developed based on these findings. This chapter describes the overarching strategy, design, and methodology used in the study to accomplish the goals of each paper published in this study. The following topics are covered in this chapter: 1) The Study Area; 2) Field Sampling Design; and 3) Summary. A discussion of research methodologies is provided in detail in Chapters 4-7, which corresponds to the stated aim and objectives of this Thesis.

3.2. The study area

Benguet is situated in the northern-central region of Luzon and the southernmost area of the Cordillera Administrative Region (CAR) (figure 6). The month of May through October is the wet season, with the rest of the year being relatively dry. Parao et al. (2016), the average temperature from January to June is between 17.3 and 20.7 degrees Celsius. Mount Pulag, at 2,926 meters above sea level, is the highest point in the province (Doyog et al., 2021). It is geographically situated between 16°11’ and 16°56’ north latitudes and 120°28' to 120°53' east longitude. It has 2,826.59 km^2 area and is bordered by the Mountain Province on the north, Pangasinan on the south, Ifugao and Nueva Vizcaya on the east, and La Union and Ilocos Sur on the west (Cruz et al., 2019).

The elevation gradient in the province leads to the development of three vegetation types: pine forest at 700-1,800 meters (Department of Environment and Natural Resources - Forest Management Bureau, 2011); mossy forest, found at elevations greater than 1,000 meters that have steep ridges, canyons, presence of landslides, exposed rocks, and flora that is typically

stunted, twisted, and covered in mosses, and microclimate is wet, cloudy and windy (Fernando & Cereno, 2010); and, grassland found at the highest peak of Mt Pulag and Mt Akiki which continue down to the rolling terrain, gentle slopes, and plateaus (Fernando & Cereno, 2010).

The province is divided into 13 municipalities, with La Trinidad as the capital (Figure 3.1). According to the 2015 census, Benguet has 444,224 people, accounting for 25.08% of the overall population of the CAR (Provincial Governor's Office - Information Technology, 2020).

Figure 3.1 Location of the study area (Benguet Province, Philippines)

Benguet's temperate climate is excellent for cultivating most vegetables, including carrots, cabbage, potatoes, and celery. Due to the province's extensive cultivation of temperate vegetables, it is the largest vegetable-producing region in CAR, making it the "salad bowl" capital of the Philippines (Piadozo & Fujimoto, 2007). However, the province's high vegetable output bears a greater price. In the province, competing land uses exist. Several forests in Benguet and adjacent provinces have been cleared for vegetable farms. These agricultural

activities extend even into protected forest areas (Manzano, 2019). Unprecedented urban development is also impacting the province's pristine forests. In addition, forest fires in the province are causing substantial forest destruction and disturbance. PSA (2020) presented that around 21,242.40 hectares of forests were significantly destroyed in CAR from 2008-2018. In 2020, almost 900 hectares of pristine forest lands in several municipalities in Benguet were destroyed due to forest fires (Dionisio & Agoot, 2020).

The selection of the study area is crucial because it serves as one of the foundations on which the entire investigation is established. The area must correspond with the research objectives and provide a representative sample of the phenomenon being investigated. Hence, the following considerations are taken into account for selecting the study area:

- The prevalence of three vegetation zones in the province, namely pine forest, mossy forest, and grassland summit, has received little consideration in the scientific community. Its destruction due to land-use conversion is imminent; consequently, evaluating these three distinct zones requires greater consideration.

- TMFs present challenging topographical environments that have discouraged scientific exploration. In CAR, Benguet stands out as a frequently visited province by tourists, hence a higher level of development. Therefore, research access in this province is more reliable, facilitating more opportunities for exploration and research.

- The municipalities and city take adequate measures to ensure safety and order, contributing to the area's well-deserved reputation for peace. The presence of military installations also contributes to the security.

3.3. Field sampling design

This study, particularly Objectives 2 and 3, employed a stratified random sampling approach. The research area has been divided into three strata: pine forest, mossy forest, and grassland summit. Generally, the pine forest can be found in every part of the province, whereas the mossy forest and grassland summit can be found at the highest elevations of Kabayan,

Benguet. Chapter 5 details the specific methodology and sampling design for Objective number 1.

The approach described by Pearson et al. (2005) was used to compute the number of samples contained within each stratum of the study (Equation 1). Based on the findings of Lasco et al. (2005); Lasco et al. (2008); Lasco & Pulhin (2003); Avtar et al. (2020); Doyog et al. (2018) Jeyanny et al. (2014), the calculation was completed with a desired precision of 80% or 20% allowable error, a t value of 2 at 95% confidence level, and a 10 m radius sampling plot (Table 3.1). As a result, 34 samples were taken from pine forests, 12 from mossy forests, and 7 from grassland summit.

$$n_h = n\ x\ \frac{N_h\ x\ s_h}{\sum_{h=1}^{L} N_h\ x\ s_h} \qquad \textit{(Equation 1)}$$

Where:

n	=	the total number of plots,
n_h	=	the number of plots in stratum h,
N	=	the number of sampling units in the population,
N_h	=	the number of sampling units in stratum h,
s	=	the standard deviation,
s_h	=	the standard deviation in stratum h.

Additional plots representing various land use and land cover types were included for Objectives 2 and 3. These supplemental plots were included to ensure that the field data obtained is representative of a wide variety of conditions, to enhance the reliability of the regression model, mitigate the possibility of overfitting, and to yield a model with practical application in a variety of scenarios (Sarstedt & Mooi, 2018; Hastie et al., 2009).

Table 3.1 Recorded carbon pool in pine forest, mossy forest and grassland ecosystem in the Philippines and other South East Asian country.

Vegetation Type	Area	Year	Total C in Biomass (tC/ha)	Reference
Grassland	Philippines (General)	2000	6	Lasco et al. (2008)
	Leyte Philippines *(Imperata cylindrica)*	1999	8.9	Lasco et al. (2005)
	Philippines *(Saccharum spontaneum)*	1999	15.2	
	Standard deviation		**4.70**	
Mossy Forest	Malaysia	2018	253.02	Jeyanny et al. (2014)
	Philippines	2000	183.8	Lasco & Pulhin (2003)
	Ifugao, Philippines	2020	126.14	Avtar et al. (2020)
	Standard deviation		**63.53**	
Pine Forest	Philippines	2000	90.1	Lasco & Pulhin (2003)
	Sagada, Philippines	2018	411.68	Doyog et al. (2018)
	Pantabangan watershed, Philippines	2005	181.22	Lasco et al. (2005)
	Standard deviation		**140.67**	

3.4. Considerations for the field data collection

The field survey team consists of the author, the primary supervisor, and two staff members with administrative and forestry experience (Figure 3.2). The team was also accompanied by monitoring staff and park rangers from the Mt. Pulag Protected Landscape (MPPL) park ranger offices in Tabayo and Babalak, Kabayan Benguet, and personnel from the Baguio City Environment and Parks Management Office (CEPMO).

Figure 3.2 The field survey team

Several factors were considered during field data collection. First, proper coordination has been taken to government offices for the conduct of the study. A letter requesting approval of the thesis data collection has been sent to the Department of Environment and Natural Resources – Cordillera Administrative Region (DENR – CAR). Similarly, the thesis and purpose of the data collection were presented to the Mount Pulag Protected Landscape – Protected Area Management Board (MPPL-PAMB) on 4 November 2023 via online conference. The author was provided with PAMB resolution number 24 series of 2022, which authorized data collection in the MPPL. In addition, data collection was also coordinated with the City Mayor of Baguio through the City Environment and Parks Management Office (CEPMO), the Superintendent of the Philippine Military Academy (PMA), MPPL – Protected Area Superintendent (Figure 3.3), and the Watershed and Water Resources Research Development and Extension Center – Ecosystems Research and Development Bureau (WWRRDEC – ERDB).

Figure 3.3 Courtesy call by the field survey team to the MPPL-Park Superintendent

Accessibility to the plot is crucial, with locations near roads or paths given preference, and extremely steep slopes were avoided for safety reasons. The plot's location is determined by locating a tree as the center of the plot and recording its coordinates with a Garmin etrex10 handheld GPS device. A layout of the 10-m radius plot was laid, subdivided into four quadrants (Figure 3.4).

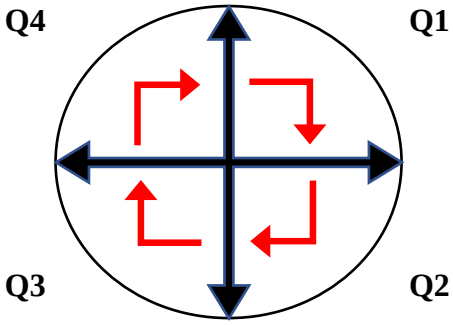

Figure 3.4 The 10-m radius plot layout divided into four quadrants

All trees, including the saplings/wildlings, with a circumference equal to or greater than 5 cm were recorded, and their diameter at breast height (DBH) was measured at 1.3m above the ground using a diameter tape. Height measurements were taken using a clinometer and laser

finder. All data were recorded in the field data sheet. Only living trees are considered during the data collection. Three readings of the densiometer were taken at the center of the plot to estimate the canopy cover. The FAO national forest inventory guidelines for measuring tree height and DBH are followed (FAO, 2016). Measurements of individual tree data were systematically done and graphically presented in Figure 3.5.

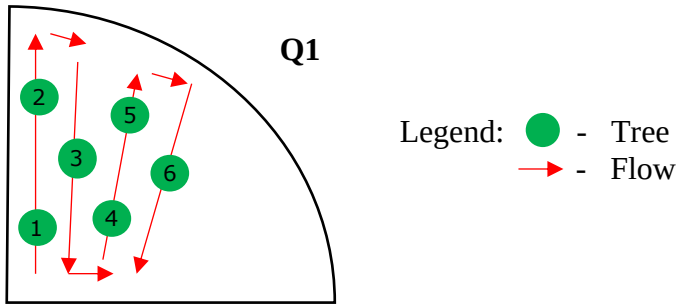

Figure 3.5 The systematic collection of vegetation parameters within the study plot's quadrat

After data collection was completed in one plot, the next was established approximately 50 meters away from the first plot. To save time and resources, the plot's locations of plots were selected in relatively flat terrain and easy access (Figures 3.6-3.8). Personnel from local government agencies, such as the CEPMO, were requested to guide the team during data collection on the ground.

Figure 3.6 Data gathering in a pine forest in Baguio City with CEPMO personnel

Figure 3.7 Lay outing of plot in a mossy forest in Mt Tabeyoc, Kabayan, Benguet

Figure 3.8 Data collection on the dwarf bamboo (*Yushania niitakayamensis*) at an elevation of 2,867 meters on Mount Pulag

3.5. Satellite imagery acquisition

The majority of satellite imagery used in Chapters 5-7 came from Sentinel-1 (Synthetic Aperture Radar (SAR) data) and -2 (Optical Sensor data). The succeeding chapters describe the dates and numbers of Sentinel-1 and -2 imagery. Likewise, each technical chapter of this thesis contains a comprehensive discussion of additional satellite imagery to supplement the analysis.

The Sentinel-1 data were acquired at the Alaska Satellite Facility (ASF) of NASA Earthdata, specifically the Earth Observing System Data and Information System (EOSDIS) of NASA. The imagery came from the Sentinel-1 mission, which consists of two polar-orbiting satellites (Sentinel-1A and Sentinel-1B) equipped with a C-band SAR instrument operating at a center frequency of 5,405.5 GHz. It functions day and night and acquires images regardless of illuminating and weather conditions, with a 250 km swath at 5 m to 20 m spatial resolution and a 6-day revisit period (Filipponi, 2019). The standard format for Sentinel-1 data is Ground Range Detected (GRD) for this study. They were acquired using Interferometric Wide Swath. The polarizations have been captured in the VV and VH in descending orbital directions. The

pixel dimensions and resolutions are measured in 10 meters for range and azimuth directions (Table 3.2).

The Sentinel-2 mission consists of two satellite configurations (Sentinel-2A and Sentinel-2B) in polar sun-synchronous orbit. Sentinel-2 data provides a combination of capabilities suitable for various applications (Meygret et al., 2009). The imagery has a 290 km wide field of view, a 5-day high revisit, a high spatial resolution of 10m, 20 m, and 60 m, and multispectral imagery (13 bands in the visible and short-wave infrared spectrum). The Sentinel-2 data were accessed through the Copernicus Open Access Hub in Bottom-of-Atmosphere (BOA) and level 2A format. Cloud cover is 0-30% and is collected in descending orbital with a 100 x 100 m tile dimension and a 290 km swath width. Bands 2-8a and 11-12 were considered for the deforestation, successional stages mapping, and carbon stocks estimation. B1, which corresponds to coastal aerosol; B9, which corresponds to water vapour; and B10, which corresponds to cirrus clouds, were the excluded bands in this study (Table 3.2).

Table 3.2 Principal features of the Sentinel-1 and -2 imagery

Sentinel 1 features	
Band	C (center frequency of 5.405 GHz)
Mode	Interferometric Wide Swath
Product Type	Ground Range Detected
Pixel Spacing	10 m in the ground resolution
Orbit	Descending
Polarization	VV & VH
Swath Width	250 km
Incidence angle (°)	29.1°–46.0°
Map projection	WGS84(DD)
Sentinel 2 features	
Bands (10 m resolution)	B2 – Blue, 492.4 nm (S-2A), 492.1 nm (S–2B) B3 – Green, 559.8 nm (S-2A), 559.0 nm (S–2B) B4 – Red, 664.6 nm (S-2A), 665.0 nm (S–2B) B8 – NIR, 832.8 nm (S-2A), 833.0 nm (S–2B)
Bands (20 m resolution)	B5 – Vegetation red edge, 704.1 nm (S-2A), 703.8 nm (S–2B) B6 – Vegetation red edge, 782.8 nm (S-2A), 739.1 nm (S–2B) B7 vegetation red edge, 782.8 nm (S-2A), 779.7 nm (S–2B) B8a – narrow NIR, 864.7 nm (S-2A), 864.0 nm (S–2B) B11 – SWIR, 1613.7 nm (S-2A), 1610.4 nm (S–2B) B12 – SWIR, 2202.4 nm (S-2A), 2185.7 nm (S–2B)
Swath width	290 km
Tile size	100 x 100 km
Cloud cover	0–30%
Map projection	WGS84(DD)

3.6. Satellite imagery processing

The Sentinel-1 and -2 data processing was primarily done in the Sentinel Application Platform (SNAP) software 2.80 (SNAP Development Team, n.d.).

The Sentinel-1 GRD imagery follows the pre-processing steps proposed by Filipponi (2019). To ensure that the whole study area was captured in the images, SAR mosaic was used. The orbit file was then applied to correct the orbital orientation of the images. Thermal and GRD boundary noise were removed to enhance the images further. Finally, the VV and VH coefficients of the backscattering were converted to sigma nought (σ°). The speckle problem was subsequently addressed by implementating Refined Lee filter. The images were geocoded with SRTM at a 1 sec 30 m resolution, and then linear to decibel (dB) was calculated.

In order to apply a scene classification, atmospheric correction, and subsequent conversion into an ortho-image Level-2A Bottom-of-Atmosphere (BOA) reflectance product, the Sentinel 2 Level-1C Top-of-Atmosphere (TOA) images are run through the Sen2Cor, a prototype processor for Sentinel-2 Level 2A product formatting and processing (Mueller-Wilm et al., 2016). This step was skipped over as most imagery used in this study was obtained from the Copernicus Hub, which provides Sentinel-2 data in L2A format. The bands B5 – B7, B8a, B11 – B12 were resampled to a 10 x 10-meter resolution using a bilinear interpolation method in SNAP software to match the other bands. The imagery was subjected to a subset to get the entirety of the study area. Finally, the clouds were masked using the land-sea masked operation.

3.7. Summary

The study area is Benguet Province, Philippines. The area was chosen because of the following reasons:

- the province's three vegetation types—pine forest, mossy forest, and grassland summit—have been understudied by researchers. As land-use modification threatens its survival, analyzing these three types is crucial;

- the TMFs' challenging topography has hindered scientific research;

- Benguet province is a tourist destination in CAR, and it is under increasing pressure for land development. Research access in this province is more reliable, enabling more accessible exploration and study options; and,

- the area is generally peaceful. The municipalities and city employ appropriate safety and order measures, and the presence of military installations enhances security.

Field sampling was conducted in the province's three vegetation types from December 2022 to January 2023. Stratified random sampling was used in this study, and the radius of the circular sampling plots was set at 10 meters. The calculated number of samples for the pine forest was 34, 12 for the mossy forests, and 7 for the grassland summit. The survey field team, composed of four personnel, was accompanied by MPPL monitoring staff and park rangers, as well as the personnel from CEPMO of Baguio City. In addition, the satellite imagery used to attain Objectives 1-3 were Sentinel-1 and -2 acquired from the Alaska Satellite Facility and Copernicus Open Access Hub, respectively. Appropriate pre-processing steps were employed before the data were subjected to higher analysis. The next chapters presented the details of the other types of satellite imagery used, other pre-processing steps, and how auxiliary variables were created. The pre-processing of Sentinel-1 and -2 images was primarily performed in the SNAP software. Finally, the specific ML and DL techniques employed were discussed in the next sections.

The following chapter, Chapter 4, introduces the first technical chapter that includes the published paper entitled "*Spaceborne Satellite Remote Sensing of Tropical Montane Forests: A Review of Applications and Future Trends*." This published paper will discuss the current state of spaceborne RS applied to TMFs around the world and the future of the RS techniques in TMF research.

CHAPTER 4: PAPER 1 - SPACEBORNE SATELLITE REMOTE SENSING OF TROPICAL MONTANE FORESTS

4.1. Introduction

In Chapter 2, the emphasis was on providing a comprehensive overview of tropical montane forests (TMFs), delving into their distributions, current status, and threats they face. This publication investigates the implications of remote sensing (RS) for evaluating TMFs. In this chapter, the applications of spaceborne remote sensing techniques tailored explicitly to TMFs across the globe were intensely described. While Chapter 2 lays the groundwork by providing an overview of TMFs and introducing RS as a valuable tool, this chapter builds upon that foundation by advancing the discussion. Special emphasis is placed on a variety of factors, including temporal considerations, spatial distribution, journal publication records, methodologies employed, research themes, sensor systems employed, vegetation zones under investigation, urgent research needs, and the most effective techniques. In addition, this chapter investigates the challenges and opportunities associated with applying RS to the conservation and management of TMFs. This publication further provides a comprehensive view of how RS technologies can be optimally utilized to protect these vital ecosystems.

4.2. Published paper

The following page is a version of the article published in *Geocarto International*. The journal is Q1 (i.e., top 25% of journals in the list) under the Geography, Planning and Development, and published by Taylor & Francis with a source normalized impact per publication (SNIP) of 1.26, impact factor (IF) of 3.8 in 2022, and an h-index of 53.

4.3. Summary and links

This chapter presents a systematic literature review that describes the current state of research into using spaceborne RS to study TMFs. It was disclosed that the number of papers published between 1997 and 2021 increased significantly, with extensive studies done in the Americas leaving other countries behind. Due to the rapid degradation of TMF in these less-studied countries, knowledge of TMF dynamics, mainly deforestation, successional stages, and carbon stocks, could be lost in the near future. There is also a knowledge gap pertaining to the location and size of TMFs in these countries that must be addressed. The use of optical sensors with low to medium spatial resolution was favored by researchers (85.76%), while synthetic aperture radar received little attention (12.70%). In order to get the intended outcome from any investigation, it is crucial to carefully select the appropriate spatial resolution of satellite imagery for TMF assessment. The majority of studies have been undertaken in the areas of forestry (42.66%), climate science (11.01%), and disaster management (9.63%). Finally, since RS evolves over time, it is advantageous to employ this technology in TMFs for enhanced assessments. The same holds true for the modernization of statistical and technological tools, including artificial intelligence, the Internet of Things, cloud computing, and machine, and deep learning.

The mapping of deforestation using the fusion of Sentinel-1, -2, and biophysical data is presented in the next Chapter (Chapter 5), along with a comparative evaluation of a traditional classifier, three machine learning algorithms, and a deep learning algorithm for land use land cover classification.

CHAPTER 5: PAPER 2 - DEFORESTATION ASSESSMENT IN A TROPICAL MONTANE FOREST USING DEEP LEARNING AND REMOTE SENSING

5.1. Introduction

In the previous chapter (Chapter 4), a comprehensive and systematic review of spaceborne remote sensing (RS) to tropical montane forests (TMFs) across the globe is discussed. In this chapter, the usage of Sentinel-1 (S-1) and Sentinel-2 (S-2) and their fusion as input for land use land cover (LULC) mapping of Benguet, Philippines, was examined. Three different modelling classifiers—the classic Maximum Likelihood Classifier (MLC), the machine learning algorithms – Random Forest (RF), K Nearest Neighbor (KNN), and KD Tree Nearest Neighbor (KD Tree), and the deep learning approach U-Net were tested to gauge their predictive capabilities in terms of deforestation mapping. Finally, this study characterized the occurrence of deforestation based on proximity factors such as distance from roads, built-up area, agriculture, and waterbody, as well as topographic factors such as elevation, slope, and aspects.

5.2. Published paper

The succeeding page is a copy of the study that was published in a Q1 (top 25% under Computer in Earth Sciences) journal titled *Remote Sensing Applications: Society and Environment* by Elsevier. In 2022, the journal's source normalized impact per publication (SNIP) was 1.32 and its impact factor (IF) was 4.7. Its h-index is 37.

5.3. Summary and links

This chapter (Chapter 5) shows the potential of traditional classifier, machine learning, and deep learning algorithms in demarcating deforestation in conjunction with the use of Sentinel-1 and Sentinel-2 imagery, in addition to auxiliary variables such as vegetation indices, biophysical data, and GLCM textures. The fusion of these imagery became more advantageous in LULC analysis. It is found that Sentinel-1 and -2 have a strong complementary feature. In terms of classifiers, the traditional MLC was best in binary satellite imagery classification. The RF proves robust in LULC classification compared to all other ML algorithms tested. U-Net deep learning outperformed traditional and machine learning classifiers when a more sophisticated LULC categorization was applied to the imagery. The best LULC model showed that 417.93 km^2 of the research site was deforested from 2015 to 2022. This study further found that the closer a forest is to a human settlement or agricultural land, the more likely a forest will be removed for human use. Deforestation can occur in remote areas, even without roads or bodies of water. This study also suggests that anthropogenic deforestation can occur even in land areas with high elevations. This situation is not unique to the Philippines; it could occur anywhere in the globe. Hence, there is a strong need for its preservation and sustainable management. It is recommended that future research take into account the dynamics of ecological succession in the study area. Finally, policymakers and legislators can use the findings of this study to develop a comprehensive strategy for protecting and conserving the Benguet's TMF.

The next chapter details how machine learning can be applied to satellite imagery including Interferometric Synthetic Aperture Radar imagery, the Global Ecosystem Dynamics Investigation data, Sentinel products, and biophysical data to assess and create maps of successional stages for the three vegetation zones in the Benguet Province.

CHAPTER 6: PAPER 3 - MAPPING THE TROPICAL MONTANE FOREST'S SUCCESSIONAL STAGES

6.1. Introduction

In Chapter 5, the data from Sentinel-1 (S-1) and Sentinel-2 (S-2) imagery, as well as their fusion, was examined for land use land cover (LULC) mapping of Benguet, Philippines. The predictive skills of a traditional classifier, three machine learning (ML) algorithms, and a deep learning algorithm have been evaluated for deforestation mapping. In this present Chapter, the use of Interferometric Synthetic Aperture Radar (InSAR) imagery and the Global Ecosystem Dynamics Investigation (GEDI) data were tested to model canopy height as one of the variables in predicting successional stages (SS) in the three different vegetation types of the study area. S-1, S-2, and biophysical data, including elevation, were also added in the modelling of SS using ML. This study aimed to add to the growing body of literature on employing InSAR and GEDI data with ML-based spatially explicit regression for tropical montane forests.

6.2. Published paper

The next page contains a copy of the article and is under review in the *Remote Sensing Applications: Society and Environment* by Elsevier. The journal is among the top 25% (Q1) in the field of Computers in Earth Sciences. The source normalized impact per publication (SNIP) of this journal in 2022 is 1.32 and has an impact factor (IF) of 4.7. The journal's h-index is 37.

Integrated multi-satellite data and machine learning approach in mapping the successional stages of forest types in a tropical montane forest

Richard Dein D. Altarez [a,b*], Armando Apan[a,b,c], Tek Maraseni[a,d]

[a] *Institute for Life Sciences and the Environment, University of Southern Queensland, Toowoomba, Queensland 4350, Australia*
[b] *School of Surveying and Built Environment, University of Southern Queensland, Toowoomba, Queensland 4350, Australia*
[c] *University of the Philippines Diliman, Institute of Environmental Science and Meteorology, Quezon City 1101, Philippines*
[d] *Northwest Institute of Eco-Environment and Resources, Chinese Academy of Sciences, Lanzhou 730000, China*

Abstract

The knowledge of successional stages in a tropical montane forest (TMF) has a profound implication for improving its preservation and management. This study examined Sentinel-1, Sentinel-2, InSAR, GEDI, and machine learning to map the successional stages of different forest types in a Philippines' TMF. Field data were collected from December to January 2023 for the creation and validation of successional stages models. Multiple correlation analysis revealed that Sentinel-1 interferogram, unwrapped interferogram, and coherence exhibited weak positive correlations with canopy height (r^2 = 0.18). Incorporating GEDI with InSAR to predict canopy height presents less accurate outputs (r = –0.2 to 0.04; RMSE = 12 to 13 m). Integrating the optical and radar data, along with auxiliary variables yielded an overall accuracy of 79.56% and a kappa value of 75.74%. Employing Random Forest's top 10 feature importance enhanced the accuracy (84.22%) and kappa value (81.19%). Elevation has significantly influenced forest type distribution, with mature and young pine forest dominating lower elevation (700-1,400m), while the mossy forest dominating the higher area (>1,400m). The disturbances across forest types emphasize the need for a solid preservation efforts and sustainable management of the TMFs. The results of this study can be applied to other TMFs other than the Philippines to understand their ecological significance. Future research should examine other factors of successional stages such as a time series evaluation to account the disturbances and patters of vegetation changes. The optimization of the RF's parameters for regression and classification, and comparing it with a much-sophisticated algorithms is also a potential avenue of improvement.

Keywords: Forest succession stages, Sentinel-1, Sentinel-2, InSAR, GEDI, Machine learning

1. Introduction

Understanding the forest succession stages is crucial for improving forest conservation and monitoring forest health (Bispo et al., 2019). Forest succession stages is the changes in vegetation composition over time and space (Taylor et al., 2009). Identifying these stages accurately is vital for reforestation projects and assessing the uncertainty in biomass and carbon storage, especially in challenging environments like tropical montane forests (TMF). This information can also help policymakers develop strategies on planting and managing native species to protect biodiversity and preserve critical habitats (Maraseni et al., 2012). While mapping land use land cover (LULC) and successional stages in tropical regions has focused on flatter areas, more research is needed for TMFs with steep slopes and multiple forest types (Carreiras et al., 2017).

The environment of TMFs are influenced by a range of climatic and site factors (Altarez et al., 2023b). Its vegetation responds to the variations in this climate and physical factors, leading to changes in composition and structure (Crausbay & Martin, 2016). These dynamics are vital for biodiversity and hydroclimatic cycle (Paulick et al., 2017). Despite these significant characteristics, our grasp of TMFs successional stages is limited. This gap limits our ability to comprehend spatial vegetation patterns, which are essential for the protection and sustainable management of these forests. In addition, understanding these dynamics in TMFs have a direct impact on forest productivity and carbon storage. Studies have shown that young or early successional stages have lower wood density than mature forests, suggesting that carbon stock is likely to change overtime (Nyirambangutse et al., 2017). TMFs are rapidly degrading due to the expansion of urban and agriculture (Kumaran et al., 2011; Altarez et al., 2022), highlighting the urgency for scientific studies on their successional stages to prevent their loss from both anthropogenic and natural causes.

Traditionally, forest successional stages are mapped using field data (Helmer et al., 2000). Although this method is accurate, it is costly and limited to a specific spatial extent. Fieldwork in mountainous forests is time-consuming and labor-intensive (Liu & Wang, 2022). Integrating field data with remotely sensed information can generate meaningful extrapolated maps of forest successional stages. In recent years, remote sensing has become more robust because it is fast, efficient, and relatively accurate. Challenges such as cloud cover and atmospheric disturbances remains the negative feature in satellite images (Liu et al., 2008). This challenge was later addressed by the rise of other groundbreaking technologies, such as the Synthetic Aperture Radar (SAR) and Light Detection and Ranging (LiDAR). While these technologies become powerful remote sensing tools, they come with drawbacks such as the technical complexity of their use, availability of data and cost. To mitigate these drawbacks, the optical remote sensing data, which are easier to handle and more cost effective, are coupled with field information. A growing number of literature combines remote sensing with field gathered information. Caughlin et al. (2021) assessed successional stages in a tropical forest by alleviating the uncertainties of Landsat imagery with field information. Szostak et al., (2018) and Chraibi et al. (2021) on the other hand, explored the integration of Sentinel data and field data to automate forest succession detection, and patterns of forest regeneration, respectively. Bispo et al. (2019) and Berveglieri et al. (2018) have demonstrated how forest succession can be studied through height estimation as generated by SAR interferometry and airborne photogrammetric imagery. The potential applications of digital surface model for forest growth, on the other hand, have been investigated by Berveglieri et al. (2016). Additionally, the utilization of LiDAR technology (van Ewijk et al., 2011), and fusion of optical and radar data (Carreiras et al., 2017) were found significant in successional dynamics studies. They also highlighted that determining the stages of forest succession requires detection of more subtle differences in vegetation properties. Hence, mapping of forest succession with remotely sensed imagery requires more detailed reference information (Helmer et al., 2000).

The assessment of forest succession stages requires age and other physiological characteristics of vegetation including height, diameter at breast height (DBH), and basal area (Lu et al., 2003). These three dimensional variables are poorly detected in most passive optical sensor (Falkowski et al., 2009). Nevertheless, advancements in technology such as LiDAR and Interferometric or Polarimetric SAR (In/Pol InSAR), now offer solutions to this challenges (Bispo et al., 2019). Despite their applicability for detecting these required variable for forest succession, their

availability is limited (Wedajo, 2017). While LiDAR is a powerful tool, its cost and the need for historical data can hinder long-term time series analysis (Berveglieri et al., 2016). On the other hand, In/Pol-InSAR faces its own set of limitations. Spaceborne In/Pol-InSAR data are acquired in repeat-pass mode, which can lead to decorrelation of radar signals and inaccurate forest height measurements (Bispo et al., 2019). Yet, the success of new technologies in remote sensing is still paving the way to bridge the gaps in forest succession assessment.

The NASA Global Ecosystem Dynamics Investigation (GEDI) collects vegetation structure data since April 2019 (Potapov et al., 2021). This GEDI instrument has a full-waveform sampling system. Despite this capability, it still contains weak, overlapping, and vast echoes, particularly in densely forested mountainous terrain that poses errors in forest height estimate (Liu & Wang, 2022). With the use of optical imagery and machine learning (ML), the gaps in the use of GEDI may be resolved (Potapov et al., 2021; Gupta & Sharma, 2022). ML proved to give accurate and interpretable results (Lary et al., 2016). In addition, the use of Interferometric SAR (InSAR), growing in popularity, faces challenges in mountains (Kumar & Krishna, 2019; Loong et al., 2013), although alternatives exist (De Petris et al., 2022). Combining Sentinel products with machine learned canopy height offers spatially explicit outcomes (Torres de Almeida et al., 2022). The technique has now been accepted in the literature, as InSAR relates significantly with forest parameters and shows promising results (Olesk et al., 2016).

Despite these advancements, there remains a gap in the literature regarding the application of GEDI and Sentinel-1 InSAR for successional stages in TMFs. Hence, this study aims to examine GEDI, Sentinel-1 InSAR data, Sentinel-1 VV, VH and GLCM textures and Sentinel 2 spectral bands, biophysical attributes, along with machine learning regression, to map successional stages of a TMF in the Philippines. By pioneering this approach in the region, this study seeks to contribute to the growing interest in remote sensing technologies for carbon and biodiversity-related goals in TMFs.

This study employs GEDI and Sentinel-1 InSAR to refine the classification and map successional stages of a TMF in the Philippines based on forest types as determined by topographic factors. Its innovative approach aims to contribute to the growing interest in the use of GEDI and InSAR in a TMF utilizing ML regression for canopy height modelling. The novelty of the paper are as follows: First, the study evaluated the use of GEDI and InSAR for successional stages mapping which is first to be used in the Philippine's TMF. Second, explicit machine learning regression to produce a continuous successional stages map is not common in most of the literature that performs classification of satellite imagery pixels and detection of objects for TMFs. Third, this study is one of the pioneering studies in the Philippines and Southeast Asia to map successional stages in a TMF using emerging remote sensing technologies. The results of this study can be employed in similar topographic and climatic region, and can assist policy makers at achieving carbon and biodiversity-related goals in TMFs.

2. Materials and methods

This section details the data and steps involved to attain the objectives set in Section 1. The main steps involved are as follows: the Sentinel-1 and Sentinel-2 data were processed and prepared, canopy height maps using GEDI and Sentinel-1 InSAR data were modelled through RF regression together with field derived data, testing of the variables for successional stages using RF classifier, and finally, assessing the accuracy of the results (Figure 1).

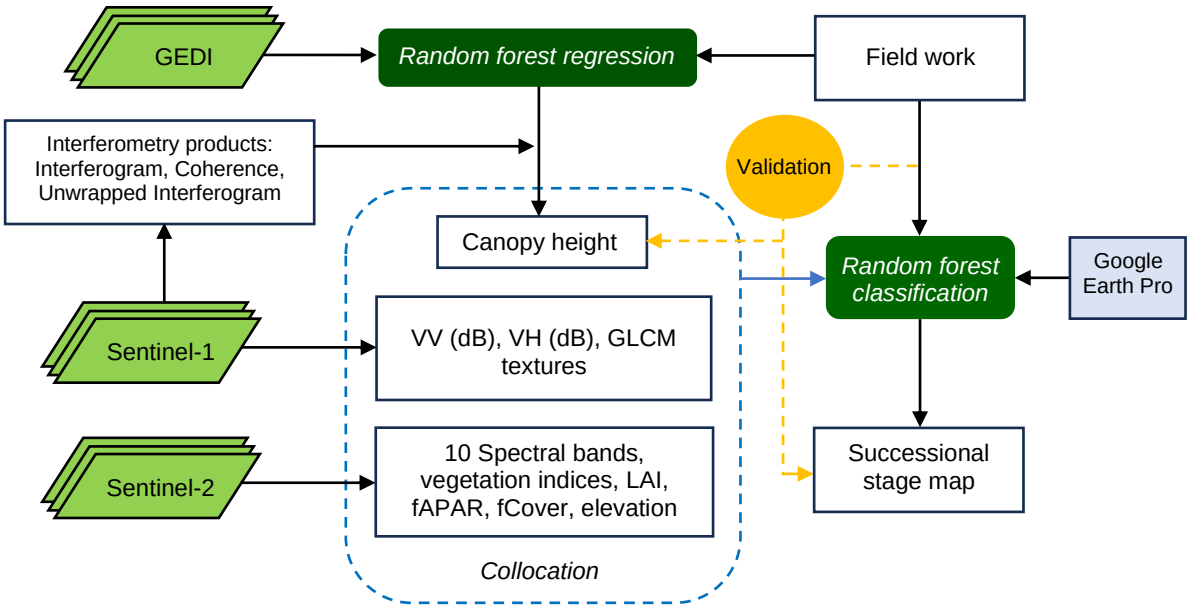

Figure 1. The overall workflow to map the successional stages of forest types in a tropical montane forest

2.1. Study area

The study area is in Benguet, Philippines with a total land area of 2,826.59 km2 (Provincial Governor's Office - Information Technology, 2020). Rainy season runs from May to October, and dry for the rest of the year. The average temperature is from January to June is 17.3 to 20.7 °C (Parao et al., 2016). The highest elevation is found in Mt Pulag at 2,926 masl (Doyog et al., 2021). The towering elevation results to the formation of three vegetation structures: pine forest at 700-1,800 meter (DENR - FMB, 2011); mossy forest, found over 1,000 meters (Fernando & Cereno, 2010); and grassland summit (figure 2).

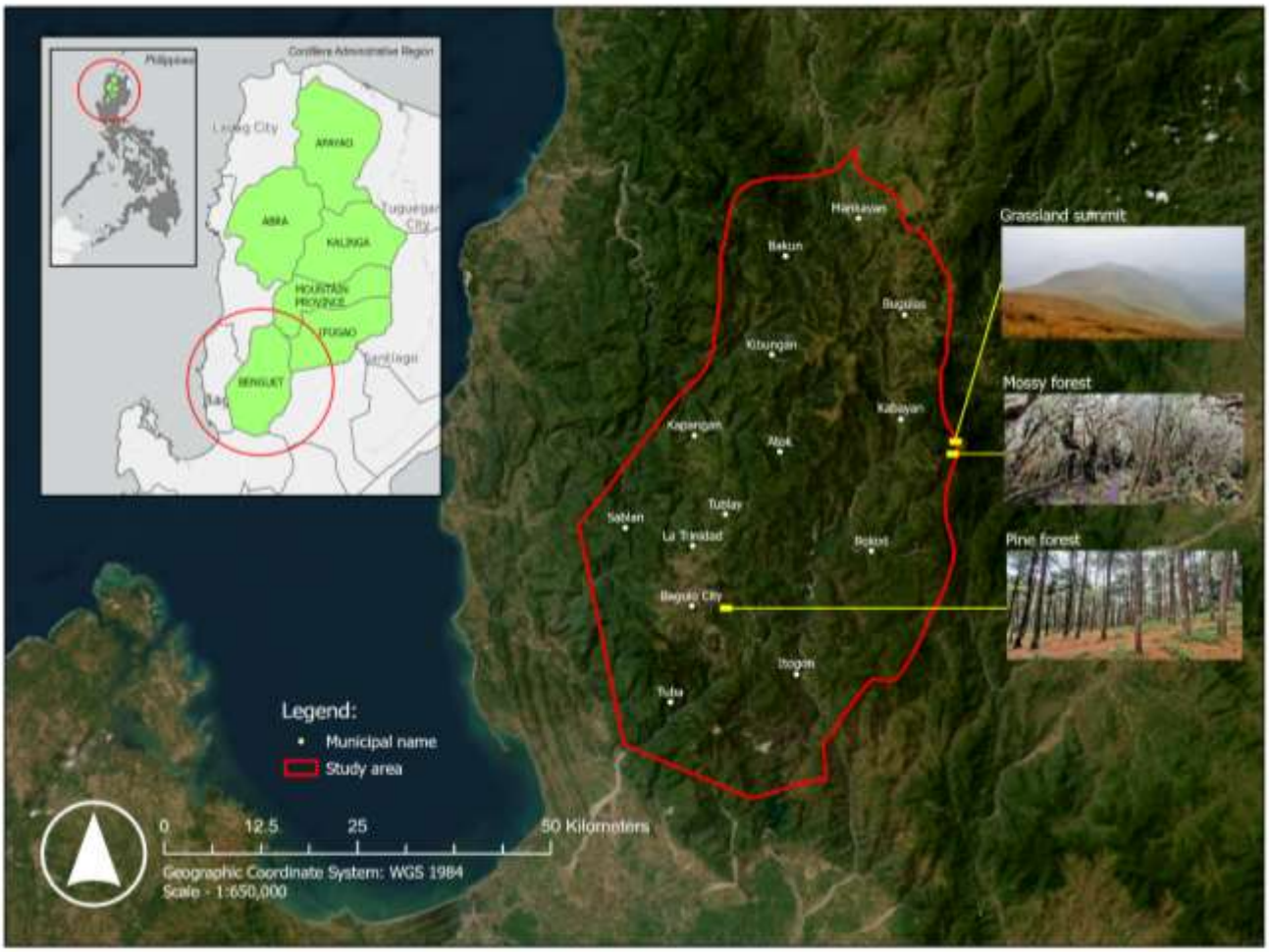

Figure 2. Location of the study area (Benguet Province, Philippines) and the three vegetation zones found in the province

2.2. Data collection

Field and satellite data were collected from December 10, 2022, to January 08, 2023. The absence of forest age data led to the adoption of the following forest succession classes found in figure 3. Table 1 further defined the successional classes through "general structure" or how vegetation is arranged, and "composition" or the identity and abundance of different species present, including the forest vertical stratification (e.g., undergrowth, canopy, and emergent layer). It is assumed that the mixed forest at the defined elevation, which exhibits the same characteristics of pine forests, may contain both young and mature pine trees. A total of 359 polygons with a uniform area of 314 m^2 were generated for the classification. These were taken from both field work, and satellite imagery interpretation. Information taken for the field data includes DBH, canopy height through clinometer and laser finder; canopy cover using a densiometer; and general condition of the area (e.g., vegetations' dominant maturity condition, regenerants, man-made and natural disturbances, and local knowledge). 737 random points were taken for each class for validation from Google Earth pro.

Figure 3. The forest succession stages in the study area. A. Grassland summit; B. Mature mossy forest; C. Young mossy forest; D. Mature pine forest; E. Young pine forest; F. Grassland patches near pine tree stands.

2.3. Satellite data

The GEDI LiDAR was used with field-derived data to produce forest height maps. It acquires data over eight tracks with a footprint spacing of 60 m along the track and 600 m across the tracks (Ngo et al., 2023). This five GEDI L2A version 2 h5 files were downloaded from the USGS LP DAAC server (Table 2). The GEDI L2A version 2 has improved geolocation error from 20.9 meters to 10.3 meters (Beck et al., 2021).

The Sentinel-1 data were acquired at the Alaska Satellite Facility (ASF) of NASA Earthdata. Two formats were used in this study, the Single Look Complex (SLC) for the interferometric analysis, and the Ground Range Detected (GRD) for the mapping of successional stages (Table 2). On the other hand, a single imagery from Sentinel-2 level 2A (Table 2) acquired from Copernicus Open Access Hub were utilized. The cloud cover is 0-30% and collected in descending orbital format with a tile size of 100 x 100 m and a swath width of 290 km. Bands 2-8a and 11-12 were considered for the mapping of successional dynamics.

Table 1. The general structure and composition of successional stage classes used in this study area.

Class	Structure	Composition
GRM	Located on the summit, composed generally of dwarfed bamboo and other grasses.	Vegetation is simple, no complex vegetation composition, but can be found in higher elevations. The dwarf bamboo (*Yushania niitakayamensis*) can be found here.
MMF	Closed canopy cover, varied tree DBH, and various heights of trees.	Vertical stratification is present, occurrence of rich undergrowth, and trees are covered with mosses and other epiphytic plants. Some dwarfed trees common

		in this zone *are Lithocarpus jordanae, L. luzoniensis, and L. woodie*
YMF	Open canopy cover, less vegetation, and the presence of wildlings.	Generally, bare and vertical stratification is not present, usually close to human or natural disturbance.
MPF	Closed canopy cover; presence of wide tree DBH; and tall pine trees.	Diverse vegetation, and undergrowth such as grasses and other plants are present. Benguet pines (*Pinus kesiya*) are found thriving in this zone.
YPF	Open canopy cover; less vegetation; pine trees usually have smaller DBH and height, and presence of wildlings.	Grasses and wildings exist, and man-made and natural disturbance is present.
GRP	Located in the lower elevation, composed generally of weeds and grasses.	Vegetation is simple, no complex vegetation composition, but can be found in lower elevations.

Table 2. Date of satellite imagery used in this study.

Satellite	Utilization	Date
GEDI	Forest height	10/10/2022 10/21/2022 09/13/2022 11/17/2022 02/10/2023
Sentinel-1	Interferometry	02/22/2023 12/12/2022 12/24/2022
	Successional stages	12/12/2022
Sentinel-2	Successional stages	02/11/2023

2.4. Pre-processing of satellite data

The GEDI L2A h5 files were processed in Jupyter Notebook Python version 3.0 based on the steps of Krehbiel (2021). The GEDI relative height (RH) metric 98 was chosen to represent the canopy height based on the previous literature (Lang et al., 2021; Ngo et al., 2023). Other RH metrics, such as RH95 and RH90 overestimate (Potapov et al., 2021) and underestimate (Dorado-Roda et al., 2021) canopy height, respectively. This pre-processing has resulted in 10,977 shots left for the training and validation of canopy height modeling.

The Sentinel-1 SLC imagery was processed in SNAP 8.0 software, following the pre-processing steps of Braun (2021). Two images per date were mosaiced using slice assembly to cover the entire area. The Sentinel-1 GRD imagery, on the other hand, was also pre-processed using the same software. The pre-processing undertaken was based on the steps proposed by Filipponi (2019). For the Sentinel 2 L2A imagery, they were resampled to a 10 x 10-meter resolution using a bilinear

interpolation method in SNAP 8.0. The imagery was subjected to a subset to get the entirety of the study area. Finally, the clouds were masked using the land-sea masked operation.

2.5. Auxiliary features for Sentinel-1 and 2 imagery

All the auxiliary features were generated in SNAP 8.0. The Sentinel-1 GLCM were generated for both VV and VH polarization. The Sentinel-2 vegetation indices were carefully selected as they are widely examined and applied for vegetation analysis (Table 3). Likewise, the SRTM 30 m resolution elevation data was also added. The biophysical data added in the Sentinel-2 imagery were leaf area index (LAI), the fraction of absorbed photosynthetically active radiation (fAPAR), and the fraction of vegetation cover (fCover). According to Kamenova & Dimitrov (2021), LAI, fAPAR, and fCover are three biophysical parameters often linked with vegetation growth.

Table 3. Vegetation indices generated using Sentinel-2 imagery.

Vegetation Index	S-2 Band Use	Importance
Normalize Difference Vegetation Index (NDVI)	(B8-B4) / (B8+B4)	Highly correlates with vegetation.
Enhanced Vegetation Index (EVI)	2.5 x (B8a – B4) / (B8 + 6 x B4 – 7.5 x B2 + 1)	Quantifies vegetation greenness and corrects atmospheric conditions (Xu et al., 2022).
Normalized Difference Moisture Index (NDMI)	(B8 – B11) / (B8 + B11)	Strongly associated with forest health, water content, canopy cover, and biomass. It also provides forest loss information (Wilson & Sader, 2002).
Bare Soil Index (BSI)	(B11 + B4) – (B8 + B2) / (B11 + B4) + (B8 + B2)	Beneficial for soil mapping and crop identification (Akike & Samanta, 2016).
Normalized Burned Ratio (NBR)	NBRI (Sentinel 2) = (B8 – B12) / (B8 + B12)	Detects burnt and healthy vegetation, dry and brown vegetation, and bare soil (García & Caselles, 1991).
Optimized Soil Adjusted Vegetation Index (OSAVI)	(1 + 0.16) * (B08– B04) / (B08 + B04 + 0.16)	Better differentiates soil and canopy cover (Rondeaux et al., 1996).

2.6. Modelling of canopy heights using ML

Continuous canopy height models were created in Whitebox Runner, an analytical back-end for other GIS and remote sensing software, and the front end for running geospatial tools of the Whitebox Geospatial Analysts Tools (Whitebox GAT) (Lindsay, 2014).

The Random Forest (RF) algorithm was used for the spatially explicit regression. The forest is comprised of 100 trees, with a minimum of one sample required per leaf and a minimum of two samples needed to split a node. Additionally, a test proportion of 70% training and 30% validation was employed. RF has been widely utilized for modelling and classification applications for TMF studies (Altarez et al., 2022). The bands produced from interferometric computation were tasted

as predictors of canopy height. Interferogram is highly correlated with terrain topography, unwrapped interferogram can reveal subtle changes in ground elevation that might occur during succession, while coherence indicates how well each pixel between two SAR images reflect each other (Braun, 2021). Previous studies in the literature have demonstrated the utilization of interferograms products to model canopy heights (Loong et al., 2013; Olesk et al., 2016; Kumar & Krishna, 2019; De Petris et al., 2022; Torres de Almeida et al., 2022). Interferogram, coherence, and unwrapped interferogram, were combined differently. The canopy height derived from fieldwork and GEDI was also tested to evaluate which combination can give a better model. These variable combinations were then iterated based on December 2022 and February 2023 imagery. The dependent variable data was divided into 70% training and 30% validation. R coefficient and root mean square error (RMSE) were used to measure the validity of the model outputs.

2.7. Mapping of successional dynamics

Successional stage mapping was done in SNAP 8.0 through Random Forest Classifier, with parameters set to 5,000 number of training samples, 10 for the number of trees, and a minimum and maximum power set of 2 and 7, respectively. The layers used were the Sentinel-1 VV and VH, GLCM textures, Sentinel-2 bands, vegetation indices, and biophysical parameters, including RF derived canopy height. The field and satellite-derived 359 training polygons, with uniform size and shape, were used to classify the study area. Different layer combinations were tested: All variables, top 10 variables, top 5 variables, Sentinel 1 with textures, Sentinel 2 with vegetation indices, and biophysical parameters. The selection of the top features combination was based on the conservative approach recommended by Guyon & Elisseeff (2003). A confusion matrix assessed the map validity.

2.8. Characterization of successional stages in different forest types

Using the best model for the classification, vegetation types were characterized based on elevation. This characterization was done in the ArcGIS Pro. The elevation gradients used are described in the literature (Whitford, 1911; DENR - FMB, 2011; Fernando & Cereno, 2010). We defined pine forests situated at 700 – 1,400 meters, mossy forests at 1,400 – 2,600 meters, and grassland summit over 2,600 meters. These assumptions were based on the literature, satellite data inspection, and fieldwork observations.

3. Results

3.1. Canopy height

A multiple correlation coefficient (R) analysis of the interferometric product combinations versus field-derived height revealed weak positive correlation (Henseler et al., 2009) with R-square values ranging from 0.1817 to 0.1826 (Table 4), despite an overall significance of less than a = 0.05. This shows that 18% of the variability in field canopy height can be explained by the interferometric product combinations.

Validation tests for the canopy height models, using field data only as variable, produced accurate results with an r coefficient ranging from 0.5 to 0.8 and RMSE between 4 to 6 meters (Figure 4). Adding GEDI and field canopy height, regardless of interferometric product combinations, resulted in less accurate outputs (r = –0.2 to 0.04; RMSE = 12 to 13 m) (Figure 5). This implies that GEDI data is not suitable for the modelling TMFs' canopy height, which can be attributed to its geolocation error (Shendryk et al., 2021). Two months were selected to determine if moisture affects the model. The December model was more accurate, with the unwrapped interferogram and coherence combination as the most valid (r = 0.808; RMSE = 4.24 m), followed by the interferogram and coherence combination (r = 0.740; RMSE = 4.81 m). It can be noticed in the models that the month of December provide better distinction of the surface (figure 5). The map exhibits various patterns, with darker shades representing urban areas, bare soil, and water bodies, and lighter colors representing vegetation.

Table 4. Multiple correlation coefficient (R) of three predictor combinations for the dependent variable canopy height.

Predictors	R square	Adjusted R Square	P-Value
Interferogram, Unwrapped Interferogram and Coherence	0.1826	0.1669	6.49×10^{-7}
Interferogram and Coherence	0.1817	0.1712	1.46×10^{-7}
Unwrapped Interferogram and Coherence	0.1817	0.1712	1.46×10^{-7}

Table 5 presents the accuracy of integrating all layers to classify successional stages in different forest types. The all-layer combination model achieved an over-all accuracy (OA) of 79.56% and a kappa index (KI) of 75.74%. Isolated group layers based on Sentinel-1 (OA = 53.79%; KI = 44.61%), Sentinel-2 (OA = 67.64%; KI = 61.59%), and biophysical data (OA = 65.78%; KI = 56.03%), shows a lower OA and KI. One-way ANOVA revealed a significant difference between the OA and KI of the layer combinations (p-value = 0.027; a = 0.05), indicating that the all- layer predictors outperform the other combinations.

The feature importance from the RF classification was used to refine the model. The top 10 variables among the 43 layers were Elevation, σ° VH Angular Second Moment (ASM), BSI, fCover, σ° VH GLCM Variance, fAPAR, σ° VV GLCM Correlation, σ° VV Homogeneity, σ° VH GLCM Correlation, and σ° VH GLCM Mean (figure 7). Elevation has the highest importance among the top 10 variables at 72%. Also, 60% of the factors are GLCM textures, followed by biophysical layers at 30%. The least is the optical layers at 10%. Using the identified top 10 features enhanced the OA and KI by 5.53% and 6.71%, respectively, compared to the all-feature combination (84.22%; 81.19%). Testing the top 5 variables resulted to an OA and KI of 83.82% and 80.75%, respectively (Table 6). The choice of the top 10 layers is preferred over the top 5.

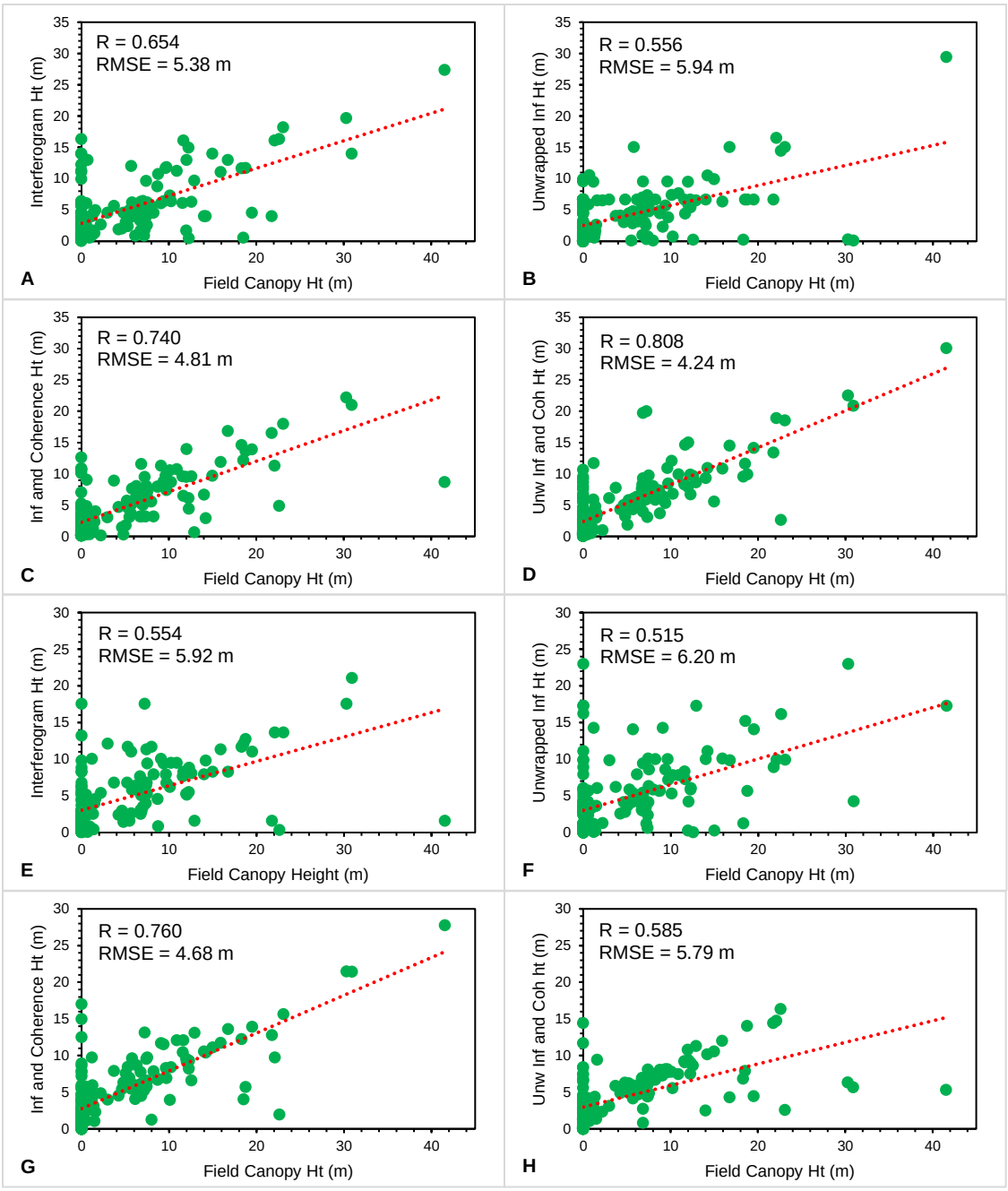

Figure 4. Validity evaluations of continuous canopy height models developed from interferometric product combinations and field data for December 2022 and February 2023: A-D. Interferometric product combinations vs field canopy height for December 2022. E-H. Interferometric product combinations vs field canopy height for February 2023.

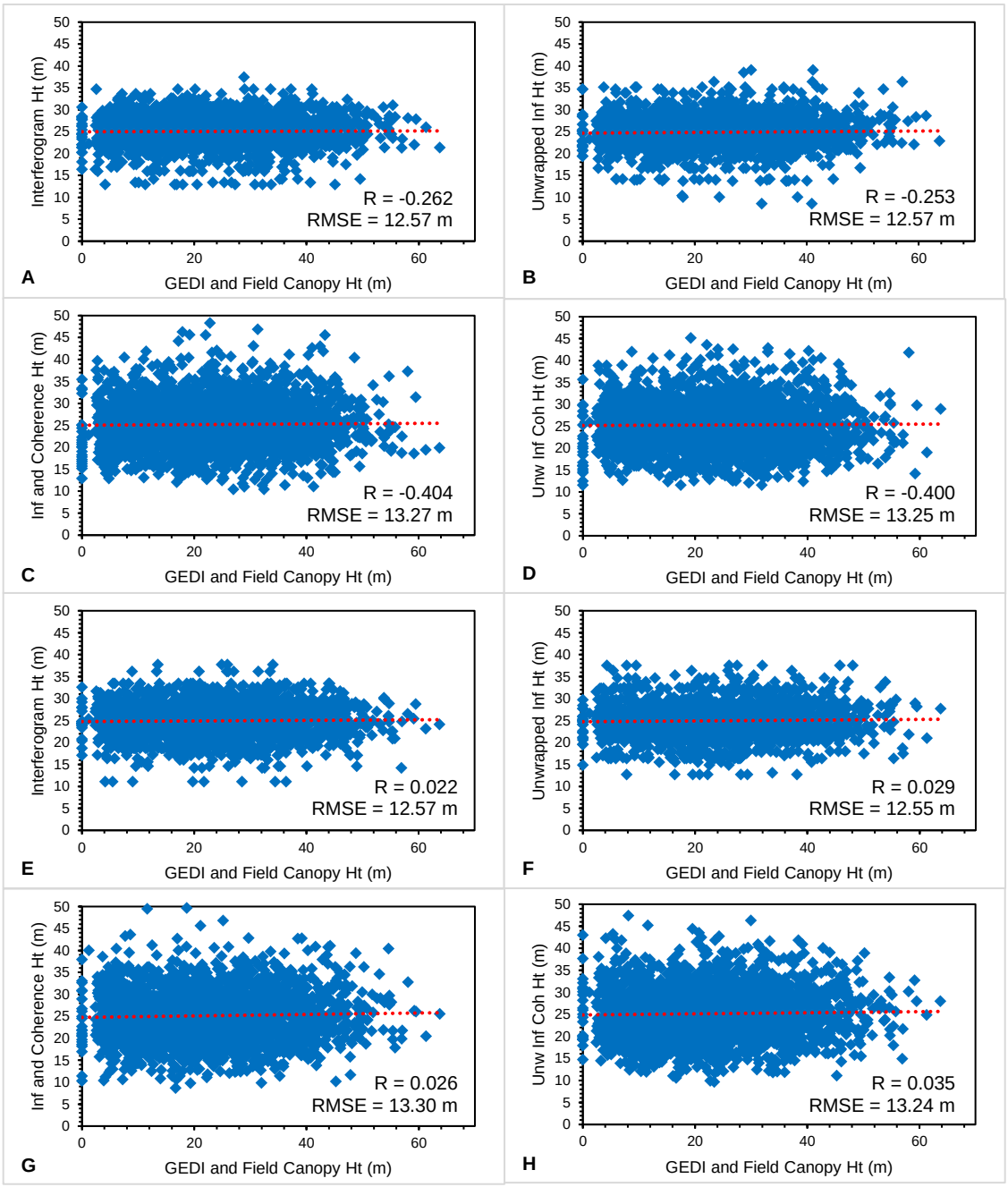

Figure 5. Validity evaluations of continuous canopy height models developed from interferometric product combinations and combined GEDI & field data for December 2022 and February 2023: A-D. Interferometric product combinations vs GEDI and field canopy height for December 2022. E-H. Interferometric product combinations vs GEDI and field canopy height for February 2023.

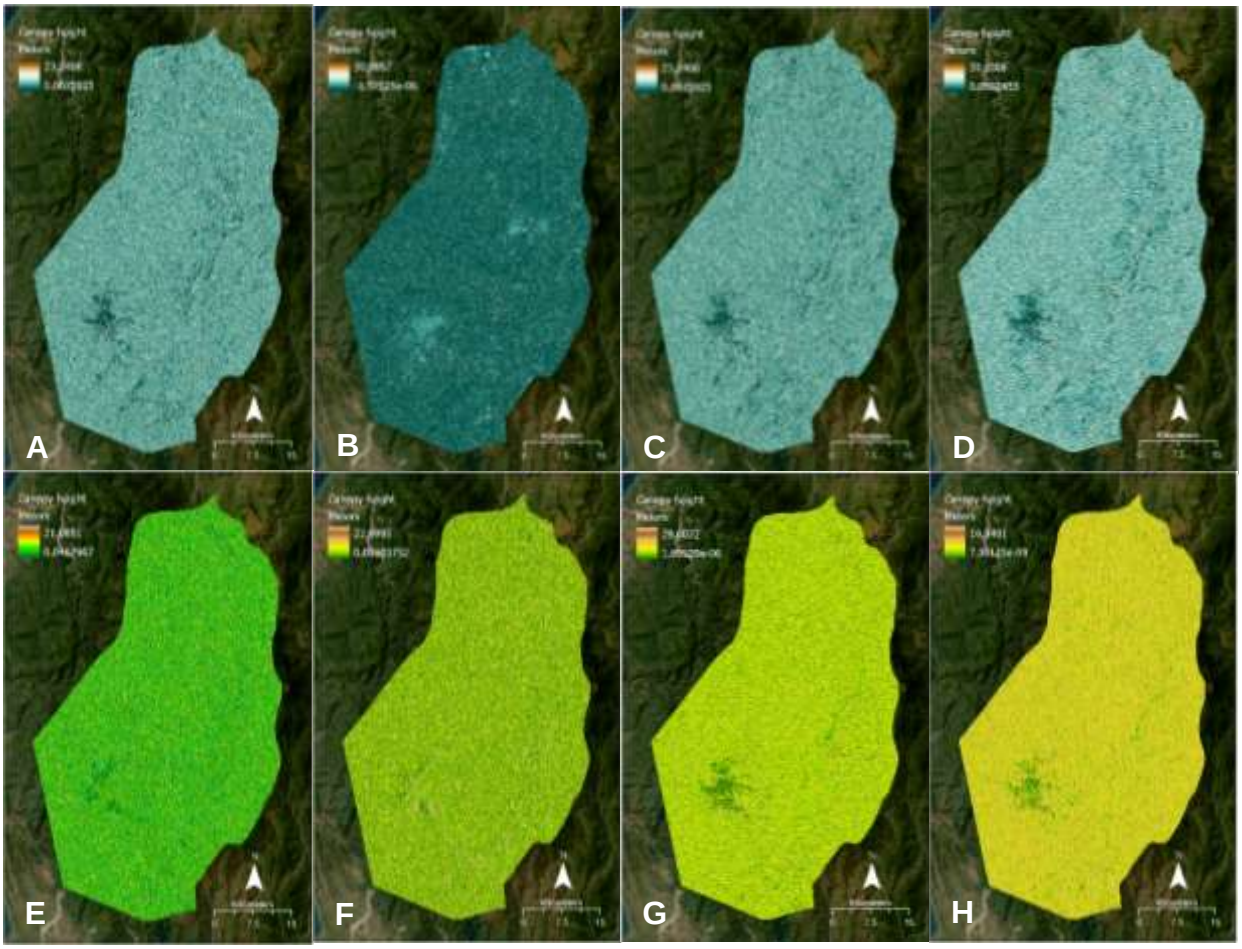

Figure 6. Validity evaluations of continuous canopy height models developed from interferometric product combinations and combined GEDI & field data for December 2022 and February 2023: A-D. Interferometric product combinations vs GEDI and field canopy height for December 2022. E-H. Interferometric product combinations vs GEDI and field canopy height for February 2023.

3.2. Best combination for the successional stages map

Table 5. OA and KI of layer combinations used to classify the successional stages in different forest types of the study area.

Layer predictor	**OA**	**KI**
All Predictors Sentinel-1: VV and VH GLCM textures – Contrast, Dissimilarity, Homogeneity, ASM, Energy, Max, Entropy, Mean, Variance, Correlation σ° VV & VH (db) (12/2022) Sentinel-2: B2,3,4,5,6,7,8,8A,11,12 NDVI, EVI, NDMI, BSI, NBR, OSAVI Biophysical: Elevation Canopy height derived from Unwrapped Interferogram and Coherence, LAI, fAPAR, fCover	79.56	75.74
Sentinel-1 data: VV and VH GLCM textures – Contrast, Dissimilarity, Homogeneity, ASM, Energy, Max, Entropy, mean, Variance, Correlation σ° VV and VH (db) (12/2022)	53.79	44.61
Sentinel-2 data: B2,3,4,5,6,7,8,8A,11,12 NDVI, EVI, NDMI, BSI, NBR, OSAVI	67.64	61.59
Biophysical data: Elevation Canopy height derived from Unwrapped Interferogram and Coherence LAI, fAPAR, fCover	65.78	56.03

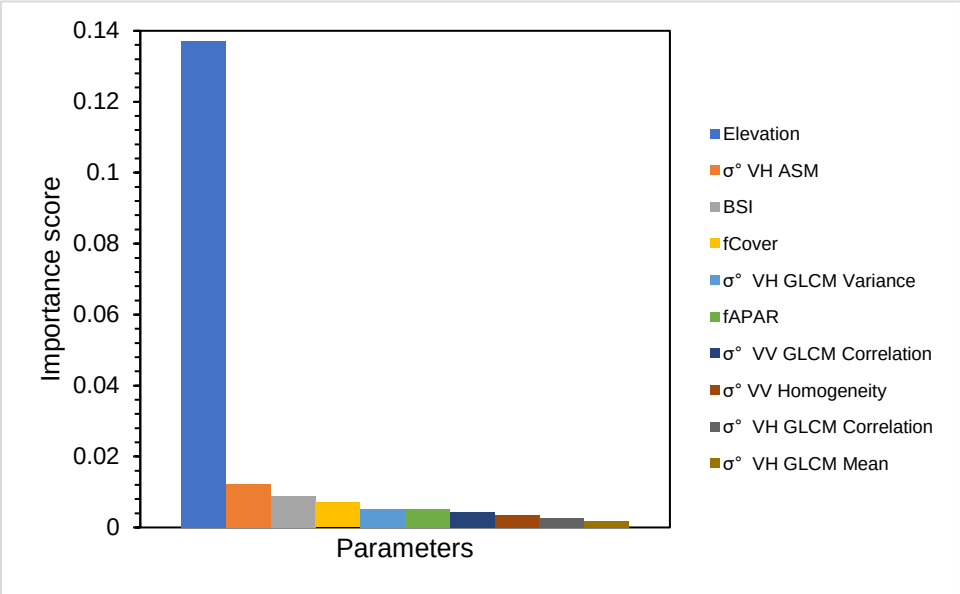

Figure 7. Top 10 variables' importance score in RF classification of successional stages in different forest types

Table 6. OA and KI of successional stage classification using RF importance features.

Predictors	**OA**	**KI**
Top 10 variables: Elevation, σ° VH ASM, BSI, fcover, σ° VH GLCM Variance, fAPAR, σ° VV GLCM Correlation, σ° VV Homogeneity, σ° VH GLCM Correlation, σ° VH GLCM Mean	84.22	81.19
Top 5 variables: Elevation, Sigma0_VH_ASM, BSI, fcover, Sigma0_VH_GLCM Variance	83.82	80.75

The successional stage map produced from the top 10 features with the highest OA and KI is shown in Figure 8. MMF and YMF are mostly found on high mountains of Kabayan, Bugias, Bokod, and Kibungan. MPF and YPF are widespread across the province. NFO is mainly in Baguio city, indicating urban areas. Other NFO areas are water bodies and bare soil, mostly in Itogon and Bokod. Table 7 displays the area and percentage distribution of succession stage classes. MPF covers the largest area at 40.38%, while MMF-YMF-GRM cover s less than 10%. A little percentage, 1.31%, is classified "No data". This is primarily due to cloud coverage, a limitation inherent to topical forest studies that are often covered by clouds.

Table 7. Area and percentage of successional stages in the study area.

Classes	Area (hectares)	Percentage
GRM	2,989	1.16
MMF	6,608	2.56
YMF	8,486	3.29
MPF	104,230	40.38
YPF	61,812	23.94
GRP	20,355	7.88
NFO	50,279	19.48
No data	3,393	1.31
Total	**258,152**	**100**

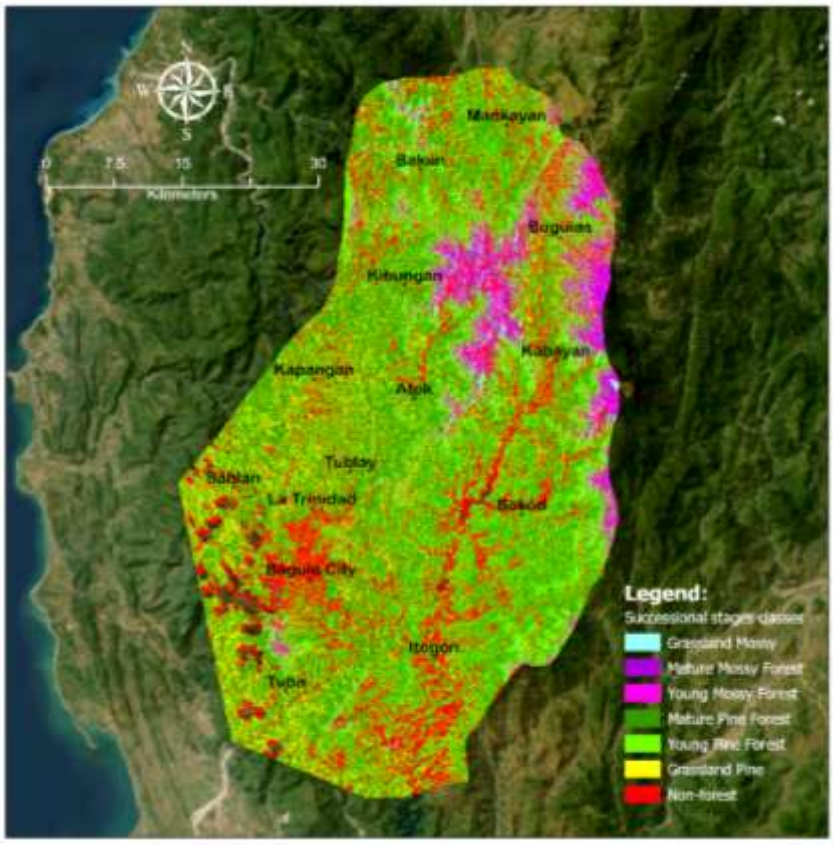

Figure 8. The successional stages map in different forest types of the study area using the Top 10 variables as the basemap

3.3. Characterization of successional stages per forest types

Table 8 displays successional stage classes by elevation gradient. MPF dominates (42.90%), followed by GRP (17.38%), and NFO (25.34%) below 700m elevation. GRM, MMF, and YMF are expected to be low at a total of 1% as the conditions are not ideal for their survival and growth. In the 700-1,400 m elevation, MPF and YPF dominate (67%), while NFO covers 21.93% due to urban areas. From 1,400 to 2,600m, MMF, YMF, and GRM prevail (17%) because its physical conditions are optimal for their growth. Above 2,600 meters, GRM, MMF, and YMF cover 88.5% with minimal YMF and YPF (0.67%). The vegetation shifts from pine forest from lower elevation to mossy forest and grassland at a higher elevation, with mossy forests becoming prominent at higher elevations. NFO is consistent, covering less than 30% coverage across elevations. Missing areas are scattered but minor in proportion.

4. Discussion

4.1. The role of canopy height in TMF successional stages

Canopy height is a critical parameter for understanding the dynamics of ecological succession (Bispo et al., 2019). This study shows that interferometric products exhibit a weak positive correlation with field canopy height. The addition of coherence improves the accuracy of height estimation, aligning with the study of Olesk et al. (2016) and Ghosh et al. (2020). Coherence provides information about the spatial distribution and structure of vegetation, making it a complementary predictor for forest canopy height (Liao et al., 2019).

Similarly, De Luca et al. (2022) exploited SAR coherence to enhance forest classification accuracy. However, the result of this study contrasts with the result of De Petris et al. (2022), wherein unwrapped phase interferogram and coherence presented a better spatially explicit canopy height model. It should be noted that different methods were applied to produce the height model. On the other hand, using GEDI data to derive height estimation corroborate with the results of Liu & Wang (2022). GEDI is limited to highly dense mountainous areas, which may be attributed to its restriction with slope affecting tree height estimation (Potapov et al., 2021). Careful consideration should be applied when using GEDI data for estimating canopy height in tropical forests (Oliveira et al., 2023). It is advised that GEDI can be used in lower elevations that is easier to discern than mountainous areas (Gupta & Sharma, 2022).

Even though canopy height was hypothesized to be crucial for TMF successional stages, the results obtained contradicted the initial hypothesis, showing that canopy height did not significantly influence the variability of the successional stages. The unexpected outcome may be attributed to unique environmental factors in the study area (Altarez et al., 2023a). Notably, elevation is the dominant factor affecting vegetation. As the elevation increases, the environmental factors change, influencing the growth and structure of vegetation (Crausbay & Martin, 2016). In the future, integrating biophysical parameters, Sentinel-1, and Sentinel-2 data could enhance the accuracy of canopy height model. In addition, fine tuning the RF regression model for canopy height could potentially enhance the result of the canopy height estimation.

Table 8. The area and percentage of successional stages in vegetation types with respect to elevation.

Elevation (m)	General Land Cover	LULC	Area (hectares)	Percentage
0-700	Others	GRM	13	0.05
		MMF	2	0.01
		YMF	22	0.09
		MPF	10,425	42.90
		YPF	2,840	11.69
		GRP	4,222	17.38
		NFO	6,158	25.34
		No data	616	2.54
	Sub-total		24,298	100
700-1,400	Pine Forest	GRM	142	0.11
		MMF	14	0.01
		YMF	68	0.05
		MPF	61,551	47.20
		YPF	25,905	19.87
		GRP	12,455	9.55
		NFO	27,895	21.39
		No data	2,364	1.81
	Sub-total		130,394	100
1,400 - 2,600	Mossy Forest	GRM	2,721	2.65
		MMF	6,366	6.19
		YMF	8,200	7.97
		MPF	32,244	31.35
		YPF	33,041	32.12
		GRP	3,674	3.57
		NFO	16,178	15.73
		No data	436	0.42
	Sub-total		102,860	100
>2,600	Grassland summit	GRM	113	18.83
		MMF	225	37.50
		YMF	193	32.17
		MPF	4	0.67
		YPF	20	3.33
		GRP	1	0.17
		NFO	44	7.33
	Sub-total		600	100
	Total		**258,152**	**100**

4.2. The role of satellite imagery in mapping TMF successional stages

A study in the Philippine's TMF presents that combining optical, radar, and biophysical data with deep learning improved complex LULC classification (Altarez et al., 2023). Another study on the use of ML algorithms revealed similar accurate predictions (Chachondhia et al., 2021). The effective classification of optical and radar satellite imagery highlights their complementary properties, allowing for more precise surface feature recognition.

Implementing the RF's feature importance further enhances the classification accuracy. Although deep learning's popularity emerges considerably in remote sensing (Ma et al., 2019), ML has proven its superiority for image classification over the last decades (Sheykhmousa et al., 2020). The successional stages map result of this study is comparable with the Environmental Systems Research Institute's (ESRI) LULC map with an OA of 85% (Karra et al., 2021), and European Space Agency (ESA) WorldCover with an OA of 74.4% (Zanaga et al., 2021).

It was found that elevation significantly influences the classification. The general trend observed in increased elevation is a decrease in woody plant vegetation (Bruijnzeel et al., 2011), this changes in wood physiology may be attributed to the involvement of other parameters, such as the shift of climatic variables. Wallis et al. (2019) found that elevation gradient significantly influences forest biomass and productivity.
Sentinel-2 data provides crucial information on vegetation composition, but its quality is affected by atmospheric disturbances. The presence of clouds affects the LAI, fAPAR, and fCover. The morphological features of vegetation can be better understood by examining these layers. Muhe & Argaw (2022) show that integrating them improves the estimation of forest above-ground biomass in a TMF.

In addition, Sentinel-1 is advantageous over areas with excessive cloud coverage. The SAR's sensitivity to surface roughness using GLCM textures provides constant and reliable separation of LULC. The GLCM texture generally relates to the structure of the different LULC and successional stages (Huang et al., 2014). The application of GLCM textures has proven to be effective in LULC assessment, in habitat structure or species richness (Wallis et al., 2017) and biomass modeling (Wallis et al., 2019).

In this study, the top 10 remote sensing variables including, elevation, σ° VH ASM, BSI, fcover, σ° VH GLCM variance, fAPAR, σ° VV GLCM correlation, σ° VV homogeneity, σ° VH GLCM correlation, and σ° VH GLCM mean are effective layers for mapping successional stages. Careful selection of data layers can leverage the successional stage classification. Our knowledge of the dynamics of successional stages can create evidence-based decisions for conserving and managing this environment in a sustainable manner.

4.3. The successional stages in different forest types

The different vegetation types are significantly influenced by elevation. MPF and YPF generally dominate the low elevation, while mossy forests prevail at higher elevations. Mossy forests are better adapted to low temperatures and wetter environments (Kappelle, 2004; Bruijnzeel et al., 2011; Wallis et al., 2019). Changes in pine forest growth are prevalent in the study region. The

MPF and YPF areas are significantly easier to access by humans, resulting to their conversion. Changes in the mossy forest are also prevalent, evidence by news reports documented the conversions to agricultural farms (Lasco, 2022). These disturbances pave the way for changes in their ecological makeup (Balangen et al., 2023). Similar TMFs changes are happening in Malaysia (Kumaran et al., 2011), even in other locations across the globe (Crausbay & Martin, 2016). Deforestation in the Philippines remains rampant, even in areas that is declared protected under law (Apan et al., 2017).

The result of this study underscores the necessity of protecting and limiting human disturbances in the TMFs. Scientific evidence indicates that TMF recovery takes 65–85 years, with 50 years for epiphytic plant and flora regeneration (Kappelle, 2004). Therefore, TMF conservation and management are necessary. A targeted conservation strategy can be crafted for each forest type. These findings have major implications for accomplishing climate change, ecological conservation, and sustainable use of natural resources goals like the conservation of biological diversity (CBD) and Nationally Determined Contributions (NDC) goals.

5. Conclusion

Interferometric products have a weak positive correlation with the field canopy height. The use of GEDI requires careful consideration for estimating canopy height in TMFs. Combining Sentinel-1 and Seninel-2 data, and auxiliary variables effectively classify successional stages with an OA of 79.56% and a KI of 75.74%. Using RF feature importance improved the model by 5.53% OA (i.e., 84.22%) and KI by 6.71% (i.e., 81.19%). This study also found that elevation significantly influenced the distribution of forest types. This is because elevation primarily drives the environmental condition such as temperature, water, and soil fertility, which significantly affects vegetation growth. Mature and young pine forest dominated the lower elevation, while the higher areas become dominated by mossy forest, indicating their preference for cooler and wetter condition. The presence disturbances observed in different forest types call for the need to pursue strong conservation efforts. Evidence-based decision-making is crucial to attaining climate change mitigation, ecological conservation, and sustainable resource use goals. This study can be applied to TMFs other than the Philippines to better understand this diverse and ecologically significant environment. Policymakers can use this study to establish plans for native plants, inhibit invasive species, and conserve biodiversity by identifying critical habitats for different species. Future research should examine other successional stages factors, and a time series successional stages map to account the disturbances and patterns of the vegetation changes. Fine tuning the RF model for both regression and classification presents a fundamental improvement for future research. Similarly, investigating additional variables to incorporate with GEDI is also recommended.

Acknowledgement

The authors acknowledge the University of Southern Queensland. RDDA was funded by the Philippines Department of Science and Technology Science Education Institute. The following were instrumental in realizing this research: Mt Pulag Protected Landscape – Protected Area Management Board (MPPL-PAMB), MPPL – Protected Area Management Office (PAMO), City Government of Baguio and the City Environment and Parks Management Office (CEPMO),

Philippine Military Academy, Watershed and Water Resources Research, Development and Extension Center, Ecosystem Research and Development Bureau, Department of Environment and Natural Resources (CAR). The following individuals were essential assets during the fieldwork: Mr. Donald Apan and Ms. Armina Apan. RDDA is also thankful to Superintendent Emerita Albas and Forester Floro Bastian of CEPMO.

Contribution statement

RDDA was responsible for the conceptualization, collection and processing of data, analysis and evaluation, writing, review and editing. **AA** was responsible for supervision, conceptualization, data collection, validation, review, and editing. **TM** was responsible for supervision, analysis, and review.

Declarations

Conflict of interest: The authors assert that there are no conflicting financial or personal interests that potentially influence the findings presented in this study.

Data availability

This investigation utilized Sentinel-1 and Sentinel-2 imagery, which can be downloaded from the ESA Copernicus Open Access Hub website, and GEDI data that is freely available at the USGS LP DAAC server. To acquire field data on the mossy forest and grassland summit in the province of Benguet, proper permissions must be obtained from the MPPL-PAMB and the MPPL-PAMO. Other data supporting this study are accessible upon reasonable request to the corresponding author and with the permission of the other authors.

References:

Akike, S., & Samanta, S. (2016). Land Use/Land Cover and Forest Canopy Density Monitoring of Wafi-Golpu Project Area, Papua New Guinea. *Journal of Geoscience and Environment Protection*, *04*(08), 1–14. https://doi.org/10.4236/gep.2016.48001

Altarez, R. D. D., Apan, A., & Maraseni, T. (2022). Spaceborne satellite remote sensing of tropical montane forests: a review of applications and future trends. *Geocarto International*, *0*(0), 1–29. https://doi.org/10.1080/10106049.2022.2060330

Altarez, R. D. D., Apan, A., & Maraseni, T. (2023a). Deep learning U-Net classification of Sentinel-1 and 2 fusions effectively demarcates tropical montane forest's deforestation. *Remote Sensing Applications: Society and Environment*, *29*(September 2022), 100887. https://doi.org/10.1016/j.rsase.2022.100887

Altarez, R. D. D., Apan, A., & Maraseni, T. (2023b). Uncovering the Hidden Carbon Treasures of the Philippines' Towering Mountains: A Synergistic Exploration Using Satellite Imagery and Machine Learning. *PFG - Journal of Photogrammetry, Remote Sensing and Geoinformation Science*, *0123456789*. https://doi.org/10.1007/s41064-023-00264-w

Apan, A., Suarez, L. A., Maraseni, T., & Castillo, J. A. (2017). The rate, extent and spatial predictors of forest loss (2000–2012) in the terrestrial protected areas of the Philippines. *Applied Geography*, *81*, 32–42. https://doi.org/10.1016/j.apgeog.2017.02.007

Balangen, D. A., Catones, M. S., Bayeng, J. M., & Napaldet, J. T. (2023). Intensities of human

disturbance dictate the floral diversity in tropical forest: the case of a secondary forest in Benguet, Philippines. *Journal of Mountain Science*, *20*(6), 1575–1588. https://doi.org/10.1007/s11629-022-7830-7

Berveglieri, A., Imai, N. N., Tommaselli, A. M. G., Casagrande, B., & Honkavaara, E. (2018). Successional stages and their evolution in tropical forests using multi-temporal photogrammetric surface models and superpixels. *ISPRS Journal of Photogrammetry and Remote Sensing*, *146*(September 2017), 548–558. https://doi.org/10.1016/j.isprsjprs.2018.11.002

Berveglieri, A., Tommaselli, A. M. G., Imai, N. N., Ribeiro, E. A. W., Guimarães, R. B., & Honkavaara, E. (2016). Identification of Successional Stages and Cover Changes of Tropical Forest Based on Digital Surface Model Analysis. *IEEE Journal of Selected Topics in Applied Earth Observations and Remote Sensing*, *9*(12), 5385–5397. https://doi.org/10.1109/JSTARS.2016.2606320

Bispo, P. D. C., Pardini, M., Papathanassiou, K. P., Kugler, F., Balzter, H., Rains, D., dos Santos, J. R., Rizaev, I. G., Tansey, K., dos Santos, M. N., & Spinelli Araujo, L. (2019). Mapping forest successional stages in the Brazilian Amazon using forest heights derived from TanDEM-X SAR interferometry. *Remote Sensing of Environment*, *232*(May), 111194. https://doi.org/10.1016/j.rse.2019.05.013

Braun, A. (2021). *Sentinel-1 Toolbox TOPS Interferometry Tutorial*. *June*, 1–25.

Bruijnzeel, L. A., Kappelle, M., Mulligan, M., & Scatena, F. N. (2011). Tropical montane cloud forests: State of knowledge and sustainability perspectives in a changing world. In *Tropical Montane Cloud Forests: Science for Conservation and Management* (Issue December 2015). https://doi.org/10.1017/CBO9780511778384.074

Carreiras, J. M. B., Jones, J., Lucas, R. M., & Shimabukuro, Y. E. (2017). Mapping major land cover types and retrieving the age of secondary forests in the Brazilian Amazon by combining single-date optical and radar remote sensing data. *Remote Sensing of Environment*, *194*, 16–32. https://doi.org/10.1016/j.rse.2017.03.016

Caughlin, T. T., Barber, C., Asner, G. P., Glenn, N. F., Bohlman, S. A., & Wilson, C. H. (2021). Monitoring tropical forest succession at landscape scales despite uncertainty in Landsat time series. *Ecological Applications*, *31*(1), 1–18. https://doi.org/10.1002/eap.2208

Chachondhia, P., Shakya, A., & Kumar, G. (2021). Performance evaluation of machine learning algorithms using optical and microwave data for LULC classification. *Remote Sensing Applications: Society and Environment*, *23*(July), 100599. https://doi.org/10.1016/j.rsase.2021.100599

Chraibi, E., Arnold, H., Luque, S., Deacon, A., Magurran, A. E., & Féret, J. B. (2021). A remote sensing approach to understanding patterns of secondary succession in tropical forest. *Remote Sensing*, *13*(11). https://doi.org/10.3390/rs13112148

Crausbay, S. D., & Martin, P. H. (2016). Natural disturbance, vegetation patterns and ecological dynamics in tropical montane forests. *Journal of Tropical Ecology*, *32*(5), 384–403. https://doi.org/10.1017/S0266467416000328

De Luca, G., M. N. Silva, J., Di Fazio, S., & Modica, G. (2022). Integrated use of Sentinel-1 and Sentinel-2 data and open-source machine learning algorithms for land cover mapping in a Mediterranean region. *European Journal of Remote Sensing*, *55*(1), 52–70. https://doi.org/10.1080/22797254.2021.2018667

De Petris, S., Cuozzo, G., Notarnicola, C., & Borgogno-Mondino, E. (2022). Forest Height Estimation Using Sentinel-1 Interferometry. A Phase Unwrapping-Free Method Based on

Least Squares Adjustment. In *Communications in Computer and Information Science: Vol. 1651 CCIS*. Springer International Publishing. https://doi.org/10.1007/978-3-031-17439-1_18

Dorado-Roda, I., Pascual, A., Godinho, S., Silva, C. A., Botequim, B., Rodríguez-Gonzálvez, P., González-Ferreiro, E., & Guerra-Hernández, J. (2021). Assessing the accuracy of gedi data for canopy height and aboveground biomass estimates in mediterranean forests. *Remote Sensing*, *13*(12). https://doi.org/10.3390/rs13122279

Doyog, N. D., Lumbres, R. I. C., & Baoanan, Z. G. (2021). Monitoring of land use and land cover changes in Mt. Pulag national park using landsat and sentinel imageries. *Philippine Journal of Science*, *150*(4), 723–734. https://doi.org/10.56899/150.04.10

Falkowski, M. J., Evans, J. S., Martinuzzi, S., Gessler, P. E., & Hudak, A. T. (2009). Characterizing forest succession with lidar data: An evaluation for the Inland Northwest, USA. *Remote Sensing of Environment*, *113*(5), 946–956. https://doi.org/10.1016/j.rse.2009.01.003

Filipponi, F. (2019). *Conferecne Paper.Pdf*. *3*(June), 2–6.

García, M. J. L., & Caselles, V. (1991). Mapping burns and natural reforestation using thematic mapper data. *Geocarto International*, *6*(1), 31–37. https://doi.org/10.1080/10106049109354290

Ghosh, S. M., Behera, M. D., & Paramanik, S. (2020). Canopy height estimation using sentinel series images through machine learning models in a Mangrove Forest. *Remote Sensing*, *12*(9), 1–21. https://doi.org/10.3390/RS12091519

Gupta, R., & Sharma, L. K. (2022). Mixed tropical forests canopy height mapping from spaceborne LiDAR GEDI and multisensor imagery using machine learning models. *Remote Sensing Applications: Society and Environment*, *27*(October 2021), 100817. https://doi.org/10.1016/j.rsase.2022.100817

Guyon, I., & Elisseeff, A. (2003). An Introduction to Variable and Feature Selection Isabelle. *Journal OfMachine Learning Research*, *3*, 1157–1182.

Helmer, E. H., Brown, S., & Cohen, W. B. (2000). Mapping montane tropical forest successional stage and land use with multi-date Landsat imagery. *International Journal of Remote Sensing*, *21*(11), 2163–2183. https://doi.org/10.1080/01431160050029495

Henseler, J., Ringle, C. M., & Sinkovics, R. R. (2009). The use of partial least squares path modeling in international marketing. *Advances in International Marketing*, *20*(May), 277–319. https://doi.org/10.1108/S1474-7979(2009)0000020014

Huang, X., Liu, X., & Zhang, L. (2014). A multichannel gray level co-occurrence matrix for multi/hyperspectral image texture representation. *Remote Sensing*, *6*(9), 8424–8445. https://doi.org/10.3390/rs6098424

Kamenova, I., & Dimitrov, P. (2021). Evaluation of Sentinel-2 vegetation indices for prediction of LAI, fAPAR and fCover of winter wheat in Bulgaria. *European Journal of Remote Sensing*, *54*(sup1), 89–108. https://doi.org/10.1080/22797254.2020.1839359

Kappelle, M. (2004). TROPICAL FORESTS | Tropical Montane Forests. *Encyclopedia of Forest Sciences*, *1981*, 1782–1792. https://doi.org/10.1016/b0-12-145160-7/00175-7

Karra, K., Kontgis, C., Statman-Weil, Z., Mazzariello, J. C., Mathis, M., & Brumby, S. P. (2021). Global Land Use/Land Cover With Sentinel 2 and Deep Learning. *International Geoscience and Remote Sensing Symposium (IGARSS)*, *2021-July*, 4704–4707. https://doi.org/10.1109/IGARSS47720.2021.9553499

Kumar, P., & Krishna, A. P. (2019). InSAR-Based Tree Height Estimation of Hilly Forest Using

Multitemporal Radarsat-1 and Sentinel-1 SAR Data. *IEEE Journal of Selected Topics in Applied Earth Observations and Remote Sensing*, *12*(12), 5147–5152. https://doi.org/10.1109/JSTARS.2019.2963443

Kumaran, S., Perumal, B., Davison, G., Ainuddin, A. N., Lee, M. S., & Bruijnzeel, L. A. (2011). Tropical montane cloud forests in Malaysia: Current state of knowledge. *Tropical Montane Cloud Forests: Science for Conservation and Management*, 113–120. https://doi.org/10.1017/CBO9780511778384.011

Lang, N., Kalischek, N., Armston, J., Schindler, K., Dubayah, R., & Wegner, J. D. (2021). *Waveforms With Deep Ensembles*. *2018*.

Lary, D. J., Alavi, A. H., Gandomi, A. H., & Walker, A. L. (2016). Machine learning in geosciences and remote sensing. *Geoscience Frontiers*, *7*(1), 3–10. https://doi.org/10.1016/j.gsf.2015.07.003

Lasco, G. (2022). *From mossy forests to vegetable farms | Inquirer Opinion*. https://opinion.inquirer.net/154083/from-mossy-forests-to-vegetable-farms?fbclid=IwAR1bSDaa-pPE8q6Dm_qre42toHIUg2FQ0yPPFy44XRzkhePXw8fJrt1C0cU

Liao, Z., He, B., Quan, X., van Dijk, A. I. J. M., Qiu, S., & Yin, C. (2019). Biomass estimation in dense tropical forest using multiple information from single-baseline P-band PolInSAR data. *Remote Sensing of Environment*, *221*(December 2018), 489–507. https://doi.org/10.1016/j.rse.2018.11.027

Lindsay, J. B. (2014). The Whitebox Geospatial Analysis Tools project and open-access GIS. *Proceedings of the GIS Research UK 22nd Annual Conference*, *April 2014*.

Liu, C., & Wang, S. (2022). Estimating Tree Canopy Height in Densely Forest-Covered Mountainous Areas Using Gedi Spaceborne Full-Waveform Data. *ISPRS Annals of the Photogrammetry, Remote Sensing and Spatial Information Sciences*, *5*(1), 25–32. https://doi.org/10.5194/isprs-annals-V-1-2022-25-2022

Liu, W., Song, C., Schroeder, T. A., & Cohen, W. B. (2008). Predicting forest successional stages using multitemporal Landsat imagery with forest inventory and analysis data. *International Journal of Remote Sensing*, *29*(13), 3855–3872. https://doi.org/10.1080/01431160701840166

Loong, C. K., Kanniah, K. D., & Pohl, C. (2013). *Oil Palm Tree Height Estimation Using InSAR*. 2–5. http://www.a-a-r-s.org/acrs/administrator/components/com_jresearch/files/publications/Ab 0061.pdf

Lu, D., Mausel, P., Brondízio, E., & Moran, E. (2003). Classification of successional forest stages in the Brazilian Amazon basin. *Forest Ecology and Management*, *181*(3), 301–312. https://doi.org/10.1016/S0378-1127(03)00003-3

Ma, L., Liu, Y., Zhang, X., Ye, Y., Yin, G., & Johnson, B. A. (2019). Deep learning in remote sensing applications: A meta-analysis and review. *ISPRS Journal of Photogrammetry and Remote Sensing*, *152*(March), 166–177. https://doi.org/10.1016/j.isprsjprs.2019.04.015

Maraseni, T. N., Cockfield, G., Cadman, T., Chen, G., & Qu, J. (2012). Enhancing the value of multiple use plantations: A case study from southeast Queensland, Australia. *Agroforestry Systems*, *86*(3), 451–462. https://doi.org/10.1007/s10457-012-9506-8

Muhe, S., & Argaw, M. (2022). Estimation of above-ground biomass in tropical afro-montane forest using Sentinel-2 derived indices. *Environmental Systems Research*, *11*(1). https://doi.org/10.1186/s40068-022-00250-y

Ngo, Y. N., Ho Tong Minh, D., Baghdadi, N., & Fayad, I. (2023). Tropical Forest Top Height by

GEDI: From Sparse Coverage to Continuous Data. *Remote Sensing*, *15*(4), 0–16. https://doi.org/10.3390/rs15040975

Nyirambangutse, B., Zibera, E., Uwizeye, F. K., Nsabimana, D., Bizuru, E., Pleijel, H., Uddling, J., & Wallin, G. (2017). Carbon stocks and dynamics at different successional stages in an Afromontane tropical forest. *Biogeosciences*, *14*(5), 1285–1303. https://doi.org/10.5194/bg-14-1285-2017

Olesk, A., Praks, J., Antropov, O., Zalite, K., Arumäe, T., & Voormansik, K. (2016). Interferometric SAR coherence models for Characterization of hemiboreal forests using TanDEM-X dssata. *Remote Sensing*, *8*(9). https://doi.org/10.3390/rs8090700

Oliveira, P. V. C., Zhang, X., Peterson, B., & Ometto, J. P. (2023). Using simulated GEDI waveforms to evaluate the effects of beam sensitivity and terrain slope on GEDI L2A relative height metrics over the Brazilian Amazon Forest. *Science of Remote Sensing*, *7*(March), 100083. https://doi.org/10.1016/j.srs.2023.100083

Parao, M. R., Pablo, J. P., Wagan, A. M., Nestor, J., Garcia, M., & Medina, S. M. (2016). Climate Change Vulnerability Assessment in Selected Highland Areas of Benguet: An Application of VAST-Agro Tool. *Mountain Journal of Science and Interdisciplinary Research*, *77*(September 2016), 1–15.

Paulick, S., Dislich, C., Homeier, J., Fischer, R., & Huth, A. (2017). The carbon fluxes in different successional stages: modelling the dynamics of tropical montane forests in South Ecuador. *Forest Ecosystems*, *4*(1). https://doi.org/10.1186/s40663-017-0092-0

Potapov, P., Li, X., Hernandez-Serna, A., Tyukavina, A., Hansen, M. C., Kommareddy, A., Pickens, A., Turubanova, S., Tang, H., Silva, C. E., Armston, J., Dubayah, R., Blair, J. B., & Hofton, M. (2021a). Mapping global forest canopy height through integration of GEDI and Landsat data. *Remote Sensing of Environment*, *253*, 1–27. https://doi.org/10.1016/j.rse.2020.112165

Potapov, P., Li, X., Hernandez-Serna, A., Tyukavina, A., Hansen, M. C., Kommareddy, A., Pickens, A., Turubanova, S., Tang, H., Silva, C. E., Armston, J., Dubayah, R., Blair, J. B., & Hofton, M. (2021b). Mapping global forest canopy height through integration of GEDI and Landsat data. *Remote Sensing of Environment*, *253*(October 2020), 112165. https://doi.org/10.1016/j.rse.2020.112165

Provincial Governor's Office - Information Technology. (2020). *About the Province – Province of Benguet*. Province of Be. http://benguet.gov.ph/about-the-province/

Rondeaux, G., Steven, M., & Baret, F. (1996). Optimization of soil-adjusted vegetation indices. *Remote Sensing of Environment*, *55*(2), 95–107. https://doi.org/10.1016/0034-4257(95)00186-7

Shendryk, Y., Davy, R., & Thorburn, P. (2021). Integrating satellite imagery and environmental data to predict field-level cane and sugar yields in Australia using machine learning. *Field Crops Research*, *260*. https://doi.org/10.1016/j.fcr.2020.107984

Sheykhmousa, M., Mahdianpari, M., Ghanbari, H., Mohammadimanesh, F., Ghamisi, P., & Homayouni, S. (2020). Support Vector Machine Versus Random Forest for Remote Sensing Image Classification: A Meta-Analysis and Systematic Review. *IEEE Journal of Selected Topics in Applied Earth Observations and Remote Sensing*, *13*, 6308–6325. https://doi.org/10.1109/JSTARS.2020.3026724

Szostak, M., Hawryło, P., & Piela, D. (2018). Using of Sentinel-2 images for automation of the forest succession detection. *European Journal of Remote Sensing*, *51*(1), 142–149. https://doi.org/10.1080/22797254.2017.1412272

Taylor, A. R., Chen, H. Y. H., & VanDamme, L. (2009). A review of forest succession models and their suitability for forest management planning. *Forest Science*, *55*(1), 23–36.

Torres de Almeida, C., Gerente, J., Rodrigo dos Prazeres Campos, J., Caruso Gomes Junior, F., Providelo, L. A., Marchiori, G., & Chen, X. (2022). Canopy Height Mapping by Sentinel 1 and 2 Satellite Images, Airborne LiDAR Data, and Machine Learning. *Remote Sensing*, *14*(16), 1–21. https://doi.org/10.3390/rs14164112

van Ewijk, K. Y., Treitz, P. M., & Scott, N. A. (2011). Characterizing forest succession in central Ontario using lidar-derived indices. *Photogrammetric Engineering and Remote Sensing*, *77*(3), 261–269. https://doi.org/10.14358/PERS.77.3.261

Wallis, C. I. B., Brehm, G., Donoso, D. A., Fiedler, K., Homeier, J., Paulsch, D., Süßenbach, D., Tiede, Y., Brandl, R., Farwig, N., & Bendix, J. (2017). Remote sensing improves prediction of tropical montane species diversity but performance differs among taxa. *Ecological Indicators*, *83*, 538–549. https://doi.org/10.1016/j.ecolind.2017.01.022

Wallis, C. I. B., Homeier, J., Peña, J., Brandl, R., Farwig, N., & Bendix, J. (2019). Modeling tropical montane forest biomass, productivity and canopy traits with multispectral remote sensing data. *Remote Sensing of Environment*, *225*(January), 77–92. https://doi.org/10.1016/j.rse.2019.02.021

Wedajo, G. K. (2017). LiDAR DEM Data for Flood Mapping and Assessment; Opportunities and Challenges: A Review. *Journal of Remote Sensing & GIS*, *06*(04), 2015–2018. https://doi.org/10.4172/2469-4134.1000211

Wilson, E. H., & Sader, S. A. (2002). Detection of forest harvest type using multiple dates of Landsat TM imagery. *Remote Sensing of Environment*, *80*(3), 385–396. https://doi.org/10.1016/S0034-4257(01)00318-2

Xu, C., Ding, Y., Zheng, X., Wang, Y., Zhang, R., Zhang, H., Dai, Z., & Xie, Q. (2022). A Comprehensive Comparison of Machine Learning and Feature Selection Methods for Maize Biomass Estimation Using Sentinel-1 SAR, Sentinel-2 Vegetation Indices, and Biophysical Variables. *Remote Sensing*, *14*(16). https://doi.org/10.3390/rs14164083

Zanaga, D., Van De Kerchove, R., De Keersmaecker, W., Souverijns, N., Brockmann, C., Quast, R., Wevers, J., Grosu, A., Paccini, A., Vergnaud, S., Cartus, O., Santoro, M., Fritz, S., Georgieva, I., Lesiv, M., Carter, S., Herold, M., Li, L., Tsendbazar, N.-E., … Arino, O. (2021). *ESA WorldCover 10 m 2020 v100*. https://doi.org/10.5281/ZENODO.5571936

6.3. Summary and links

This study explored the mapping of successional stages in different forest types in Benguet province, Philippines. The study also demonstrated the significance of modelling canopy height along with other variables to understand the succession levels in the three types of vegetation found in the study area. The correlation between InSAR products and field canopy height was found to be weak positive ($r^2 = 0.18$). This study confirms that using GEDI data in locations with undulating terrain and dense vegetation might result in inaccurate data. Combining S-1, S-2, auxiliary variables, and biophysical data effectively classifies successional stages with an Overall Accuracy (OA) of 79.56% and a Kappa Index (KI) of 75.74%. Utilizing the top 10 variables specified by random forest (RF) feature importance improved the model with an OA of 84.22% and a KI of 81.19%. It was also determined that elevation had the greatest influence on forest types distribution of all the variables subjected to modelling. Pine forests, both mature and young, dominated the lower elevations, while mossy forests are generally located in higher elevations, indicating their preference for cooler and wetter conditions. In addition, this study calls for a strong conservation effort, as the assessment found the presence of non-forests and disturbances in all areas. A carbon stock analysis is beneficial in understanding the forest dynamics in the study area. Finally, this research can be used by policymakers to protect native plants, reduce the spread of invasive species, and conserve biodiversity by identifying critical habitats.

A comprehensive analysis of above-ground biomass and carbon density across the three vegetation types of Benguet province is presented in the next chapter (Chapter 7). This study combines satellite imagery and machine learning techniques to create statistical and spatially explicit carbon stock models.

CHAPTER 7: PAPER 4 – ABOVE-GROUND CARBON AND DENSITY OF THE PHILIPPINE'S TOWERING MOUNTAINS

7.1. Introduction

The discussion on machine learning (ML)-based mapping of successional stages in the province of Benguet using Interferometric Synthetic Aperture Radar (InSAR) imagery, the Global Ecosystem Dynamics Investigation data (GEDI), Sentinel products, and biophysical data was provided in the previous chapter (Chapter 6). In the current chapter, a non-destructive estimation of above-ground biomass (AGB) and above-ground carbon (AGC) using Sentinel-1 (S-1), Sentinel-2 (S-2) and biophysical data with machine learning (ML) is presented. Similarly, this article explores various ML applications (i.e., statistical regression, spatially explicit model, and feature selection). Another innovation of this article is the allometric equation for the dwarf bamboo *(Yushania niitakayamensis)* that thrives at Mt. Pulag National Park's summit. In addition, different ML algorithms in the WEKA statistical software were pitted against one another to evaluate their ability to predict AGB.

7.2. Published paper

The subsequent page contains the published version of the article in *PFG – Journal of Photogrammetry, Remote Sensing and Geoinformation Science* (Q1 – top 25% in Earth and Planetary Sciences field). The journal's publisher is Springer International Publishing AG. Its source normalized impact per publication (SNIP) in 2022 is 1.17 and has an impact factor (IF) of 3.2. The journal's h-index is 29.

Appendix 1. ***AGB modelling for Yushania niitakayamensis (dwarf bamboo)***

The absence of live specimens and established allometric equations for the dwarf bamboo *Yushania niitakayamensis* in the study area was addressed by creating an alternative allometric equation based on the collected data, namely clump basal diameter and height. The absence of live specimen collection is attributed to the legal protection measures implemented by the Republic of the Philippines, namely Republic Act No. 1586 and DENR-PAMB Resolution No. 24 series of 2022. These regulations specifically outline the requirement for non-destructive data gathering methods inside the study area. To accomplish the crafting of the allometric equation, 19 samples were randomly selected from the study site, and their fresh weight was calculated using the formula for the volume of a cylinder ($\pi r^2 h$) multiplied by the specific gravity 0.4g/cm^3 and then converted to kg. The specific gravity of different bamboo species varies from 0.4 to 0.8 g/cm^3 (Wakchaure & Kute, 2012), with some species possessing even higher values. Based on this range, the chosen value of 0.4 g/cm^3 lies within the reported range's lower end and is thus a conservative estimate of the specific gravity of dwarf bamboo. The dry weight, in this study interchangeably referred to as the pseudo AGB, was calculated as the difference between the fresh weight and the assumed moisture content of 80% (Wakchaure & Kute, 2012). However, the validity of this assumption may vary depending on the age and species of the bamboo (Wi et al., 2017). Hence, this assumption must be used cautiously in future studies.

Five allometric models were created using height (ht), clump base diameter (cbd), and dry weight, including a simple linear regression model and logarithmic transformations in which either one or both variables were log-transformed. In addition, a Bayesian linear regression model was created to investigate the relationship between the variables in greater depth (Appendix table 1).

The modeling was performed using the statistical programming language R version 4.2.2. Using the lm function, linear regression was performed. Logarithmic models were fitted by transforming the variables with the log function and then fitting them with the lm function. In addition, the final model was estimated using the log-transformed dependent and independent variables and the bayeslm function.

Appendix table 1. The generated models for *Yushania niitakayamensis*

Model	Allometric Equation
Linear regression formula (model 1)	AGB (kg) = -16.53 + 0.1 * ht + 0.45 * cbd
Log height formula (model 2)	AGB (kg)= -41.13+ 7.80*LN(Ht) + 0.43* cbd
Log basal diameter formula (model 3)	AGB (kg)= -61.34 + 0.10 * Height + 17.46* LN(cbd)
Log ht cbd formula (model 4)	AGB (kg)= -82.89 + 7.38 * LN(Ht) + 16.80 * LN(cbd)
Bayesian linear regression (model 5)	AGB (kg) = exp(-9.39) * height^0.95 * cbd^1.98

A scatterplot was created to compare the predicted performance of the five AGB models against the pseudo AGB (Appendix figure 1). The dashed line represents the dry weight assumed as the pseudo AGB values, and the dots are the predicted values by the models as represented by the varying colors. The result indicates that all models could predict the AGB with certain levels of accuracy. Model 1, in particular, appears to overpredict the AGB, while models 2 to 5 produced a better prediction.

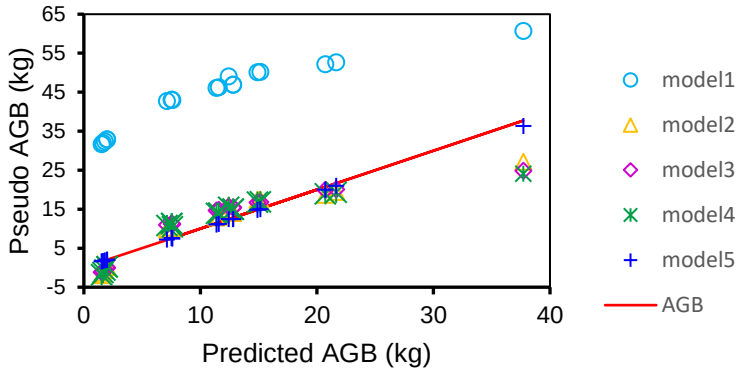

Appendix figure 1. Scatter plot showing the AGB prediction of five models vs the pseudo AGB of *Yushania niitakayamensis*

Appendix table 2 compares the five different model predictions of AGB vs. the pseudo value of AGB using root mean square error, r coefficient and adjusted r squared as basis. In general, it is inferred that model 5 best fits the AGB based on low RMSE and a value of R-squared close to 1. This is consistent with the result shown in appendix figure 1, where most of the predicted values of model 5 almost fit along the pseudo AGB values. However, it is also important to remember that the models developed in this study were based on proxy values and not the actual AGB obtained through the destructive method of generating an allometric equation. Therefore, future applications of these models must be approached with extreme caution. It may be necessary to conduct additional research to confirm the applicability and dependability of the models for predicting AGB in other settings or under different conditions.

Appendix table 2. Model validation of predicted AGB against the estimated AGB of *Yushania niitakayamensis* using field data

Model	RMSE	r coefficient	Adjusted r^2
Model 1	143.3376	0.9306	0.85375
Model 2	0.752	0.9240	0.83125
Model 3	10.489972	0.8894	0.76375
Model 4	0.037206	0.8839	0.7525
Model 5	0.905928	0.9998	0.98875

Appendix table 3. The machine learning algorithm tested in this study and its general description based on Frank et al., (2016) and at this website: https://weka.sourceforge.io/doc.dev/overview-summary.html

	Algorithm	Type	Description
1.	Additive Regression	Meta	Enhances the regression base classifier performance.
2.	Alternating model tree	Trees	In a single tree structure, this algorithm provides the predictive power of the decision tree ensembles.
3.	Bagging	Meta	Reduces variance by bagging a classifier.
4.	Decision Stump	Trees	A simple one-level binary tree builder with missing value handling.
5.	Decision Table	Rules	Utilizes best-first search to evaluate feature subsets and perform evaluation using cross-validation.
6.	ElasticNet	Functions	Performs linear regression by using elastic method.
7.	Gaussian Processes	Functions	Performs non-linear regression with Bayesian Gaussian process technique implementation.
8.	IBk	Lazy	Implements the simplest lazy learner k-nearest-neighbor classifier.
9.	Isotonic Regression	Functions	Uses the attributes that came from the lowest squared error.
10.	Iterative Absolute Error Regression	Meta	Uses Schlossmacher's iteratively reweighted least squares method to fits model with minimized absolute error.
11.	K*	Lazy	Generalizes distance function through transformation.
12.	LeastMedSq	Functions	Generated from random subsamples of the data, and uses the lowest median squared error as the model.
13.	Linear regression	Functions	Performs regression with attribute selection, either greedily or by dropping terms based on standardized coefficients until a stopping criteria is met.
14.	LWL	Lazy	An algorithm for locally weighted learning.
15.	M5P	Trees	A variation of M5.
16.	M5P Rules	Rules	Acquires regression rules from M5.
17.	Multilayer Perceptron	Functions	Trained using back propagation and is a type of neural network.
18.	Random Forest	Trees	Builds random forests by constructing ensembles of randomized trees through bagging.
19.	Random Sub Space	Meta	Creates an ensemble classifier that is trained through randomly selected attributes as input.
20.	Random Tree	Trees	Randomly builds tree through feature selection at each node without pruning.
21.	Random Committee	Meta	Builds ensemble of base classifiers and averages the resulting predictions.
22.	Randomisable Filtered Classifier	Meta	A class designed to execute any classifier on data that has been pre-processed by an arbitrary filter.
23.	Regression by Discretization	Meta	Discretizes the class attribute into specified number of bins and employs a classifier.
24.	RepTree	Trees	Optimizes decision or regression tree using information gain/ variance and reduced error pruning.
25.	SMOreg	Functions	Uses the sequential minimal optimization algorithm.

Appendix table 4: The machine learning algorithms tested in various predictor categories used in this study, showing the Pearson's r correlation coefficient and RMSE.

Algorithms	Biophysical		Optical index		Optical		Radar index		Radar index with elev		Radar	
	r	RMSE	r	RMSE	r	RMSE	r	RMSE	r	RMSE	r	RMSE
Additive Regression	0.712	135.807	0.710	140.399	0.677	144.171	0.377	177.633	0.458	170.183	0.471	167.441
Alternating model tree	0.753	148.011	0.064	2808.629	0.421	231.722	0.149	282.205	0.288	223.822	0.157	250.773
Bagging	0.753	124.700	0.724	130.927	0.689	138.678	0.301	181.118	0.362	176.426	0.369	176.588
Decision Stump	0.689	137.113	0.677	140.034	0.703	134.526	0.212	186.828	0.212	186.828	0.317	179.260
Decision Table	0.696	140.373	0.712	133.741	0.769	121.210	0.267	187.638	0.248	196.567	0.267	187.638
ElasticNet	0.686	137.804	0.697	135.769	0.678	139.369	0.259	182.852	0.256	182.677	0.286	181.112
Gaussian Processes	0.619	150.663	0.698	135.864	0.658	142.559	0.268	182.145	0.250	183.063	0.301	180.971
IBk	0.786	131.591	0.647	174.402	0.567	176.147	0.266	229.533	0.217	242.542	0.094	240.071
Isotonic Regression	0.716	132.705	0.749	127.108	0.685	138.487	0.165	190.711	0.165	190.711	0.255	183.507
Iterative Absolute Error Regression	0.693	137.467	0.682	139.676	0.709	135.090	0.202	193.942	0.202	193.942	0.161	203.574
*K**	0.827	107.795	0.669	149.847	0.684	148.189	0.213	224.713	0.328	198.602	0.225	206.045
LeastMedSq	0.070	220.207	0.106	220.227	0.186	220.091	0.024	220.258	-0.001	220.293	0.015	220.283
Linear regression	0.684	137.962	0.702	135.829	0.657	143.964	0.187	188.772	0.183	189.287	0.181	188.133
LWL	0.687	138.530	0.685	138.429	0.718	131.714	0.341	178.874	0.358	177.264	0.448	169.804
M5P	0.716	132.509	0.718	135.509	0.668	144.879	0.338	178.745	0.295	182.891	0.404	173.403
M5P Rules	0.713	133.443	0.709	137.856	0.609	161.522	0.347	178.196	0.205	195.351	0.400	174.596
Multilayer Perceptron	0.685	152.217	0.667	171.316	0.616	175.477	0.295	206.658	0.370	195.672	0.285	194.006
Random Forest	0.821	108.478	0.709	136.401	0.768	121.460	0.391	175.642	0.460	168.280	0.430	172.922
Random Sub Space	0.750	124.963	0.711	132.818	0.725	130.206	0.345	177.433	0.417	172.582	0.450	169.784
Random Tree	0.694	151.048	0.596	179.459	0.629	169.430	0.103	261.783	0.318	208.834	0.232	244.759
RandomCommittee	0.778	122.860	0.670	150.436	0.750	129.627	0.358	187.043	0.478	170.074	0.397	183.512
RandomisableFilteredClassifier	0.784	131.586	0.647	170.809	0.641	159.900	0.108	269.431	0.181	240.789	0.215	227.449
Regression by Discretization	0.716	140.229	0.675	146.134	0.619	161.762	0.146	212.464	0.287	203.572	0.330	194.284
RepTree	0.683	140.484	0.681	140.052	0.651	145.589	0.235	193.423	0.379	180.757	0.311	184.384
SMOreg	0.669	146.146	0.708	135.313	0.672	145.178	0.187	200.916	0.183	200.608	0.218	202.795

Appendix table 4: Continuation.

Algorithms	All Predictors		Selected features top 5		Selected features top 10	
	r	RMSE	r	RMSE	r	RMSE
Additive Regression	0.678	151.106	0.773	123.324	0.706	137.979
Alternating model tree	0.571	203.408	0.674	156.003	0.749	152.026
Bagging	0.771	120.693	0.767	121.742	0.785	117.490
Decision Stump	0.677	140.034	0.711	133.319	0.670	140.891
Decision Table	0.636	152.538	0.657	147.780	0.664	144.639
ElasticNet	0.708	133.469	0.687	137.594	0.708	133.507
Gaussian Processes	0.705	134.169	0.662	142.102	0.702	134.730
IBk	0.658	154.402	0.779	130.246	0.761	133.017
Isotonic Regression	0.749	127.108	0.749	127.108	0.671	143.151
Iterative Absolute Error Regression	0.682	139.676	0.715	133.656	0.676	140.899
*K**	0.713	142.433	0.832	106.682	0.835	107.335
LeastMedSq	-0.015	220.403	0.059	220.219	0.023	220.318
Linear regression	0.629	158.256	0.673	140.225	0.698	137.080
LWL	0.700	135.365	0.697	136.058	0.696	136.045
M5P	0.746	126.764	0.765	121.864	0.804	112.791
M5P Rules	0.714	136.903	0.739	129.545	0.757	129.779
Multilayer Perceptron	0.548	198.032	0.689	151.035	0.763	133.183
Random Forest	0.786	117.244	0.822	108.226	0.819	108.933
Random Sub Space	0.726	130.121	0.787	116.823	0.765	121.711
Random Tree	0.635	166.050	0.752	141.800	0.625	170.481
RandomCommittee	0.779	119.557	0.824	109.449	0.814	111.049
RandomisableFilteredClassifier	0.580	181.427	0.756	138.363	0.782	124.949
Regression by Discretization	0.668	152.245	0.775	130.008	0.759	125.406
RepTree	0.634	149.801	0.707	137.514	0.681	147.494
SMOreg	0.674	140.357	0.665	146.631	0.683	139.758

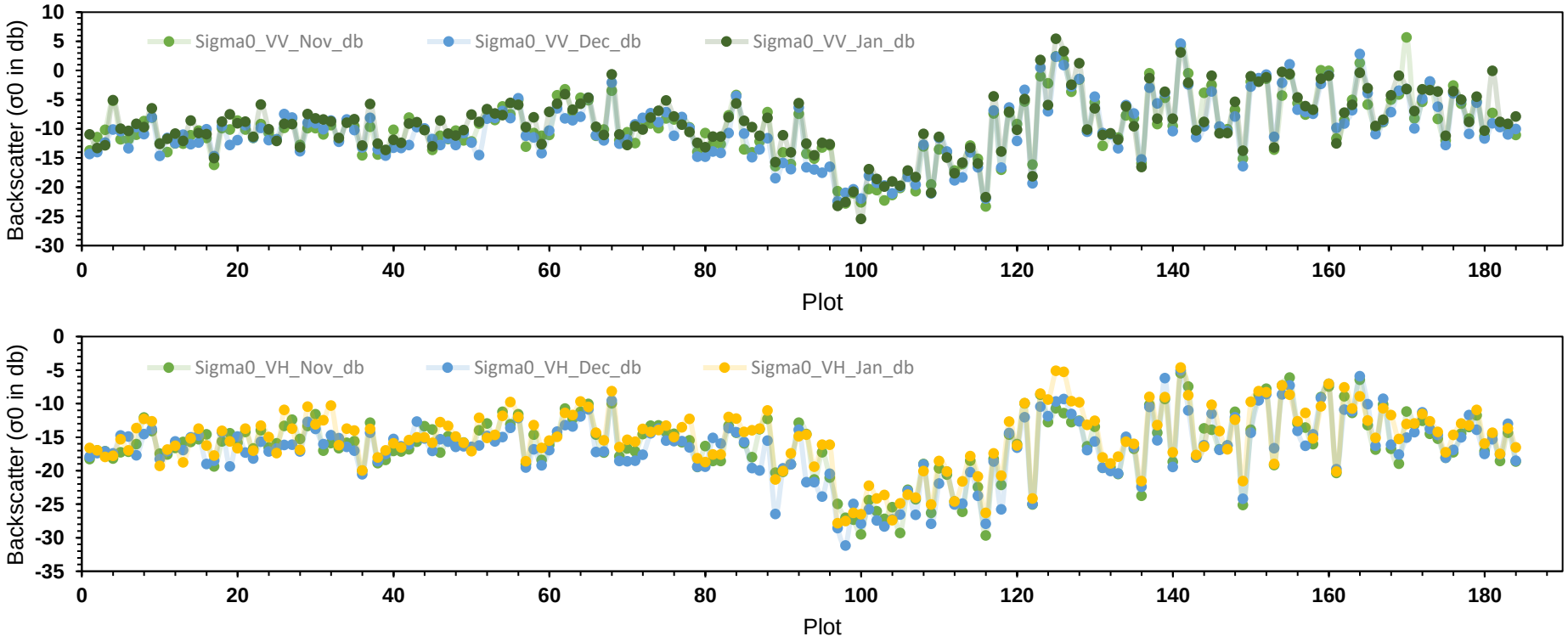

Appendix figure 2. The trend of Sentinel-1 VV and VH backscatter for November 2022, December 2022 and January 2023 per sampling plots

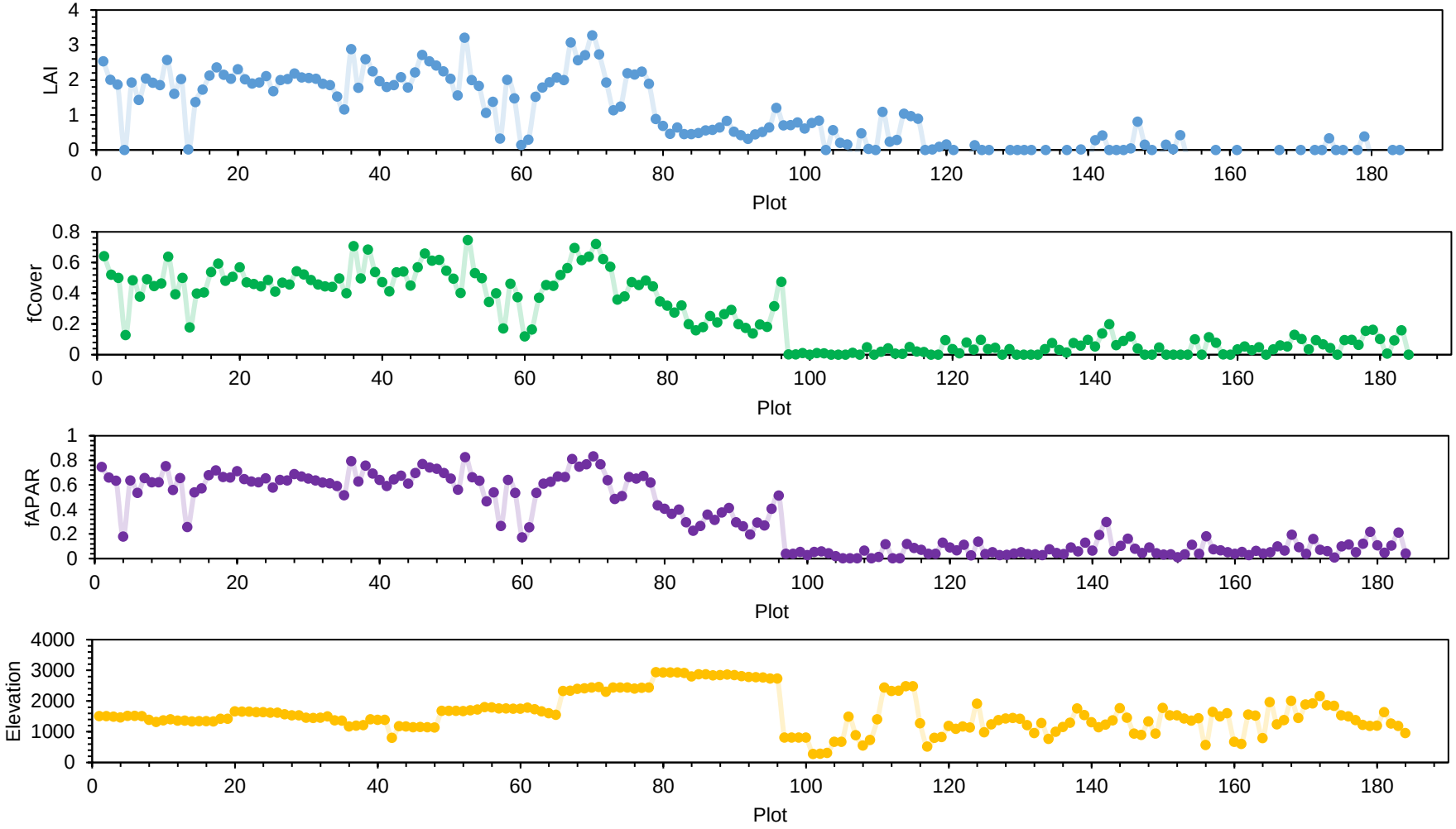

Appendix figure 3. The trend of LAI, fCover, fAPAR and Elevation per sampling plots

References:

Frank, E., Hall, M. A., & Witten, I. H. (2016). The WEKA workbench. In M. Kaufmann (Ed.), *Online Appendix for "Data Mining: Practical Machine Learning Tools and Techniques"* (Fourth Edi).

Wakchaure, M. R., & Kute, S. Y. (2012). Effect of moisture content on physical and mechanical properties of bamboo. *Asian Journal of Civil Engineering*, *13*(6), 753–763.

Wi, S. G., Lee, D. S., Nguyen, Q. A., & Bae, H. J. (2017). Evaluation of biomass quality in short-rotation bamboo (Phyllostachys pubescens) for bioenergy products. *Biotechnology for Biofuels*, *10*(1), 1–11. https://doi.org/10.1186/s13068-017-0818-9

7.3. Summary and links

This chapter presented the synergistic approach of ML, S-1, S-2, and other biophysical parameters to explore the estimation of AGB and AGC in the province of Benguet, Philippines. This research has demonstrated the efficacy of optical and radar satellite imagery, in conjunction with ML, to accurately predict AGB and AGC across various vegetation types within a tropical montane forest. The combination of the elevation band with other biophysical data from S-2 consisting of LAI, fAPAR, and fCover and vegetation indices such as NDVI can accurately predict AGB (r = 0.657 to 0.832; RMSE = 106.682 Mgha-1 to 156.03 Mgha-1) and circumvent the challenges of TMFs assessment. This study also discussed the importance of multi-date S-1, radar vegetation index and elevation in AGB estimation.

A significant contribution of this study lies in its statement that replicating ML algorithm models possess challenges. ML models are inherently stochastic, with random inputs resulting in variable predictions even with a consistent algorithm across different software platforms. In contrast, this stochasticity is important to ML because it maintains the input randomness while still employing training samples that may represent the underlying variability of data in its natural environment. In addition, random forest (RF) proved its effectiveness in selecting important features for AGB. Among all other ML algorithms tested for spatially explicit modelling, RF has accurately predicted the study site's AGB (r = 0.962; RMSE = 53.980 Mgha-1). The study area's AGC ranges from 0 to 434.94 $Mgha^{-1}$. Higher-elevation forests in Benguet were potentially significant for carbon sequestration and forest conservation. Evidence from this study suggests that carbon sequestration capacity in these carbon-rich locations can be commercialized through REDD+ initiatives. In order to safeguard and preserve the province's remaining forests, a strong commitment is required to craft conservation and management policies and ensure their implementation.

The last chapter (Chapter 8) synthesizes and explores the core findings of all the preceding chapters, conclusions, and the limitations and potential for further study.

CHAPTER 8: CONCLUSION

8.1. Introduction

The aim of this study was to evaluate deforestation, successional stages (SS), and carbon stocks of a tropical montane forest (TMF) in the Province of Benguet, Philippines using Sentinel-1 (S-1), Sentinel-2 (S-2) and biophysical data with machine learning (ML). To achieve this goal, the research was divided into three objectives, which were addressed in Chapters 4 to 7.

The traditional, ML, and deep learning (DL) classifiers and the variable combination of S-1, S-2, and biophysical data were tested for deforestation mapping. The SS was assessed using InSAR imagery, GEDI data, S-1, S-2, and other biophysical characteristics. This research discusses ML's use in feature selection, regression analysis, and spatially explicit modelling. The non-destructive assessment of above-ground biomass (AGB) and carbon (AGC) was also studied using radar, optical, and biophysical data. This study also compared ML algorithms for statistical AGB prediction and spatially modelled its concentration in the province. All investigations in this thesis used field observation data from December 2022 to January 2023 and spaceborne remote sensing (RS) datasets.

Several novel aspects are introduced in this study: First, it examines forest evaluations in a TMF that has not been studied extensively because of its difficult terrain and steep slopes. It is also the first attempt in Southeast Asia to employ InSAR and GEDI to evaluate successional stages. The use of ML algorithms for statistical regression to predict AGB is novel in TMF research. More so, AGB modelling for TMF and forest research in the Philippines is greatly improved by the combination of spatially explicit regression through ML and spaceborne RS. The development of an allometric equation for dwarf bamboo in the Mount Pulag protected landscape (MPPL) is an important addition to the existing body of knowledge. Finally, a DL classification of land use land cover (LULC) has been tested, particularly the U-Net Convolutional Neural Network (CNN), believed to be the first of its kind in the Philippines.

8.2. Summary of findings

The following provides an in-depth summary of the findings of each study that has been published in four different Q1 journals:

a. **Paper 1** – *Spaceborne Satellite Remote Sensing of Tropical Montane Forests: A review of applications and future trends*

- The number of published TMF studies between 1997 and 2021 grew dramatically, with the majority done in the Americas, putting other countries behind. These less-studied countries, particularly Asia, Africa and Oceania, are under rapid deforestation threat, thereby putting the information of TMF dynamics in danger. There is also an information gap about TMF location and size in these nations. According to the literature, researchers preferred optical sensors with low to medium spatial resolution (85.76%), than SAR (12.70%). To acquire the desired result from any inquiry, satellite imaging spatial resolution for TMF assessment must be properly chosen. Further, spaceborne RS applications to TMF are concentrated in the realm of forestry (42.66%), climate science (11.01%), and disaster management (9.63%). Finally, since RS technology evolves, TMFs benefit from these for better assessments. The continuous rise of artificial intelligence, the Internet of Things (IoT), cloud computing, ML and DL, and other statistical and technological tools should also be considered to improve TMF research.

b. **Paper 2** – *Deep Learning U-Net Classification of Sentinel-1 and -2 Fusions Effectively Demarcates Tropical Montane Forest's Deforestation*

- Fusion of S-1, S-2, Biophysical data and other auxiliary variables improved land use land cover (LULC) analysis. The traditional Maximum Likelihood Classifier (MLC) classified satellite imagery adequately in binary categories (mean Overall Accuracy (OA) – 95.22% and mean Kappa Index (KI) – 90.39%). Among the ML methods examined, the RF is robust in LULC classification (mean OA – 94.49% and mean KI – 90.39%). With a more complex LULC categorization of the imagery, U-Net DL beat the traditional

and ML classifiers (mean OA – 86.77% and mean KI – 78.89%). The best LULC model recorded a deforested area of 417.93 km^2 in the study site from 2015 to 2022. This study also indicated that forests near human settlements or agriculture are more likely to be converted for human use. Remote locations without roads or water can face deforestation too. Deforestation is also present in high-elevation areas and will occur in any part of the world. Therefore, TMF preservation and sustainable management are crucial. Future studies should consider ecological succession dynamics in the study area. Finally, policymakers and legislators can use this data to create Benguet'scomprehensive TMF conservation strategy.

c. Paper 3 – *Integrated multi-satellite data and machine learning approach in mapping the successional stages of forest types in a tropical montane forest*

- The study showed the importance of modelling canopy height and using it with other variables to explain SS in the three vegetation types of Benguet province, Philippines. InSAR products and field canopy height have a weak positive correlation. Incorporating GEDI with InSAR to predict canopy height presents less accurate outputs (r = –0.2 to 0.04; RMSE = 12 to 13 m). Further, this study shows that GEDI may produce erroneous data in TMF with undulating terrain and dense vegetation. SS can be modelled using S-1, S-2, auxiliary variables, and biophysical data, generating an Overall Accuracy (OA) of 79.56% and a Kappa Index (KI) of 75.74%. Using the top 10 random forest (RF) feature importance variables, improved the model by 5.53% OA (84.22%) and 6.71% KI (81.19%). Among all the variables considered in the model, it was found that elevation had the greatest influence on the forest type distribution. Young and mature pine forests dominate Benguet, whereas mossy forests are generally found in higher elevations with colder, wetter, and windy microclimate. The study also discovered non-forests and disturbances in all locations, necessitating a major conservation effort. An assessment of carbon stock may further help to understand forest dynamics in the area of study. Lastly, policymakers can use this data to safeguard native plants, control invasive species, and maintain biodiversity by identifying crucial habitats in the ecosystems.

d. **Paper 4** – *Uncovering the Hidden Carbon Treasures of the Philippine's Towering Mountains: A synergistic exploration using satellite imagery and machine learning*

- Optical and radar satellite imagery and ML can accurately predict AGB and AGC across TMF vegetation types. The elevation band, LAI, fAPAR, fCover, and vegetation indices such as NDVI from S-2 may accurately predict AGB (r = 0.657 to 0.832; RMSE = 106.682 Mgha-1 to 156.03 $Mgha^{-1}$). RF proved to be superior in selecting important features for AGB estimation. Of the spatially explicit ML methods examined, RF accurately predicted the study site's AGB (r = 0.962; RMSE = 53.980 $Mgha^{-1}$). AGC ranged from 0 to 434.94 $Mgha^{-1}$ in the research area. Forests in higher elevations in Benguet have potential significance for carbon sequestration and forest conservation. This study implies that REDD+ projects can commercialise carbon sequestration capacity in these carbon-rich locations. Conserving and managing the province's remaining forests requires a significant commitment to policy creation and its implementation.

8.3. Conclusion

The findings of this investigation indicate that deforestation remains an issue in Benguet. From 2015-2022, using the fusion of S-1, S-2 and auxiliary variables and U-Net DL, an area of 417.93 km^2 in the study site was deforested. Based on forest characterization, it was found that the closer a forest is to human settlement or agricultural land, the more susceptible it is to be converted. Additionally, deforestation occurs in areas remote from roads and bodies of water. This phenomenon indicates that forest degradation occurs in inaccessible areas. Additionally, the study confirms that deforestation occurs even at high elevations. This assessment of deforestation was conducted predominantly using RS and ML. The fusion of S-1, S-2, auxiliary variables including the grey level co-occurrence matrix (GLCM), vegetation indices and biophysical data were the best combination for LULC assessment. In terms of classifiers, it was determined that traditional MLC is more advantageous for binary LULC classification, but RF remains the best among all ML algorithms. Nonetheless,

when compared to six (6) LULC categories, the U-Net proved to be superior than traditional and ML algorithms.

The assessment of SS provides a fundamental understanding of TMF's dynamics, which is geared towards its preservation and monitoring of degradation and regeneration. The study found that mature and young pine forests dominate the lower elevations, and mossy forests dominate the higher elevations. Pine forest growth has changed dramatically in the studied region, which is attributable to its accessibility. News reports additionally reveal changes in mossy forests. The presence of non-forests and disturbances emphasizes the need to preserve the remaining forests and reduce human disturbances. According to available literature, TMF recovery takes 65–85 years, and epiphytic plants and other flora regenerate in 50 years. ML-based SS assessment demonstrated that S-1, S-2, auxiliary variables, and biophysical data work successfully for SS mapping. This study shows that InSAR products have a weak positive correlation with field canopy height and that coherence improves its accuracy. The findings further support the literature that GEDI was unsuitable for canopy height modelling in heavily vegetated mountainous locations. However, RF improves SS mapping by finding the ten most important features that significantly influence the model. This study also showed that elevation greatly affected the province's forest types. This condition happens because temperature, moisture, and soil quality influenced by elevation, positively affect plant development.

The AGB of the study site was calculated using a non-destructive field observation method. Results showed that the mean AGB in pine forest is 284.75 $Mgha^{-1}$, 380.33 $Mgha^{-1}$ in mossy forest, and in the grassland summit is 39.93 $Mgha^{-1}$. This study discovered that the mean AGB of 251.79 $Mgha^{-1}$ in the entire province is 17% higher than the literature-reported AGB in 2000. The mean AGC was calculated to be 118.341 $Mgha^{-1}$, which is comparable to what has been found in the majority of published papers. Despite the steep elevation of the study site, the results indicate that the area contains significant amounts of carbon. Thus, indicating the province as potential target for conservation, and a good sign to incentivize its carbon sequestration through REDD+ interventions. The biophysical data derived from S-2 comprising of LAI, fAPAR, fCover, the vegetation index NDVI and elevation accurately predicted AGB through RF. Unfortunately, using multi-date S-1, radar vegetation index, and S-1-derived auxiliary variables shows weak correlation with field AGB. It was further found

that the RF, among other ML algorithms, proved to be superior in feature selection, statistical regression and spatially explicit modelling of carbon stock.

In general, this research highlights the value of SAR and optical imagery. These two types of RS technology are gaining prominence in TMF evaluations. Using RS technology to circumvent the harshness of TMF when conducting field assessments emphasizes the crucial need to utilize and develop them. Also, the potential of ML in enhancing LULC analysis, deforestation mapping, SS modelling, and AGB and AGC estimation has been demonstrated by the effective implementation of ML and DL techniques such as RF and U-Net. The results of this research have implications for environmental policy on a global level. Deforestation, for instance, may have universal causes. The conditions that lead to it may be the same everywhere. Given the global scope of deforestation, it is crucial that forests be protected. The identified disturbances in the study area call for intensified conservation efforts. Protecting important habitats and controlling the damage caused by invasive species are both crucial. Information presented in this thesis can be used by policymakers in the Philippines and other regions with similar forest types to guide land use planning and establish policies that encourage sustainable resource management and conservation initiatives.

The findings of this study advance our understanding of TMFs, and it provides valuable information for lawmakers and authorities. Ultimately, this study underscores the importance of the continued and shared responsibility of safeguarding the remaining forests for future generations.

8.4. Recommendation

This study highlights the critical importance of studying the Benguet's TMF. The research in this thesis must be refined and improved to better our understanding and craft suitable TMF conservation and management strategies. The following are suggested areas for further study:

- For the deforestation and LULC study, the reliance on selected GLCM textures potentially affected analysis result. There is a need to explore adding other GLCM textures in the analysis in the future to test their influence on improving the

assessment. The use of other optical sensors, such as those provided by commercial satellites (e.g., IKONOS, QuickBird, SPOT, etc.), could be explored. Likewise, the utility of other SAR satellites (ALOS-PALSAR, NovaSAR, etc.) with longer wavelengths should also be considered. The LULC classification results may also benefit from the use of other vegetation indices that highly correspond to forest analysis. Further, other DL classifiers or CNN types (ResNet, PSPNet and DeepLabV3) can be pitted against each other to test their effectiveness in LULC assessment. Finally, future research is strongly encouraged to take seasonal variation into account.

- The diverse nature of the factors that affect TMF ecological succession calls for an in-depth investigation into the SS in future studies. The age of the trees, soil qualities, microclimate, and biodiversity indicators might all be analysed thoroughly to shed light on their role in SS. Adding a time-series SS map to the TMF would also be beneficial for recognising temporal trends and disturbances in the study area. Finally, using state-of-the-art technology like Light Detection and Ranging (LiDAR) could provide insights into the in-depth structural dimension of TMFs that is important for ecological succession. The use of hyperspectral imagery could also improve the spectral dimensions requirement for studying SS.

- Future research should develop species-specific allometric models for mossy forest trees and dwarf bamboo to enhance carbon estimation accuracy. To evaluate the carbon sequestration interventions in Benguet's TMF, carbon stock should be monitored throughout time. Additional biophysical data (such as soil fertility) and study plots should be examined for better correlational studies. The AGB estimation can be improved using LiDAR data, which matches vegetation structural components. SAR data with longer wavelengths (S-, L-, and P-bands) and hyperspectral optical imaging should be tried to improve biomass and carbon stock estimates. Including below-ground biomass (BGB) is also recommended for future study to account for the total carbon stock of the study area.

REFERENCES

Ahrends, A., Bulling, M. T., Platts, P. J., Swetnam, R., Ryan, C., Doggart, N., Hollingsworth, P. M., Marchant, R., Balmford, A., Harris, D. J., Gross-Camp, N., Sumbi, P., Munishi, P., Madoffe, S., Mhoro, B., Leonard, C., Bracebridge, C., Doody, K., Wilkins, V., … Burgess, N. D. (2021). Detecting and predicting forest degradation: A comparison of ground surveys and remote sensing in Tanzanian forests. In *Plants People Planet* (Vol. 3, Issue 3, pp. 268–281). https://doi.org/10.1002/ppp3.10189

Albrich, K., Rammer, W., & Seidl, R. (2020). *Climate change causes critical transitions and irreversible alterations of mountain forests*. *July 2019*, 4013–4027. https://doi.org/10.1111/gcb.15118

Alloghani, M., Al-Jumeily, D., Mustafina, J., Hussain, A., & Aljaaf, A. J. (2020). A Systematic Review on Supervised and Unsupervised Machine Learning Algorithms for Data Science. In *Unsupervised and Semi-Supervised Learning*.

Altarez, R. D. D., Apan, A., & Maraseni, T. (2022). Spaceborne satellite remote sensing of tropical montane forests: a review of applications and future trends. *Geocarto International*, *0*(0), 1–29. https://doi.org/10.1080/10106049.2022.2060330

Anderson-Teixeira, K. J., Wang, M. M. H., Mcgarvey, J. C., & Lebauer, D. S. (2016). Carbon dynamics of mature and regrowth tropical forests derived from a pantropical database (TropForC-db). *Global Change Biology*, *22*(5), 1690–1709. https://doi.org/10.1111/gcb.13226

Apan, A., Suarez, L. A., Maraseni, T., & Castillo, J. A. (2017). The rate, extent and spatial predictors of forest loss (2000–2012) in the terrestrial protected areas of the Philippines. *Applied Geography*, *81*, 32–42. https://doi.org/10.1016/j.apgeog.2017.02.007

Argamosa, J. L., Blanco, R. C., Baloloy, A. B., Candido, A. G., Dumalag, C., DImapilis, L. C., & Paringit, E. (2018). Modelling above ground biomass of mangrove forest using Sentinel-1 imagery. *ISPRS Annals of the Photogrammetry, Remote Sensing and Spatial Information Sciences*, *4*(3), 13–20. https://doi.org/10.5194/isprs-annals-IV-3-13-2018

Aslan, A., Rahman, A. F., & Robeson, S. M. (2018). Investigating the use of Alos Prism data in detecting mangrove succession through canopy height estimation. *Ecological Indicators*, *87*(December 2017), 136–143. https://doi.org/10.1016/j.ecolind.2017.12.008

Avtar, R., Tsusaka, K., & Herath, S. (2020). Assessment of forest carbon stocks for REDD+ implementation in the muyong forest system of Ifugao, Philippines. *Environmental Monitoring and Assessment*, *192*(9). https://doi.org/10.1007/s10661-020-08531-8

Banaticla, M. R., Sales, R., & Lasco, R. (2007). Biomass Equations for Tropical Tree Plantation Species in Young Stands Using Secondary Data from the Philippines. *Annals of Tropical Research*, *Parde 1980*, 73–90. https://doi.org/10.32945/atr2937.2007

Belgiu, M., & Drăgu, L. (2016). Random forest in remote sensing: A review of applications and future directions. *ISPRS Journal of Photogrammetry and Remote Sensing*, *114*, 24–31. https://doi.org/10.1016/j.isprsjprs.2016.01.011

Benner, J., Vitousek, P. M., & Ostertag, R. (2011). Nutrient cycling and nutrient limitation in tropical montane cloud forests. *Tropical Montane Cloud Forests: Science for Conservation and Management*, 90–100. https://doi.org/10.1017/CBO9780511778384.009

Berveglieri, A., Tommaselli, A. M. G., Imai, N. N., Ribeiro, E. A. W., Guimarães, R. B., & Honkavaara, E. (2016). Identification of Successional Stages and Cover Changes of Tropical Forest Based on Digital Surface Model Analysis. *IEEE Journal of Selected Topics in Applied Earth Observations and Remote Sensing*, *9*(12), 5385–5397.

https://doi.org/10.1109/JSTARS.2016.2606320
Biggs, T., Dunne, T., Roberts, D. A., & Matricardi, E. (2008). The Rate and Extent of Deforestation in Watersheds of the Southwestern Amazon Basin. *Ecological Applications*, *18*(1), 31–48.
Bispo, P. D. C., Pardini, M., Papathanassiou, K. P., Kugler, F., Balzter, H., Rains, D., dos Santos, J. R., Rizaev, I. G., Tansey, K., dos Santos, M. N., & Spinelli Araujo, L. (2019). Mapping forest successional stages in the Brazilian Amazon using forest heights derived from TanDEM-X SAR interferometry. *Remote Sensing of Environment*, *232*(May), 111194. https://doi.org/10.1016/j.rse.2019.05.013
Brenning, A., Schwinn, M., Ruiz-Páez, A. P., & Muenchow, J. (2015). Landslide susceptibility near highways is increased by 1 order of magnitude in the Andes of southern Ecuador, Loja province. *Natural Hazards and Earth System Sciences*, *15*(1), 45–57. https://doi.org/10.5194/nhess-15-45-2015
Brown, S. (1997). Estimating Biomass and Biomass Change of Tropical Forests: a Primer. (FAO Forestry Paper - 134), Available at http://www.fao.org/docrep/w4095e/w4095e00.htm. *FAO Forestry Paper 134*, *January 1997*, 1–4.
Brown, S., & Lugo, A. (1990). Tropical secondary forests. *Journal of Tropical Ecology*, *6*, 1–32. https://doi.org/10.1177/030913339501900201
Bruijnzeel, L. A., & Veneklaas, E. J. (1998). Climatic conditions and tropical montane forest productivity: The fog has not lifted yet. *Ecology*, *79*(1), 3–9. https://doi.org/10.1890/0012-9658(1998)079[0003:CCATMF]2.0.CO;2
Buchanan, G. M., Butchart, S. H. M., Dutson, G., Pilgrim, J. D., Steininger, M. K., Bishop, K. D., & Mayaux, P. (2008). Using remote sensing to inform conservation status assessment: Estimates of recent deforestation rates on New Britain and the impacts upon endemic birds. *Biological Conservation*, *141*(1), 56–66. https://doi.org/10.1016/j.biocon.2007.08.023
Cadman, T., Maraseni, T., Sarker, T., & Hwan, O. M. (2017). Comparative evaluation of zero deforestation governance. In *ETFRN News 58* (Vol. 58).
Camarretta, N., Harrison, P. A., Bailey, T., Potts, B., Lucieer, A., Davidson, N., & Hunt, M. (2019). Monitoring forest structure to guide adaptive management of forest restoration : a review of remote sensing approaches. *New Forests*, *0123456789*. https://doi.org/10.1007/s11056-019-09754-5
Camps-Valls, G. (2009). Machine learning in remote sensing dataprocessing. *Machine Learning for Signal Processing XIX - Proceedings of the 2009 IEEE Signal Processing Society Workshop, MLSP 2009*, *September 2009*. https://doi.org/10.1109/MLSP.2009.5306233
Carandang, A. P., Bugayong, L. A., Dolom, P. C., Garcia, L. N., Villanueva, M. M. B., Espiritu, N. O., & Forestry Development Center, U. of the P. L. B.-C. of F. and N. R. (2013). *Analysis of Key Drivers of Deforestation and Forest Degradation in the Philippines*. Deutsche Gesellschaft für Internationale Zusammenarbeit (GIZ).
Castel, T., Beaudoin, A., Picard, G., Le Toan, T., Caraglio, Y., & Houllier, F. (2000). Accurate analysis of L-band SAR backscatter sensitivity to forest biomass. *International Geoscience and Remote Sensing Symposium (IGARSS)*, *6*(1), 2564–2566. https://doi.org/10.1109/igarss.2000.859641
Castillo, J. A. A., Apan, A. A., Maraseni, T. N., & Salmo, S. G. (2017). Estimation and mapping of above-ground biomass of mangrove forests and their replacement land uses in the Philippines using Sentinel imagery. *ISPRS Journal of Photogrammetry and Remote Sensing*, *134*, 70–85. https://doi.org/10.1016/j.isprsjprs.2017.10.016
Caughlin, T. T., Barber, C., Asner, G. P., Glenn, N. F., Bohlman, S. A., & Wilson, C. H.

(2021). Monitoring tropical forest succession at landscape scales despite uncertainty in Landsat time series. *Ecological Applications*, *31*(1), 1–18. https://doi.org/10.1002/eap.2208

Chapman, H., Cordeiro, N. J., Dutton, P., Wenny, D., Kitamura, S., Kaplin, B., Melo, F. P. L., & Lawes, M. J. (2016). Seed-dispersal ecology of tropical montane forests. *Journal of Tropical Ecology*, *32*(5), 437–454. https://doi.org/10.1017/S0266467416000389

Chave, J., Réjou-Méchain, M., Búrquez, A., Chidumayo, E., Colgan, M. S., Delitti, W. B. C., Duque, A., Eid, T., Fearnside, P. M., Goodman, R. C., Henry, M., Martínez-Yrízar, A., Mugasha, W. A., Muller-Landau, H. C., Mencuccini, M., Nelson, B. W., Ngomanda, A., Nogueira, E. M., Ortiz-Malavassi, E., … Vieilledent, G. (2014). Improved allometric models to estimate the aboveground biomass of tropical trees. *Global Change Biology*, *20*(10), 3177–3190. https://doi.org/10.1111/gcb.12629

Cronin, D. T., Libalah, M. B., Bergl, R. A., & Hearn, G. W. (2014). Biodiversity and conservation of tropical montane ecosystems in the Gulf of Guinea, West Africa. *Arctic, Antarctic, and Alpine Research*, *46*(4), 891–904. https://doi.org/10.1657/1938-4246-46.4.891

Cruz, M. N., Medina, K. C., Cabriga, A. S., Mendoza, F., & Blanco, A. C. (2019). GIS-assisted rain-induced landslide susceptibility mapping of Benguet using logistic regression model. *International Archives of the Photogrammetry, Remote Sensing and Spatial Information Sciences - ISPRS Archives*, *42*(4/W19), 157–164. https://doi.org/10.5194/isprs-archives-XLII-4-W19-157-2019

De Sy, V., Herold, M., Achard, F., Asner, G. P., Held, A., Kellndorfer, J., & Verbesselt, J. (2012). Synergies of multiple remote sensing data sources for REDD+ monitoring. *Current Opinion in Environmental Sustainability*, *4*(6), 696–706. https://doi.org/10.1016/j.cosust.2012.09.013

Department of Environment and Natural Resources. (2009). Assessing Progress Towards the 2010 Biodiversity Target: The 4th National Report to the Convention on Biological Diversity. In *Convention on Biological Diversity*. www.rufford.org/files/16.05.07 Detailed Final Report.pdf

Department of Environment and Natural Resources - Forest Management Bureau. (2011). *Watershed Characterization and Vulnerability Assessment Using Geographic Information System and Remote Sensing*. i–i. https://doi.org/10.1109/isqed.2008.4479675

Dionisio, D. J., & Agoot, L. (2020). *Almost 900 hectares of natural forest, areas razed in Benguet | Philippine News Agency*. Philippine News Agency. https://www.pna.gov.ph/articles/1094989

dos Santos, J. R., Gama, F. F., & da ConceiçãO Bispo, P. (2014). Estimating forest biomass by remote sensing radar data in brazil. *Drewno* , *57*(192), 120–132. https://doi.org/10.12841/wood.1644-3985.S01.08

Doyog, N. D., Lumbres, R. I. C., & Baoanan, Z. G. (2021). Monitoring of land use and land cover changes in Mt. Pulag national park using landsat and sentinel imageries. *Philippine Journal of Science*, *150*(4), 723–734. https://doi.org/10.56899/150.04.10

Doyog, N. D., Lumbres, R. I. C., & Lee, Y. J. (2018). Mapping of the spatial distribution of carbon storage of the Pinus kesiya Royle ex Gordon (Benguet pine) forest in Sagada, Mt. Province, Philippines. *Journal of Sustainable Forestry*, *37*(7), 661–677. https://doi.org/10.1080/10549811.2018.1450155

Elhag, M., Boteva, S., & Al-Amri, N. (2021). Forest cover assessment using remote-sensing techniques in Crete Island, Greece. *Open Geosciences*, *13*(1), 345–358. https://doi.org/10.1515/geo-2020-0235

Eller, C. B., Meireles, L. D., Sitch, S., Burgess, S. S. O., & Oliveira, R. S. (2020). How

Climate Shapes the Functioning of Tropical Montane Cloud Forests. *Current Forestry Reports*, *6*(2), 97–114. https://doi.org/10.1007/s40725-020-00115-6
Environmental Science for Social Change (ESSC). (1999). *Decline of the Philippine Forest*. https://essc.org.ph/content/archives/80/
Environmental Science for Social Change Inc. (ESSC). (2012). *Cordillera's forests, green water, and watersheds - Institute of Environmental Science for Social Change*. https://essc.org.ph/content/view/617/153/
Espírito-Santo, F. D. B., Shimabukuro, Y. E., & Kuplich, T. M. (2005). Mapping forest successional stages following deforestation in Brazilian Amazonia using multi-temporal Landsat images. *International Journal of Remote Sensing*, *26*(3), 635–642. https://doi.org/10.1080/0143116042000274078
European Space Agency. (2019). *New biomass map to take stock of the world's carbon*. https://www.esa.int/Applications/Observing_the_Earth/Space_for_our_climate/New_biomass_map_to_take_stock_of_the_world_s_carbon
FAO. (2016). Forests and agriculture: land-use challenges and opportunities. In *State of the World's Forests* (Vol. 45, Issue 12). http://ccafs.cgiar.org/news/press-releases/agriculture-and-food-production-contribute-29-percent-global-greenhouse-gas
Fernando, E., & Cereno, R. (2010). Biodiversity and Natural Resources Management in the Mt Pulag National Park, Philippines. In M. H. S. et al. Lapitan, P.G., E.S. Fernando (Ed.), *Biodiversity and Natural Resources Conservation in Protected Areas of Korea and the Philippines* (pp. 120–177). ASEAN-Korea Environmental Cooperation Unit, Seoul National University, Korea.
Ferrer Velasco, R., Lippe, M., Tamayo, F., Mfuni, T., Sales-Come, R., Mangabat, C., Schneider, T., & Günter, S. (2022). Towards accurate mapping of forest in tropical landscapes: A comparison of datasets on how forest transition matters. *Remote Sensing of Environment*, *274*(February). https://doi.org/10.1016/j.rse.2022.112997
Filipponi, F. (2019). *Conferecne Paper.Pdf*. *3*(June), 2–6.
Food and Agriculture Organization—FAO. (2015). Global Forest Resources Assessment 2015. In *Desk Reference*.
Food and Agriculture Organization [FAO]. (2001). *Global ecological zoning for the global forest resources assessment 2000*. http://www.fao.org/3/ad652e/ad652e00.htm
Food and Agriculture Organization [FAO]. (2007). Manual on deforestation, degradation, and fragmentation using remote sensing and GIS. *Food and Agriculture Organization of the United Nations*, *42*(1), 1–20.
Food and Agriculture Organization [FAO]. (2010). *Global Forest Resources Assessment 2010: Guidelines for Country Reporting to FRA 2010*.
Food and Agriculture Organization [FAO]. (2012). Global ecological zones for FAO forest reporting: 2010 Update. *Forest Resources Assessment Working Paper 179*, 42. http://www.fao.org/docrep/017/ap861e/ap861e00.pdf
Food and Agriculture Organization of the United Nations (FAO). (2016). *Field manual for national forest inventory*. *October*. http://wiki.awf.forst.uni-goettingen.de/wiki/index.php/Category:Single_tree_variables
Foody, G. M., & Curran, P. J. (1994). Estimation of Tropical Forest Extent and Regenerative Stage Using Remotely Sensed Data. *Journal of Biogeography*, *21*(3), 223. https://doi.org/10.2307/2845527
Frolking, S., Palace, M. W., Clark, D. B., Chambers, J. Q., Shugart, H. H., & Hurtt, G. C. (2009). Forest disturbance and recovery: A general review in the context of spaceborne remote sensing of impacts on aboveground biomass and canopy structure. *Journal of Geophysical Research: Biogeosciences*, *114*(3). https://doi.org/10.1029/2008JG000911
Galido-Isorena, T. (2011). Mapping Guidebook for Forest Land Use Planning. In *Philippine*

Environmental Governance Project 2.
Gao, Y., Skutsch, M., Paneque-g, J., & Ghilardi, A. (2020). *Remote sensing of forest degradation : a review. Remote sensing of forest degradation : a review*.
Gevana, D. T., & Im, S. (2016). Allometric models for Rhizophora stylosa griff. in dense monoculture plantation in the Philippines. *Malaysian Forester*, *79*(1–2), 39–53.
Ghosh, S. M., Behera, M. D., & Paramanik, S. (2020). Canopy height estimation using sentinel series images through machine learning models in a Mangrove Forest. *Remote Sensing*, *12*(9), 1–21. https://doi.org/10.3390/RS12091519
Gibbs, H. K., Brown, S., Niles, J. O., & Foley, J. A. (2007). *Monitoring and estimating tropical forest carbon stocks : making REDD a reality*. https://doi.org/10.1088/1748-9326/2/4/045023
González-Jaramillo, V., Fries, A., & Bendix, J. (2019). AGB estimation in a tropical mountain forest (TMF) by means of RGB and multispectral images using an unmanned aerial vehicle (UAV). *Remote Sensing*, *11*(12), 1–22. https://doi.org/10.3390/rs11121413
González-Jaramillo, V., Fries, A., Zeilinger, J., Homeier, J., Paladines-Benitez, J., & Bendix, J. (2018). Estimation of above ground biomass in a tropical mountain forest in southern Ecuador using airborne LiDAR data. *Remote Sensing*, *10*(5). https://doi.org/10.3390/rs10050660
Grêt-Regamey, A., & Weibel, B. (2020). Global assessment of mountain ecosystem services using earth observation data. *Ecosystem Services*, *46*. https://doi.org/10.1016/j.ecoser.2020.101213
Hansen, M. C., Potapov, P. V., Moore, R., Hancher, M., Turubanova, S. A., Tyukavina, A., Thau, D., Stehman, S. V., Goetz, S. J., Loveland, T. R., Kommareddy, A., Egorov, A., Chini, L., Justice, C. O., & Townshend, J. R. G. (2013). High-resolution global maps of 21st-century forest cover change. *Science*, *342*(6160), 850–853. https://doi.org/10.1126/science.1244693
Hastie, T., Tibshirani, R., & Friedman, J. (2009). Statistics The Elements of Statistical Learning. *Springer Series in Statistics*, *27*(2), 745. http://www.springerlink.com/index/D7X7KX6772HQ2135.pdf
Helmer, E. H., Brown, S., & Cohen, W. B. (2000). Mapping montane tropical forest successional stage and land use with multi-date Landsat imagery. *International Journal of Remote Sensing*, *21*(11), 2163–2183. https://doi.org/10.1080/01431160050029495
Hu, X., Huang, B., Verones, F., Cavalett, O., & Cherubini, F. (2021). Overview of recent land-cover changes in biodiversity hotspots. *Frontiers in Ecology and the Environment*, *19*(2), 91–97. https://doi.org/10.1002/fee.2276
Hütt, C., Koppe, W., Miao, Y., & Bareth, G. (2016). Best accuracy land use/land cover (LULC) classification to derive crop types using multitemporal, multisensor, and multi-polarization SAR satellite images. *Remote Sensing*, *8*(8). https://doi.org/10.3390/rs8080684
Intergovernmental Panel on Climate Change (IPCC). (2007). Synthesis Report. Contribution of Working Groups I, II and III to the Fourth Assess- ment Report of the Intergovernmental Panel on Climate Change. In *Intergovernmental Panel on Climate Change*. (ment Repor). IPCC. https://doi.org/10.1038/446727a
Jeyanny V.; Mha, H.; Rasidah, K.W.; Kumar, B. S. . and H. M. . (2014). Carbon stocks in different carbon pools pf a tropical lowland forest and a montane forest with vartying topography. *Journal of Tropical Forest Science*, *26*(4), 560–571.
Jin, X. M., Zhang, Y.-K., Schaepman, M. E., Clevers, J. G. P. W., & Su, Z. (2008). Impact of elevation and aspect on the spatial distribution of vegetation in the Qilian Mountain area with remote sensing data. *International Archives of the Photogrammetry, Remote*

Sensing and Spatial Information Sciences - ISPRS Archives, *37*(July), 1385–1390.
Joseph B. Manzano. (2019). *Cordillera forests on the brink of extinction - Herald Express | News in Cordillera and Northern Luzon*. Herald Express. https://www.baguioheraldexpressonline.com/cordillera-forests-extinction/
Joshi, N. P., Mitchard, E. T. A., Schumacher, J., Johannsen, V. K., Saatchi, S., & Fensholt, R. (2015). L-Band SAR Backscatter Related to Forest Cover, Height and Aboveground Biomass at Multiple Spatial Scales across Denmark. *Remote Sensing*, *7*(4), 4442–4472. https://doi.org/10.3390/rs70404442
Kappelle, M. (2004). Tropical Forest | Tropical Montane Forests. *Encyclopedia of Forest Sciences*, *1981*, 1782–1792. https://doi.org/10.1016/b0-12-145160-7/00175-7
Kauffman, J. B., & Donato, D. C. (2012). *Protocols for the measurement, monitoring and reporting of structure, biomass and carbon stocks in mangrove forests*. https://doi.org/https://doi.org/10.17528/cifor/003749
Körner, Christian; Ohsawa, Masahiko; Spehn, Eva; Berge, Erling; Bugmann, Harald; Groombridge, Brian; Hamilton, Lawrence; Hofer, Thomas; Ives, Jack; Jodha, Narpat; Messerli, Bruno; Pratt, Jane; Price, Martin; Reasoner, Mel ; Rodgers, Alan; Thonell, Jillian, M. (2005). Ecosystems and Human Well-being: Current State and Trends. In *Millennium Ecosystem Assessment* (Vol. 1).
Kowaal, N. E. (1966). *Shifting Cultivation , Fire , and Pine Forest in the Cordillera Central , Luzon , Philippines Author (s): Norman Edward Kowal Published by : Wiley on behalf of the Ecological Society of America Stable URL : https://www.jstor.org/stable/1942374 REFERENCE*. *36*(4), 389–419.
Kuyah, S., Dietz, J., Muthuri, C., Jamnadass, R., Mwangi, P., Coe, R., & Neufeldt, H. (2012). Allometric equations for estimating biomass in agricultural landscapes: I. Aboveground biomass. *Agriculture, Ecosystems and Environment*, *158*, 216–224. https://doi.org/10.1016/j.agee.2012.05.011
Lapini, A., Pettinato, S., Santi, E., Paloscia, S., Fontanelli, G., & Garzelli, A. (2020). Comparison of machine learning methods applied to SAR images for forest classification in mediterranean areas. *Remote Sensing*, *12*(3). https://doi.org/10.3390/rs12030369
Lary, D. J., Alavi, A. H., Gandomi, A. H., & Walker, A. L. (2015). Geoscience Frontiers Machine learning in geosciences and remote sensing. *Geoscience Frontiers*, 1–9. https://doi.org/10.1016/j.gsf.2015.07.003
Lary, D. J., Alavi, A. H., Gandomi, A. H., & Walker, A. L. (2016). Machine learning in geosciences and remote sensing. *Geoscience Frontiers*, *7*(1), 3–10. https://doi.org/10.1016/j.gsf.2015.07.003
Lary, D. J., Zewdie, G. K., Liu, X., Wu, D., Levetin, E., Allee, R. J., Malakar, N., Walker, A., Mussa, H., Mannino, A., & Aurin, D. (2018). Machine Learning Applications for Earth Observation. In *Earth Observation Open Science and Innovation*. https://doi.org/10.1007/978-3-319-65633-5_8
Lasco, R. D., Pulhin, F. B., Cruz, R. V. O., Pulhin, J. M., & Roy, S. S. N. (2005). Carbon Budgets Of Terrestrial Ecosystems in the Pantabangan-Carranglan Watershed 1. *Sierra*, *2005*(10), 1–23.
Lasco, R D, Pulhin, F. B., Sanchez, P. a J., Villamor, G. B., & Villegas, K. a L. (2008). Climate Change and Forest Ecosystems in the Philippines: Vulnerability, Adaptation and Mitigation. *Journal of Environmental Science and Management*, *11*(1), 1–14.
Lasco, Rodel D., & Pulhin, F. B. (2003). Philippine Forest Ecosystems and Climate Change : Carbon stocks , Rate of Sequestration and the Kyoto Protocol. *Annals of Tropical Research*, *25*(2), 37–51.
Li, G., Lu, D., Moran, E., & Hetrick, S. (2011). Land-cover classification in a moist tropical

region of Brazil with Landsat Thematic Mapper imagery. *International Journal of Remote Sensing*, *32*(23), 8207–8230. https://doi.org/10.1080/01431161.2010.532831

Liao, Z., He, B., Quan, X., van Dijk, A. I. J. M., Qiu, S., & Yin, C. (2019). Biomass estimation in dense tropical forest using multiple information from single-baseline P-band PolInSAR data. *Remote Sensing of Environment*, *221*(December 2018), 489–507. https://doi.org/10.1016/j.rse.2018.11.027

Liu, D. S., Iverson, L. R., & Brown, S. (1993). Rates and patterns of deforestation in the Philippines: application of geographic information system analysis. *Forest Ecology and Management*, *57*(1–4), 1–16. https://doi.org/10.1016/0378-1127(93)90158-J

Liu, W., Song, C., Schroeder, T. A., & Cohen, W. B. (2008). Predicting forest successional stages using multitemporal Landsat imagery with forest inventory and analysis data. *International Journal of Remote Sensing*, *29*(13), 3855–3872. https://doi.org/10.1080/01431160701840166

Liu, Z., Peng, C., Work, T., Candau, J.-N., DesRochers, A., & Kneeshaw, D. (2018). Application of machine-learning methods in forest ecology: Recent progress and future challenges. *Environmental Reviews*, *26*(4), 339–350. https://doi.org/10.1139/er-2018-0034

Loh, H. Y., James, D., Ioki, K., Wong, W. V. C., Tsuyuki, S., & Phua, M. H. (2020). Aboveground biomass changes in tropical montane forest of northern borneo estimated using spaceborne and airborne digital elevation data. *Remote Sensing*, *12*(22), 1–16. https://doi.org/10.3390/rs12223677

Lu, D. (2005). Integration of vegetation inventory data and Landsat TM image for vegetation classification in the western Brazilian Amazon. *Forest Ecology and Management*, *213*(1–3), 369–383. https://doi.org/10.1016/j.foreco.2005.04.004

Lu, Dengsheng, Mausel, P., Brondízio, E., & Moran, E. (2003). Classification of successional forest stages in the Brazilian Amazon basin. *Forest Ecology and Management*, *181*(3), 301–312. https://doi.org/10.1016/S0378-1127(03)00003-3

Ma, L., Liu, Y., Zhang, X., Ye, Y., Yin, G., & Johnson, B. A. (2019). Deep learning in remote sensing applications: A meta-analysis and review. *ISPRS Journal of Photogrammetry and Remote Sensing*, *152*(March), 166–177. https://doi.org/10.1016/j.isprsjprs.2019.04.015

Makinano-Santillan, M., Bolastig, C. G., & Santillan, J. R. (2019). Above-ground biomass estimation of mangroves in Siargao Island, Philippines. *The 40th Asian Conference on Remote Sensing*, *ACRS 2019*, 1–10.

Mantero, P., Moser, G., & Serpico, S. B. (2004). Partially supervised classification of remote sensing images using SVM-based probability density estimation. *2003 IEEE Workshop on Advances in Techniques for Analysis of Remotely Sensed Data*, *43*(3), 327–336. https://doi.org/10.1109/WARSD.2003.1295212

Martínez, M. L., Pérez-Maqueo, O., Vázquez, G., Castillo-Campos, G., García-Franco, J., Mehltreter, K., Equihua, M., & Landgrave, R. (2009). Effects of land use change on biodiversity and ecosystem services in tropical montane cloud forests of Mexico. *Forest Ecology and Management*, *258*(9), 1856–1863. https://doi.org/10.1016/j.foreco.2009.02.023

Masum, K. M., Mansor, A., Sah, S. A. M., & Lim, H. S. (2017). Effect of differential forest management on land-use change (LUC) in a tropical hill forest of Malaysia. *Journal of Environmental Management*, *200*, 468–474. https://doi.org/10.1016/j.jenvman.2017.06.009

Maxwell, A. E., Warner, T. A., & Fang, F. (2018). Implementation of machine-learning classification in remote sensing: An applied review. *International Journal of Remote Sensing*, *39*(9), 2784–2817. https://doi.org/10.1080/01431161.2018.1433343

Mc Daniel, J. (2017). *How Does Altitude Affect Vegetation?* Sciencing. https://sciencing.com/how-does-altitude-affect-vegetation-12003620.html

Meygret, A., Baillarin, S., Gascon, F., Hillairet, E., Dechoz, C., Lacherade, S., Martimort, P., Spoto, F., Henry, P., & Duca, R. (2009). SENTINEL-2 image quality and level 1 processing. *Earth Observing Systems XIV*, *7452*(August), 74520D. https://doi.org/10.1117/12.826184

Miettinen, J., Stibig, H. J., & Achard, F. (2014). Remote sensing of forest degradation in Southeast Asia-Aiming for a regional view through 5-30 m satellite data. *Global Ecology and Conservation*, *2*, 24–36. https://doi.org/10.1016/j.gecco.2014.07.007

Mitchard, E. T. A., Saatchi, S. S., Lewis, S. L., Feldpausch, T. R., Woodhouse, I. H., Sonké, B., Rowland, C., & Meir, P. (2011). Measuring biomass changes due to woody encroachment and deforestation/degradation in a forest-savanna boundary region of central Africa using multi-temporal L-band radar backscatter. *Remote Sensing of Environment*, *115*(11), 2861–2873. https://doi.org/10.1016/j.rse.2010.02.022

Monzon, A. K., Veridiano, R. K., Mendoza, G., Vinluan, R., Agoncillo, O., & De Alban, J. D. (2015). Estimating forest biomass of Northern Sierra Madre Natural Park using SAR data. *ACRS 2015 - 36th Asian Conference on Remote Sensing: Fostering Resilient Growth in Asia, Proceedings*.

Moran, E. F., Brondizio, E., Mausel, P., & Wu, Y. (1994). Integrating Amazonian vegetation, land-use, and satellite data. *BioScience*, *44*(5), 329–338. https://doi.org/10.2307/1312383

Moumni, A., Oujaoura, M., Ezzahar, J., & Lahrouni, A. (2021). A new synergistic approach for crop discrimination in a semi-arid region using Sentinel-2 time series and the multiple combination of machine learning classifiers. *Journal of Physics: Conference Series*, *1743*(1). https://doi.org/10.1088/1742-6596/1743/1/012026

Mountrakis, G., Im, J., & Ogole, C. (2011). Support vector machines in remote sensing: A review. *ISPRS Journal of Photogrammetry and Remote Sensing*, *66*(3), 247–259. https://doi.org/10.1016/j.isprsjprs.2010.11.001

Mueller-Wilm, U., Devignot, O., & Pessiot, L. (2016). Sen2Cor Configuration Manual. *Esa, Sentinel 2*.

Mukul, S. A., Herbohn, J., & Firn, J. (2016). Tropical secondary forests regenerating after shifting cultivation in the Philippines uplands are important carbon sinks. *Scientific Reports*, *6*(February), 1–12. https://doi.org/10.1038/srep22483

Napaldet, J. T., & Gomez, R. A. (2015). Allometric Models for Aboveground Biomass of Benguet Pine (Pinus kesiya). *International Journal of Scientific & Engineering Research*, *6*(3), 182–187. http://www.ijser.org

Norovsuren, B., Tseveen, B., Batomunkuev, V., Renchin, T., Natsagdorj, E., Yangiv, A., & Mart, Z. (2019). Land cover classification using maximum likelihood method (2000 and 2019) at Khandgait valley in Mongolia. *IOP Conference Series: Earth and Environmental Science*, *381*(1). https://doi.org/10.1088/1755-1315/381/1/012054

Ochego, H. (2003). Application of Remote Sensing in Deforestation Monitoring : A Case Study of the Aberdares (Kenya). *2nd FIG Regional Conference*, 1–10. https://www.fig.net/resources/proceedings/fig_proceedings/morocco/proceedings/TS11/TS11_4_ochego.pdf

Ohsawa, M. (1991). Structural comparison of tropical montane rain forests along latitudinal and altitudinal gradients in south and east Asia. *Vegetatio*, *97*(1), 1–10. https://doi.org/10.1007/BF00033897

Olaode, A., & Todd, C. (2014). Unsupervised Classification of Images : A Review. *International Journal of Image Processing*, *8*(5), 325–342.

Parao, M. R., Pablo, J. P., Wagan, A. M., Nestor, J., Garcia, M., & Medina, S. M. (2016).

Climate Change Vulnerability Assessment in Selected Highland Areas of Benguet: An Application of VAST-Agro Tool. *Mountain Journal of Science and Interdisciplinary Research*, *77*(September 2016), 1–15.
Paulick, S., Dislich, C., Homeier, J., Fischer, R., & Huth, A. (2017). The carbon fluxes in different successional stages: modelling the dynamics of tropical montane forests in South Ecuador. *Forest Ecosystems*, *4*(1). https://doi.org/10.1186/s40663-017-0092-0
Pearson, Timothy, Walker, Sarah, Brown, & Sandra. (2005). *Sourcebook for land use , land-use change and forestry projects*. https://www.winrock.org/wp-content/uploads/2016/03/Winrock-BioCarbon_Fund_Sourcebook-compressed.pdf
Perez, G. J., Comiso, J. C., Aragones, L. V, Merida, H. C., & Ong, P. S. (2020). *Reforestation and Deforestation in Northern Luzon , Philippines : Critical Issues as Observed from Space*. 1–20.
Pettorelli, N., Vik, J. O., Mysterud, A., Gaillard, J. M., Tucker, C. J., & Stenseth, N. C. (2005). Using the satellite-derived NDVI to assess ecological responses to environmental change. *Trends in Ecology and Evolution*, *20*(9), 503–510. https://doi.org/10.1016/j.tree.2005.05.011
Philippine Statistics Authority. (2020). *Regional Compendium of Environment Statistics Component 1: Environmental conditions and quality, land cover, ecosystem and biodiversity*.
Philippine Statistics Authority. (2021). Highlights of the Philippine Population 2020 Census of Population and Housing. In *2021-252*. http://web0.psa.gov.ph/content/highlights-philippine-population-2015-census-population
Pichler, M., & Hartig, F. (2023). Machine learning and deep learning—A review for ecologists. *Methods in Ecology and Evolution*, *14*(4), 994–1016. https://doi.org/10.1111/2041-210X.14061
Provincial Governor's Office - Information Technology. (2020). *About the Province – Province of Benguet*. Province of Be. http://benguet.gov.ph/about-the-province/
Pulhin, F. B., Torres, A. M., Pampolina, N. M., Lasco, R. D., & Alducente, A. M. (2020). *Vegetation Analysis of Sanctuary and Forest Areas of Kalahan Forest Reserve Nueva Vizcaya*. *150*, 271–280.
Ray, D. K. (2013). Tropical Montane Cloud Forests. In *Climate Vulnerability: Understanding and Addressing Threats to Essential Resources* (Vol. 5). Elsevier. https://doi.org/10.1016/B978-0-12-384703-4.00519-0
Reich, P. B. (2012). Key canopy traits drive forest productivity. *Proceedings of the Royal Society B: Biological Sciences*, *279*(1736), 2128–2134. https://doi.org/10.1098/rspb.2011.2270
Reiche, J., Hamunyela, E., Verbesselt, J., Hoekman, D., & Herold, M. (2018). Improving near-real time deforestation monitoring in tropical dry forests by combining dense Sentinel-1 time series with Landsat and ALOS-2 PALSAR-2. *Remote Sensing of Environment*, *204*(November 2017), 147–161. https://doi.org/10.1016/j.rse.2017.10.034
Requena-Mullor, J. M., Reyes, A., Escribano, P., & Cabello, J. (2018). Assessment of ecosystem functioning from space: Advancements in the Habitats Directive implementation. *Ecological Indicators*, *89*(December 2017), 893–902. https://doi.org/10.1016/j.ecolind.2017.12.036
Richards, D. R., & Friess, D. A. (2016). Rates and drivers of mangrove deforestation in Southeast Asia, 2000-2012. *Proceedings of the National Academy of Sciences of the United States of America*, *113*(2), 344–349. https://doi.org/10.1073/pnas.1510272113
Richter, M. (2008). Tropical mountain forests - distribution and general features. In J. H. and D. G. S.R. Gradstein (Ed.), *Tropical Mountain Forest: Patterns and Processes in a Biodiversity Hotspot* (Vol. 2, pp. 7–24). Göttingen Centre for Biodiversity and Ecology.

Rodríguez-Veiga, P., Wheeler, J., Louis, V., Tansey, K., & Balzter, H. (2017). Quantifying Forest Biomass Carbon Stocks From Space. *Current Forestry Reports*, *3*(1), 1–18. https://doi.org/10.1007/s40725-017-0052-5

Romijn, E., Lantican, C. B., Herold, M., Lindquist, E., Ochieng, R., Wijaya, A., Murdiyarso, D., & Verchot, L. (2015). Assessing change in national forest monitoring capacities of 99 tropical countries. *Forest Ecology and Management*, *352*, 109–123. https://doi.org/10.1016/j.foreco.2015.06.003

Salvaña, F. R. P., Dacutan, C. J. J., Cherie, C., & Bretaña, B. L. P. (2019). *Comparison of aboveground biomass estimation in two forest types using different allometric equations* (Vol. 8, Issue September).

Santi, E., Paloscia, S., Pettinato, S., Cuozzo, G., Padovano, A., Notarnicola, C., & Albinet, C. (2020). Machine-learning applications for the retrieval of forest biomass from airborne P-band SAR data. *Remote Sensing*, *12*(5), 1–17. https://doi.org/10.3390/rs12050804

Sarker, I. H. (2021). Machine Learning: Algorithms, Real-World Applications and Research Directions. *SN Computer Science*, *2*(3), 1–21. https://doi.org/10.1007/s42979-021-00592-x

Sarstedt, M., & Mooi, E. (2018). Regresion Analysis. In *Angewandte Chemie International Edition*. https://doi.org/10.1007/978-3-662-56707-4

Schwartz, N. B., Uriarte, M., Defries, R., Gutierrez-Velez, V. H., & Pinedo-Vasquez, M. A. (2017). Land-use dynamics influence estimates of carbon sequestration potential in tropical second-growth forest. *Environmental Research Letters*, *12*(7). https://doi.org/10.1088/1748-9326/aa708b

Shivakumar, B. R., & Rajashekararadhya, S. V. (2018). Investigation on land cover mapping capability of maximum likelihood classifier: A case study on North Canara, India. *Procedia Computer Science*, *143*, 579–586. https://doi.org/10.1016/j.procs.2018.10.434

Singh, M., Friess, D. A., Vilela, B., De Alban, J. D. T., Monzon, A. K. V., Veridiano, R. K. A., & Tumaneng, R. D. (2017). Spatial relationships between above-ground biomass and bird species biodiversity in Palawan, Philippines. *PLoS ONE*, *12*(12), 1–22. https://doi.org/10.1371/journal.pone.0186742

SNAP Development Team. (n.d.). *Sentinel Application Platform Software*. Retrieved October 11, 2023, from https://step.esa.int/main/toolboxes/snap/

Soh, M. C. K., Mitchell, N. J., Ridley, A. R., Butler, C. W., Puan, C. L., & Peh, K. S.-H. (2019). Impacts of Habitat Degradation on Tropical Montane Biodiversity and Ecosystem Services: A Systematic Map for Identifying Future Research Priorities. *Frontiers in Forests and Global Change*, *2*(December), 1–18. https://doi.org/10.3389/ffgc.2019.00083

Song, C., Woodcock, C. E., & Li, X. (2002). The spectral/temporal manifestation of forest succession in optical imagery. *Remote Sensing of Environment*, *82*(2–3), 285–302. https://doi.org/10.1016/s0034-4257(02)00046-9

Spracklen, D. V., & Righelato, R. (2014). Tropical montane forests are a larger than expected global carbon store. *Biogeosciences*, *11*(10), 2741–2754. https://doi.org/10.5194/bg-11-2741-2014

Stone, T. A., Brown, I. F., & Woodwell, G. M. (1991). Estimation, by remote sensing, of deforestation in central Rondônia, Brazil. *Forest Ecology and Management*, *38*(3–4), 291–304. https://doi.org/10.1016/0378-1127(91)90150-T

Timothy, D., Onisimo, M., Cletah, S., Adelabu, S., & Tsitsi, B. (2016). Remote sensing of aboveground forest biomass: A review. *Tropical Ecology*, *57*(2), 125–132.

Turner, I. M., Wong, Y. K., Chew, P. T., & Bin Ibrahim, A. (1996). Rapid assessment of tropical rain forest successional status using aerial photographs. *Biological Conservation*, *77*(2–3), 177–183. https://doi.org/10.1016/0006-3207(95)00145-X

Vieira, I. C. G., De Almeida, A. S., Davidson, E. A., Stone, T. A., Reis De Carvalho, C. J., & Guerrero, J. B. (2003). Classifying successional forests using Landsat spectral properties and ecological characteristics in eastern Amazônia. *Remote Sensing of Environment*, *87*(4), 470–481. https://doi.org/10.1016/j.rse.2002.09.002

Wallis, C. I. B., Brehm, G., Donoso, D. A., Fiedler, K., Homeier, J., Paulsch, D., Süßenbach, D., Tiede, Y., Brandl, R., Farwig, N., & Bendix, J. (2017). Remote sensing improves prediction of tropical montane species diversity but performance differs among taxa. *Ecological Indicators*, *83*, 538–549. https://doi.org/10.1016/j.ecolind.2017.01.022

Wallis, C. I. B., Homeier, J., Peña, J., Brandl, R., Farwig, N., & Bendix, J. (2019). Modeling tropical montane forest biomass, productivity and canopy traits with multispectral remote sensing data. *Remote Sensing of Environment*, *225*(September 2018), 496–510. https://doi.org/https://doi.org/10.1111/gcb.13907

Walpole, P. (2010). Figuring the forest figures: Understanding forest cover data in the Philippines and where we might be proceeding. *Environmental Science for Social Change, July 2010*, 37.

Washington-allen, R. (2015). *Application of remote sensing technology and ecological modeling of forest carbon stocks in Mt. Apo Natural Park, Philippines*. *May*, 195. http://search.proquest.com.ezproxy.usc.edu.ph/docview/1732362560/B553D742F31E4508PQ/3

Whitford, H. N. (1911). *Whitford_1911_Forests_of_the_Philippines.pdf*.

Wikramanayake, E. (2021). *Mindanao Montane Rainforests | One Earth*. One Earth. https://www.oneearth.org/ecoregions/mindanao-montane-rainforests/

Xu, L., Saatchi, S. S., Yang, Y., Yu, Y., & White, L. (2016). Performance of non-parametricv algorithms for spatial mapping of tropical forest structure. *Carbon Balance and Management*, *11*(1), 18–20. https://doi.org/10.1186/s13021-016-0062-9

Yanasse, C. D. C. F., Sant'Anna, S. J. S., Frery, A. C., Rennó, C. D., Soares, J. V., & Luckman, A. J. (1997). Exploratory study of the relationship between tropical forest regeneration stages and SIR-C L and C data. *Remote Sensing of Environment*, *59*(2), 180–190. https://doi.org/10.1016/S0034-4257(96)00149-6

Yuan, H., Van Der Wiele, C. F., & Khorram, S. (2009). An automated artificial neural network system for land use/land cover classification from landsat TM imagery. *Remote Sensing*, *1*(3), 243–265. https://doi.org/10.3390/rs1030243

Yuen, J. Q., Fung, T., & Ziegler, A. D. (2016). Review of allometric equations for major land covers in SE Asia: Uncertainty and implications for above- and below-ground carbon estimates. *Forest Ecology and Management*, *360*, 323–340. https://doi.org/10.1016/j.foreco.2015.09.016

APPENDIX A: FIELD PLOTS AND DATA

Appendix Table 1. Sampling plots and field collected forest data

Vegetation Type	Plot Number	Plot code	Longitude	Latitude	Elevation	Canopy cover
Pine Forest	1	P1	120.61355	16.39725	1505	93.76
	2	P2	120.6136167	16.3952	1504	75.04
	3	P3	120.6136333	16.39467	1486	83.36
	4	P4	120.6076833	16.39837	1459	0
	5	P5	120.6197667	16.41396	1508	84.4
	6	P6	120.61925	16.41407	1508	35.52
	7	P7	120.6187333	16.4149	1505	90.64
	8	P8	120.62455	16.3698	1380	96.1
	9	P9	120.6255333	16.36973	1310	79.98
	10	P10	120.6149833	16.36877	1366	88.56
	11	P11	120.618	16.36705	1400	79.98
	12	P12	120.6172667	16.36352	1357	72.96
	13	P13	120.6173333	16.36283	1360	81.02
	14	P14	120.6171167	16.36068	1332	67.24
	15	P15	120.6160833	16.36128	1341	87
	16	P16	120.6168333	16.3616	1343	84.34
	17	P17	120.6164333	16.36203	1330	81.02
	18	P18	120.6218833	16.3666	1415	72.18
	19	P19	120.6224	16.36858	1415	86.64
	20	P20	120.61975	16.4285	1657	69.32
	21	P21	120.6192833	16.42833	1651	57.62
	22	P22	120.61865	16.42848	1651	69.58
	23	P23	120.6184333	16.42792	1633	71.4
	24	P24	120.6170333	16.42795	1629	46.44
	25	P25	120.6165333	16.42722	1614	56.58
	26	P26	120.61565	16.42858	1615	67.69
	27	P27	120.6135833	16.42667	1567	75.3
	28	P28	120.6110833	16.42788	1531	79.46
	29	P29	120.61185	16.42618	1530	79.2
	30	P30	120.5998	16.40145	1448	91.16
	31	P31	120.5993167	16.40177	1442	84.93
	32	P32	120.5996667	16.40217	1448	86.74
	33	P33	120.6008	16.40207	1499	74
	34	P34	120.60165	16.39958	1365	0
	35	P35	120.6018167	16.39885	1356	0
	36	P36	120.6081333	16.36442	1168	71.14

Appendix Table 1. Sampling plots and field collected forest data (continuation)

Vegetation Type	Plot Number	Plot code	Longitude	Latitude	Elevation	Canopy cover
Pine Forest	37	P37	120.6097167	16.36465	1192	62.56
	38	P38	120.6111667	16.36423	1213	67.5
	39	P39	120.61425	16.38562	1398	64.92
	40	P40	120.6149667	16.38503	1381	65.42
	41	P41	120.6162333	16.3853	1383	66.72
	42	P42	120.6741833	16.36512	798	66.97
	43	P43	120.63985	16.36795	1178	46.7
	44	P44	120.6407667	16.36707	1166	75
	45	P45	120.6415833	16.36667	1144	70.88
	46	P46	120.6431833	16.36577	1146	76.6
	47	P47	120.6447	16.36402	1145	84.62
	48	P48	120.6448667	16.36333	1132	76.08
	49	P49	120.6491333	16.31822	1674	66.2
	50	P50	120.64875	16.31615	1677	64.64
	51	P51	120.6490333	16.31708	1675	53.46
	52	P52	120.6487	16.31535	1668	50.34
	53	P53	120.648	16.31425	1697	57.36
	54	P54	120.64865	16.31147	1720	0
	55	P55	120.6474333	16.30723	1800	0
	56	P56	120.64775	16.30598	1787	11.34
	57	P57	120.6461	16.305	1757	0
	58	P58	120.6457333	16.30392	1752	66.2
	59	P59	120.6432833	16.30285	1746	62.04
	60	P60	120.6404667	16.29997	1746	0
	61	P61	120.6389667	16.2988	1777	0
	62	P62	120.6343	16.2853	1730	50.34
	63	P63	120.6353833	16.2843	1660	19.46
	64	P64	120.6362167	16.28383	1599	70.1
	65	P65	120.6368167	16.28355	1544	75.04
Mossy Forest	66	M1	120.8780333	16.68003	2319	0
	67	M2	120.8782667	16.68055	2330	93.76
	68	M3	120.8964833	16.68163	2395	93.76
	69	M4	120.8800683	16.68187	2411	88.56
	70	M5	120.8805333	16.68222	2437	92.72
	71	M6	120.8809667	16.68263	2454	96.88
	72	M7	120.87545	16.68002	2300	0
	73	M8	120.8877167	16.6677	2431	0
	74	M9	120.8879667	16.66785	2431	0
	75	M10	120.8885167	16.66755	2431	87
	76	M11	120.8893833	16.6672	2398	78.94
	77	M12	120.8871333	16.66763	2427	84.92

Appendix Table 1. Sampling plots and field collected forest data (continuation)

Vegetation Type	Plot Number	Plot code	Longitude	Latitude	Elevation	Canopy cover
Mossy Forest	78	M13	120.8863667	16.66765	2436	63.08
Grassland Summit	79	G1	120.8987783	16.59785	2931	78.68
	80	G2	120.89885	16.59793	2928	92.72
	81	G3	120.8989	16.59808	2928	94.8
	82	G4	120.8988833	16.59815	2926	95.84
	83	G5	120.8992333	16.59807	2912	87.52
	84	G6	120.8995333	16.59735	2800	96.88
	85	G7	120.9000167	16.59812	2869	100
	86	G8	120.9003333	16.5981	2867	64.64
	87	G9	120.90175	16.59725	2835	93.76
	88	G10	120.9058333	16.59718	2843	88.56
	89	G11	120.9031833	16.5954	2854	100
	90	G12	120.9043	16.5946	2842	62.56
	91	G13	120.9054667	16.59313	2808	100
	92	G14	120.59215	16.90687	2779	79.2
	93	G15	120.9085167	16.58988	2774	93.76
	94	G16	120.90755	16.5911	2762	95.84
	95	G17	120.9091	16.58875	2727	100
	96	G18	120.9083	16.58712	2730	41.76
Other Land Use and Land Cover	97	W1	120.7439261	16.4625	803.627	0
	98	W2	120.7435844	16.47068	803.6364	0
	99	W3	120.7461299	16.48719	803.6693	0
	100	W4	120.7598651	16.48124	803.7266	0
	101	W5	120.6928911	16.20089	266.3456	0
	102	W6	120.6984255	16.218	277.8372	0
	103	W7	120.6985284	16.23408	304.6121	0
	104	W8	120.6763716	16.23448	667.9511	0
	105	W9	120.6647411	16.23928	665.1603	0
	106	W10	120.5948173	16.4106	1483.814	0
	107	W10	120.6594355	16.4002	884.6638	0
	108	W11	120.6189992	16.6282	549.4838	0
	109	W12	120.7664468	16.89733	725.0009	0
	110	W13	120.8231566	16.73217	1399.635	0
	111	W14	120.8894565	16.66763	2438.485	0
	112	W15	120.8741807	16.67789	2321.13	0
	113	W16	120.8734726	16.67922	2327.867	0
	114	W17	120.8855978	16.66742	2473.414	0
	115	W18	120.8851645	16.66856	2479.467	0
	116	W19	120.6777665	16.63714	1272.777	0
	117	BS1	120.6854992	16.23878	513.4929	0

Appendix Table 1. Sampling plots and field collected forest data (continuation)

Vegetation Type	Plot Number	Plot code	Longitude	Latitude	Elevation	Canopy cover
Other Land Use and Land Cover	118	BS2	120.6861555	16.24754	796.939	0
	119	BS3	120.7271666	16.29174	818.382	0
	120	BS4	120.7522716	16.35257	1188.591	0
	121	BS5	120.6849896	16.3432	1085.43	0
	122	BS6	120.7690672	16.44172	1164.433	0
	123	BS7	120.8470343	16.51698	1136.996	0
	124	BS8	120.7652085	16.58406	1910.588	0
	125	BS9	120.8213018	16.57687	980.8034	0
	126	BS10	120.8272901	16.59326	1234.35	0
	127	BS11	120.8130592	16.67014	1373.236	0
	128	BS12	120.820024	16.68553	1421.909	0
	129	BS13	120.7730649	16.79309	1439.875	0
	130	BS14	120.7743264	16.80819	1418.147	0
	131	BS15	120.785017	16.85052	1214.265	0
	132	BS17	120.7757504	16.85995	950.3339	0
	133	BS18	120.7193358	16.90397	1277.053	0
	134	BS19	120.7301197	16.89426	759.9238	0
	135	BS20	120.6511568	16.85845	996.8363	0
	136	BS21	120.7579657	16.81797	1152.612	0
	137	BS22	120.6493361	16.79446	1288.986	0
	138	BS23	120.6970866	16.74989	1755.087	0
	139	BS24	120.6387499	16.7152	1541.854	0
	140	BS25	120.6776846	16.63353	1306.098	0
	141	BS26	120.636194	16.62214	1137.634	0
	142	BS27	120.5776024	16.59208	1225.525	0
	143	BS28	120.6815041	16.51487	1365.684	0
	144	BS29	120.6896162	16.51101	1765.472	0
	145	BS30	120.6823997	16.47122	1451.653	0
	146	BS31	120.5097564	16.50987	935.6754	0
	147	BS32	120.5381535	16.42074	891.966	0
	148	BS33	120.5349931	16.38116	1330.354	0
	149	BS34	120.6054345	16.29291	935.2983	0
	150	BS35	120.6206268	16.26616	1772.778	0
	151	BU1	120.5992686	16.40884	1533.447	0
	152	BU2	120.6030021	16.40373	1530.273	0
	153	BU3	120.6215075	16.38071	1425.515	0
	154	BU4	120.6306038	16.36739	1356.554	0
	155	BU5	120.6200128	16.36131	1434.909	0
	156	BU6	120.5906535	16.28911	565.8144	0
	157	BU7	120.5682756	16.38273	1642.461	0
	158	BU8	120.5778344	16.37185	1494.149	0

Appendix Table 1. Sampling plots and field collected forest data (continuation)

Vegetation Type	Plot Number	Plot code	Longitude	Latitude	Elevation	Canopy cover
Other Land Use and Land Cover	159	BU9	120.5687373	16.37425	1594.766	0
	160	BU10	120.7276137	16.38701	670.1323	0
	161	BU11	120.7303443	16.39482	595.7079	0
	162	BU12	120.6547709	16.32548	1557.587	0
	163	BU13	120.6618821	16.33827	1520.122	0
	164	BU14	120.6770965	16.36017	788.2064	0
	165	BU15	120.7420295	16.5757	1957.15	0
	166	BU16	120.8386489	16.6227	1231.91	0
	167	BU17	120.8321676	16.64021	1370.197	0
	168	BU18	120.8504437	16.67274	2000.233	0
	169	BU19	120.8271476	16.71973	1438.857	0
	170	BU20	120.8685303	16.73835	1884.49	0
	171	BU21	120.8652193	16.74346	1919.451	0
	172	BU22	120.804952	16.75487	2157.995	0
	173	BU23	120.8194516	16.79217	1859.624	0
	174	BU24	120.8207195	16.8033	1841.828	0
	175	BU25	120.8173936	16.82326	1531.691	0
	176	BU26	120.7948167	16.8384	1493.819	0
	177	BU27	120.7886646	16.84588	1375.22	0
	178	BU28	120.7797686	16.86779	1216.737	0
	179	BU29	120.7528544	16.86885	1181.221	0
	180	BU30	120.6614668	16.79168	1190.257	0
	181	BU31	120.6661761	16.76394	1636.653	0
	182	BU32	120.6563179	16.69708	1259.218	0
	183	BU33	120.6239052	16.57456	1188.622	0
	184	BU35	120.6197433	16.53047	951.4916	0

**Plot code: P – Pine Forest, M – Mossy Forest, G – Grassland, W – Waterbody, BS- Bare Soil, BU – Built-up Area*

APPENDIX B: DATA SHEET

Appendix B.1. Field plot data sheet for pine and mossy forest

Plot number: _____ Location: _____ Date: _____

GPS data: Longitude (E): _____ Latitude (N): _____ Accuracy: _____ Elevation: _____

Forest type: ☐ Pine Forest ☐ Mossy Category: ☐ Small ☐ Medium ☐ Large

Canopy cover (%): _____

Number of saplings (below 5cm): Q1: _____ Q2: _____ Q3: _____ Q4: _____

Collected by: _____

Nr	Local Name/Species name	DBH	Distance	Top (angle)	Down (angle)
1					
2					
3					
4					
5					
6					
7					
8					
9					
10					
11					
12					

Code: P – Pine Forest; M – Mossy Forest; G – Grassland Summit

Appendix B.2. Field plot data sheet for grassland summit

Plot number: _____ Location: _____ Date: _____

GPS data: Longitude (E): _____ Latitude (N): _____ Accuracy: _____ Elevation: _____

Forest type: ☐ Grassland Category: ☐ Small ☐ Medium ☐ Large

Canopy cover (%): _____

Collected by: _____

Nr	Local Name/Species name	Height	Basal diameter	Number of Culm/Stem	Other note
1					
2					
3					
4					
5					
6					
7					
8					
9					
10					
11					
12					

Code: P – Pine Forest; M – Mossy Forest; G – Grassland Summit

APPENDIX C: PHOTO DOCUMENTATION

Appendix Figure C.1 Field work at Mt Tabeyoc with the monitoring staff from MPPL PMO sub-station

Appendix Figure C.2 The field survey team at Ambulalacao lake in Ballay, Kabayan, Benguet

Appendix Figure C.3 Dwarf bamboo (*Yushania niitakayamensis)* found at the summit of Mount Pulag, elevation is 2,926 meters

Appendix Figure C.4 The field survey team ascending to the summit of Mt Pulag

Appendix Figure C.5 A pine forest inside the Philippine Military Academy in Baguio City

Appendix Figure C.6 Layouting of a survey plot in one of the selected sites in Baguio City

Appendix Figure C.7 Converted pine forest into a water crest agricultural farm in Camp 8, Baguio City